NASA Contractor Report 4122

Calculation of Symmetric and Asymmetric Vortex Separation on Cones and Tangent Ogives Based on Discrete Vortex Models

S. Chin and C. Edward Lan

GRANT NSG-1629
FEBRUARY 1988

NASA

NASA Contractor Report 4122

Calculation of Symmetric and Asymmetric Vortex Separation on Cones and Tangent Ogives Based on Discrete Vortex Models

S. Chin and C. Edward Lan
Flight Research Laboratory
University of Kansas Center for Research, Inc.
Lawrence, Kansas

Prepared for
Langley Research Center
under Grant NSG-1629

National Aeronautics
and Space Administration

Scientific and Technical
Information Division

1988

SUMMARY

An inviscid discrete vortex model, with newly derived expressions for the tangential velocity imposed at the separation points, is used to investigate the symmetric and asymmetric vortex separation on cones and tangent ogives. The circumferential locations of separation are taken from experimental data. Based on a slender body theory, the resulting simultaneous nonlinear algebraic equations in a cross-flow plane are solved with Broyden's modified Newton-Raphson method. Total force coefficients are obtained through momentum principle with new expressions for nonconical flow. It is shown through the method of function deflation that multiple solutions exist at large enough angles of attack, even with symmetric separation points. These additional solutions are asymmetric in vortex separation and produce side force coefficients which agree well with data for cones and tangent ogives.

LIST OF SYMBOLS

A	Parameter of incidence ($= \alpha/\delta$)
C_L	Lift coefficient
C_{L_i}	Lift coefficient at station i
C_N	Normal force coefficient
C_{N_i}	Normal force coefficient at station i
C_y	Side force coefficient
C_{y_i}	Side force coefficient at station i
S_b	Base area of a body of revolution
U_∞	Free-stream velocity
$V_{1,2}$	Vortex core
V_{tm}	Mean tangential velocity
W	Complex potential
Z	Complex coordinate ($= \bar{y} + i\bar{z}$)
$\bar{Z}$	Complex conjugate of Z
a	Radius of a circular cross section of a body at an axial station of $\bar{x}$
a_b	Radius of the base area
n	Outward normal to a cross section of a body at $\bar{x}$
y	Nondimensional lateral coordinate ($= \bar{y}/a$)
z	Nondimensional vertical coordinate ($= \bar{z}/a$)
$\bar{x}$	Dimensional longitudinal coordinate
$\bar{y}$	Dimensional lateral coordinate
$\bar{z}$	Dimensional vertical coordinate
α	Angle of attack

β	Sideslip angle
δ	Semi-apex angle of a cone
$\theta_{1,2}$	Separation angle measured from the starboard generator
Γ	Vortex strength
γ	Nondimensional vortex strength (= $\Gamma/2\pi a\alpha U$)
ζ	Nondimensional complex coordinate (= Z/a)
$\bar{\zeta}$	Nondimensional complex conjugate coordinate (= $\bar{Z}/a$)
ζ_{S_1,S_2}	Nondimensional complex coordinate of separation position
$\bar{\zeta}_{S_1,S_2}$	Nondimensional complex conjugate coordinate of separation position
ϕ	Velocity potential

INTRODUCTION

Recent and new fighters and missiles are developed to have increased aerodynamic performance and high maneuverability. These requirements frequently involve operation at high angles of attack and consequently body separated vortices. Therefore, understanding and predicting the flow characteristics near the body can be accomplished only if these vortices are accounted for.

To represent mathematically the body vortex flow field, Bryson (Reference 1) introduced two inviscid line vortices in the leeward side of the body. He considered symmetric flow past bodies of revolution. This approach was extended by Schindel (Reference 2) to bodies of elliptic cross section and of cambered longitudinal axis. By removing restriction to laterally symmetric flow, Dyer, Fiddes, and Smith (Reference 3) extended this simple model to deal with asymmetric vortex separation on cones. In all of these investigations, a stagnation condition was imposed at the separation line as the Kutta condition. On the other hand, Moore (Reference 4) imposed a tangential velocity at the separation line based on an expression derived by Smith (Reference 5). The effect was found to be small in symmetrical flow.

Other methods used to predict the asymmetric vortex shedding include the vortex cloud method (Reference 6) and solving the complete Navier-Stokes equations (Reference 7). As described by Mendenhall et al. in their paper (Reference 6), in the vortex cloud method a perturbation to the symmetric solution must be imposed in

order to obtain an asymmetric solution. In fact, every investigator has a different means of introducing a perturbation to the symmetric solution. The method which Mendenhall et al. used is to modify the predicted symmetric separation point on either side of the body so that the separation position is not kept symmetric. By solving the complete Navier-Stokes equations at high α, the asymmetric vortex shedding was found on a cone cylinder (Reference 7). However, the asymmetry in the flow field was introduced through asymmetric numerical truncation errors with the computed side force being too small.

In the present study, different discrete vortex models will be studied in the cross-flow plane. New expressions for the tangential velocity at the separation line will be included in the models to investigate the vortex flow effect on cones and tangent ogives in both symmetric and asymmetric flows. The resulting nonlinear algebraic equations are solved for multiple solutions (i.e. both symmetric and asymmetric ones) based on a function deflation concept.

MATHEMATICAL MODEL

Slender-body theory is assumed applicable. This leads to the usual representation of the flow in terms of a streamwise disturbance velocity which depends only on the streamwise coordinate, and a quasi-two-dimensional cross flow which is independent of the Mach number. For cones, the flow is assumed to

be conical, so that the separation lines are straight lines, OS_1 and OS_2 (see Figure 1). To represent the nonconical flow, a tangent ogive is divided into several stations. Between two stations, flow properties are assumed to vary linearly (i.e. $\partial\Gamma/\partial\bar{x} = \Delta\Gamma/\Delta\bar{x} = (\Gamma_i - \Gamma_{i-1})/\Delta\bar{x}$, $\partial a/\partial\bar{x} = (a_i - a_{i-1})/\Delta\bar{x}$, etc.). The separation lines are specified by their angular coordinates, θ_1 and θ_2, measured from the starboard generator. The sign convention is that a positive value of Γ represents a circulation which is counterclockwise when viewed from downstream. With specified separation lines, the problem therefore involves six unknown quantities, which include the strengths and coordinates of two discrete vortices. These are determined by six equations obtained from the following conditions:

(i) An analogue of the Kutta condition, namely that the velocity vectors on the surface of the body at S_1 and S_2 should be directed along the separation lines, OS_1 and OS_2.

In the past investigations, either a stagnation condition (Reference 3) or a tangential velocity (Reference 4) was imposed at the separation point. Since the latter did not provide significant improvement to the solution, a new velocity condition is needed.

In the vortex cloud method (Reference 6) the relationship between the vortex strength and velocity at the boundary layer edge, U_e, is used, which is

$$\partial\Gamma/\partial t = K\frac{U_e^2}{2} \tag{1}$$

where K is an empirical factor used to reduce the strength of the shedding vorticity. In a subsonic flow, K = 0.6, a typical value suggested by most investigators. If half value of U_e is taken as the average tangential velocity at the separation point, as assumed in Smith's model (Reference 5), then

$$U\frac{\partial\Gamma}{\partial\bar{x}} = K\frac{(2V_{tm})^2}{2} \tag{2}$$

For a cone with $\partial\Gamma/\partial\bar{x} = \Gamma/\bar{x}$, the tangential velocity becomes

$$V_{tm} = \left[\frac{U}{K}\frac{\Gamma}{2\bar{x}}\right]^{1/2} = \left[\frac{U^2\alpha}{K}\frac{\pi a\Gamma}{2\pi a\bar{x}U\alpha}\right]^{1/2} = \left[\frac{U^2\alpha\delta}{K}\frac{\pi\Gamma\delta}{2\pi a\alpha U}\right]^{1/2} = \frac{U\alpha}{\sqrt{K}}\sqrt{\pi\gamma\delta/\alpha} \tag{3}$$

where γ is the nondimensionalized vortex strength, and

$$\gamma = \Gamma/2\pi a\alpha U$$

For a tangent ogive, it is assumed that

$\partial\Gamma/\partial\bar{x} = \Delta\Gamma/\Delta\bar{x}$, and therefore

$$V_{tm} = \left[\frac{U}{K}\frac{\Delta\Gamma}{2\Delta\bar{x}}\right]^{1/2} = \left[\frac{U^2\alpha}{K}\frac{\pi a_i(\Gamma_i - \Gamma_{i-1})}{2\pi a_i\Delta\bar{x}U\alpha}\right]^{1/2}$$

$$= \frac{U\alpha}{\sqrt{K}}\sqrt{\pi(a_i\gamma_i - a_{i-1}\gamma_{i-1})/\Delta\bar{x}\alpha} \tag{4}$$

where i means the present station and i-1 means the

previous station.

However, experimental data (Reference 8) show that the vortex convection speed in a shear layer is approximately

$$V_{tm} = fU_e \tag{5}$$

where f = 0.61, instead of 0.5 used in Equation (2). Then for a cone

$$V_{tm} = \frac{2fU\alpha}{\sqrt{K}} \sqrt{\pi\gamma\delta/\alpha} \tag{6}$$

and for a tangent ogive

$$V_{tm} = \frac{2fU\alpha}{\sqrt{K}} \sqrt{\pi(a_i\gamma_i - a_{i-1}\gamma_{i-1})/\Delta\bar{x}\alpha} \tag{7a}$$

Six models based on different f and K values are investigated for cones in this report. They are

1. Stagnation separation model ($V_{tm} = 0$)
2. Model 1, Smith's separation model ($V_{tm} = U\alpha\sqrt{\pi\gamma\delta/\alpha}$)
3. Model 2, f = 0.61 and K = 1.0 ($V_{tm} = 1.220\ U\alpha\sqrt{\pi\gamma\delta/\alpha}$)
4. Model 3, f = 0.61 and K = 0.6 ($V_{tm} = 1.575\ U\alpha\sqrt{\pi\gamma\delta/\alpha}$)
5. Model 4, f = 1.00 and K = 1.0 ($V_{tm} = 2.000\ U\alpha\sqrt{\pi\gamma\delta/\alpha}$)
6. Model 5, f = 1.00 and K = 0.6 ($V_{tm} = 2.582\ U\alpha\sqrt{\pi\gamma\delta/\alpha}$)

After testing, a best model with f and K values written as f_b and K_b will be chosen to investigate the asymmetric vortex separation on cones and vortex flow separation on tangent ogives. Based on f_b and k_b values, V_{tm} for tangent ogives becomes

$$V_{tm} = \frac{2f_b U\alpha}{\sqrt{K_b}} \sqrt{\pi(a_i\gamma_i - a_{i-1}\gamma_{i-1})/\Delta\bar{x}\alpha} \qquad (7b)$$

(ii) A condition based on the fact that the fluid should sustain no force.

In reality, when the flow is separated from a body, there will be a vortex sheet with small strength shedding from the body and finally rolling up into a concentrated vortex. To simplify the physical problem, only the concentrated vortex is used here; and a cut which connects the vortex core to the separation point is introduced to represent the sheet. It is required that the force on the cut must be balanced by force on the vortex, as described in Bryson's paper (Reference 1). In the vortex sheet model (Reference 9) usually a cut is introduced to connect the end of the sheet to the vortex core. The cut is much larger in the present model than that in the vortex sheet model. Although the force on the cut has always been included in the model in the past, a numerical experimentation will be conducted in the present study to determine its effect on the solution.

Following the usual development of the slender-body theory, the cross-flow velocity potential, ϕ, is constructed as a solution of the two-dimensional form of Laplace's equation in the plane of transverse coodinates y and z (see Figure 1). In a conical flow, all such planes are equivalent. The velocity components are the

same at points whose y and z coordinates are scaled by $\bar{x}$, and the vortex circulations are proportional to $\bar{x}$.

The boundary conditions for the far field and on the body are

$$\phi_z \sim U\alpha \quad \text{as} \quad |\bar{Z}| \to \infty \tag{8}$$

$$\phi_n = U\delta_{local} \quad \text{for} \quad |\bar{Z}| = \delta_{local}\bar{x} = a_{local} \tag{9}$$

where U is the free-stream speed, n is the outward normal to the cross section of the body at a constant $\bar{x}$, δ_{local} is the angle of local slope, and a_{local} is the radius of this section.

The complex potential may be written as

$$W = iU\alpha\left(Z - \frac{a^2}{\bar{Z}}\right) + Ua\frac{da}{d\bar{x}}\ell nZ + \frac{\Gamma_1}{2\pi i}\ell n\frac{Z - Z_1}{Z - (a^2/\bar{Z}_1)} - \frac{\Gamma_2}{2\pi i}\ell n\frac{Z - Z_2}{Z - (a^2/\bar{Z}_2)} \tag{10}$$

where the first term comes from the cross-flow stream in the presence of a circular body. The second term represents the area expansion in the x direction. The third and fourth terms are due to the vortices outside the body and their images inside the body.

Using the nondimensional variables $\zeta = z/a$, $\gamma = \Gamma/2\pi a\alpha U$, the Kutta condition and the force-free condition can be written as

Kutta Condition

$$V_{tm} = 2\alpha U\cos\theta_1 - \alpha U\gamma_1\frac{\zeta_1\bar{\zeta}_1 - 1}{(e^{i\theta_1} - \zeta_1)(e^{-i\theta_1} - \bar{\zeta}_1)} + \alpha U\gamma_2\frac{\zeta_2\bar{\zeta}_2 - 1}{(e^{i\theta_1} - \zeta_2)(e^{-i\theta_1} - \bar{\zeta}_2)} \tag{11}$$

$$-V_{tm} = 2\alpha U\cos\theta_2 - \alpha U\gamma_1\frac{\zeta_1\bar{\zeta}_1 - 1}{(e^{i\theta_2} - \zeta_1)(e^{-i\theta_2} - \bar{\zeta}_1)} +$$

$$\alpha U \gamma_2 \frac{\zeta_2 \bar{\zeta}_2 - 1}{(e^{i\theta_2} - \zeta_2)(e^{i\theta_2} - \bar{\zeta}_2)} \tag{12}$$

Force-Free Condition

$$-i\left(1 + \frac{1}{\zeta_1^2}\right) + \frac{1}{\zeta_1 \alpha} + i\gamma_1 \frac{\bar{\zeta}_1}{\zeta_1 \bar{\zeta}_1 - 1} + i\gamma_2 \left[\frac{\zeta_2 \bar{\zeta}_2 - 1}{(\zeta_1 - \zeta_2)(\zeta_1 \bar{\zeta}_2 - 1)}\right] -$$

$$\frac{a_i \zeta_{1_i} - a_{i-1} \zeta_{1_{i-1}}}{\alpha \Delta \bar{x}} - \frac{a_i \gamma_{1_i} - a_{i-1} \gamma_{1_{i-1}}}{\alpha \gamma_1 \Delta \bar{x}} (\bar{\zeta}_1 - \bar{\zeta}_{S_1}) = 0 \tag{13}$$

$$-i\left(1 + \frac{1}{\zeta_2^2}\right) + \frac{1}{\zeta_2 \alpha} - i\gamma_2 \frac{\bar{\zeta}_2}{\zeta_2 \bar{\zeta}_2 - 1} - i\gamma_1 \left[\frac{\zeta_1 \bar{\zeta}_1 - 1}{(\zeta_2 - \zeta_1)(\zeta_2 \bar{\zeta}_1 - 1)}\right] -$$

$$\frac{a_i \zeta_{2_i} - a_{i-1} \zeta_{2_{i-1}}}{\alpha \Delta \bar{x}} - \frac{a_i \gamma_i - a_{i-1} \gamma_{1_{i-1}}}{\alpha \gamma_1 \Delta \bar{x}} (\bar{\zeta}_2 - \bar{\zeta}_{S_2}) = 0 \tag{14}$$

where γ_1 and γ_2 are evaluated at the current station i and $\Delta \bar{x}$ is a dimensional quantity.

By separating the force-free condition into real and imaginary parts, the system of equations which needs to be solved consists of six nonlinear algebra equations of six unknowns: γ_1, γ_2, y_1, $z_1(\zeta_1 = y_1 + iz_1)$, y_2, and $z_2(\zeta_2 = y_2 + iz_2)$. The system can be rewritten--with y_1, z_1, etc., representing y_{1_i}, z_{1_i}, etc.--as

$$Fl = \gamma_1 \frac{y_1^2 + z_1^2 - 1}{(\cos\theta_1 - y_1)^2 + (\sin\theta_1 - z_1)^2} -$$

$$\gamma_2 \frac{y_2^2 + z_2^2 - 1}{(\cos\theta_1 - y_2)^2 + (\sin\theta_1 - z_2)^2} -$$

$$2\cos\theta_1 + V_{tm}/U\alpha = 0 \tag{15}$$

$$F2 = \gamma_1 \frac{y_1^2 + z_1^2 - 1}{(\cos\theta_2 - y_1)^2 + (\sin\theta_2 - z_1)^2} -$$

$$\gamma_2 \frac{y_2^2 + z_2^2 - 1}{(\cos\theta_2 - y_2)^2 + (\sin\theta_2 - z_2)^2} -$$

$$2\cos\theta_2 - V_{tm}/U\alpha = 0 \tag{16}$$

$$F3 = -2\frac{y_1 z_1}{(y_1^2 + z_1^2)^2} + \frac{1}{\alpha}\frac{a_i - a_{i-1}}{\bar{\Delta x}}\frac{y_1}{y_1^2 + z_1^2} + \gamma_1 \frac{z_1}{y_1^2 + z_1^2 - 1} +$$

$$\frac{\gamma_2(y_2^2 + z_2^2 - 1)[(z_1 - z_2)(y_1 y_2 + z_1 z_2 - 1) + (y_1 - y_2)(-y_1 z_2 + y_2 z_1)]}{[(y_1 - y_2)^2 + (z_1 - z_2)^2][(y_1 y_2 + z_1 z_2 - 1)^2 + (y_2 z_1 - y_1 z_2)^2]} -$$

$$\frac{a_i}{\alpha}\frac{y_{1_i} - y_{1_{i-1}}(a_{i-1}/a_i)}{\bar{\Delta x}} - \frac{a_i\gamma_{1_i} - a_{i-1}\gamma_{1_{i-1}}}{\alpha\bar{\Delta x}\gamma_{1_i}}(y_1 - \cos\theta_1) = 0 \tag{17}$$

$$F4 = -[1 + \frac{y_1^2 - z_1^2}{(y_1^2 - z_1^2)^2}] - \frac{1}{\alpha}\frac{a_i - a_{i-1}}{\bar{\Delta x}}\frac{z_1}{y_1^2 + z_1^2} + \frac{\gamma_1 y_1}{y_1^2 + z_1^2 - 1} +$$

$$\frac{\gamma_2(y_2^2 + z_2^2 - 1)[(y_1 - y_2)(y_1 y_2 + z_1 z_2 - 1) - (z_1 - z_2)(-y_1 z_2 + y_2 z_1)]}{[(y_1 - y_2)^2 + (z_1 - z_2)^2][(y_1 y_2 + z_1 z_2 - 1)^2 + (y_2 z_1 - y_1 z_2)^2]} +$$

$$\frac{a_i}{\alpha}\frac{z_{1_i} - z_{1_{i-1}}(a_{i-1}/a_i)}{\bar{\Delta x}} + \frac{a_i\gamma_{1_i} - a_{i-1}\gamma_{1_{i-1}}}{\alpha\bar{\Delta x}\gamma_{1_i}}(z_1 - \sin\theta_1) = 0 \tag{18}$$

$$F5 = -2\frac{y_2 z_2}{(y_2^2 + z_2^2)^2} + \frac{1}{\alpha}\frac{a_i - a_{i-1}}{\bar{\Delta x}}\frac{y_2}{y_2^2 + z_2^2} - \gamma_2 \frac{z_2}{y_2^2 + z_2^2 - 1} +$$

$$\frac{\gamma_1(y_1^2 + z_1^2 - 1)[(z_1 - z_2)(y_1y_2 + z_1z_2 - 1) + (y_1 - y_2)(-y_1z_2 + y_2z_1)]}{[(y_1 - y_2)^2 + (z_1 - z_2)^2][(y_1y_2 + z_1z_2 - 1)^2 + (y_2z_1 - y_1z_2)^2]} -$$

$$\frac{a_i}{\alpha}\frac{y_{2_i} - y_{2_{i-1}}(a_{i-1}/a_i)}{\bar{\Delta x}} - \frac{a_i\gamma_{1_i} - a_{i-1}\gamma_{1_{i-1}}}{\alpha\bar{\Delta x}\gamma_{1_i}}(y_2 - \cos\theta_2) = 0 \qquad (19)$$

$$F6 = -\left[1 + \frac{y_2^2 - z_2^2}{(y_2^2 + z_z^2)^2}\right] - \frac{1}{\alpha}\frac{a_i - a_{i-1}}{\bar{\Delta x}}\frac{z_2}{y_2^2 + z_2^2} - \gamma_2\frac{y_2}{y_2^2 + z_2^2 - 1} +$$

$$\frac{\gamma_1(y_1^2 + z_1^2 - 1)[(y_1 - y_2)(y_1y_2 + z_1z_2 - 1) - (z_1 - z_2)(-y_1z_2 + y_2z_1)}{[(y_1 - y_2)^2 + (z_1 - z_2)^2][y_1y_2 + z_1z_2 - 1)^2 + (y_2z_1 - y_1z_2)^2]} +$$

$$\frac{a_i}{\alpha}\frac{z_{2_i} - z_{2_{i-1}}(a_{i-1}/a_i)}{\bar{\Delta x}} + \frac{a_i\gamma_{1_i} - a_{i-1}\gamma_{1_{i-1}}}{\alpha\bar{\Delta x}\gamma_{1_i}}(z_2 - \sin\theta_2) = 0 \qquad (20)$$

For a cone, these equations can be simplified to

$$F1 = \gamma_1\frac{y_1^2 + z_1^2 - 1}{(\cos\theta_1 - y_1)^2 + (\sin\theta_1 - z_1)^2} -$$

$$\gamma_2\frac{y_2^2 + z_2^2 - 1}{(\cos\theta_1 - y_2)^2 + (\sin\theta_1 - z_2)^2} - 2\cos\theta_1 + V_{tm}/U\alpha = 0 \qquad (21)$$

$$F2 = \gamma_1\frac{y_1^2 + z_1^2 - 1}{(\cos\theta_2 - y_1)^2 + (\sin\theta_2 - z_1)^2} -$$

$$\gamma_2\frac{y_2^2 + z_2^2 - 1}{(\cos\theta_2 - y_2)^2 + (\sin\theta_2 - z_2)^2} - 2\cos\theta_2 - V_{tm}/U\alpha = 0 \qquad (22)$$

$$F3 = -2\frac{y_1z_1}{(y_1^2 + z_1^2)^2} + \frac{\delta}{\alpha}\frac{y_1}{y_1^2 + z_1^2} + \frac{\gamma_1z_1}{y_1^2 + z_1^2 - 1} +$$

$$\gamma_2 \frac{(y_2^2 + z_2^2 - 1)[(z_1 - z_2)(y_1y_2 + z_1z_2 - 1) + (y_1 - y_2)(-y_1z_2 + y_2z_1)]}{[(y_1 - y_2)^2 + (z_1 - z_2)^2][(y_1y_2 + z_1z_2 - 1)^2 + (y_2z_1 - y_1z_2)^2]} -$$

$$[y_1 + (y_1 - \cos\theta_1)]\delta/\alpha = 0 \qquad (23)$$

$$F4 = -\left[1 + \frac{y_1^2 - z_1^2}{(y_1^2 + z_1^2)^2}\right] - \frac{\delta}{\alpha}\frac{z_1}{y_1^2 + z_1^2} + \frac{\gamma_1 y_1}{y_1^2 + z_1^2 - 1} +$$

$$\gamma_2 \frac{(y_2^2 + z_2^2 - 1)[(y_1 - y_2)(y_1y_2 + z_1z_2 - 1) - (z_1 - z_2)(-y_1z_2 + y_2z_1)]}{[(y_1 - y_2)^2 + (z_1 - z_2)^2][y_1y_2 + z_1z_2 - 1)^2 + (y_2z_1 - y_1z_2)^2]} +$$

$$[z_1 - (\sin\theta_1 - z_1)]\delta/\alpha = 0 \qquad (24)$$

$$F5 = -2\frac{y_2z_2}{(y_2^2 + z_2^2)^2} + \frac{\delta}{\alpha}\frac{y_2}{y_2^2 + z_2^2} - \gamma_2\frac{z_2}{y_2^2 + z_2^2 - 1} +$$

$$\gamma_1 \frac{(y_1^2 + z_1^2 - 1)[(z_1 - z_2)(y_1y_2 + z_1z_2 - 1) + (y_1 - y_2)(-y_1z_2 + y_2z_1)}{[(y_1 - y_2)^2 + (z_1 - z_2)^2][(y_1y_2 + z_1z_2 - 1)^2 + (y_2z_1 - y_1z_2)^2]} -$$

$$[y_2 + (y_2 - \cos\theta_2)]\delta/\alpha = 0 \qquad (25)$$

$$F6 = -\left[1 + \frac{y_2^2 - z_2^2}{(y_2^2 + z_2^2)^2}\right] - \frac{\delta}{\alpha}\frac{z_2}{y_2^2 + z_2^2} - \gamma_2\frac{y_2}{y_2^2 + z_2^2 - 1} +$$

$$\gamma_1 \frac{(y_1^2 + z_1^2 - 1)[(y_1 - y_2)(y_1y_2 + z_1z_2 - 1) - (z_1 - z_2)(-y_1z_2 + y_2z_1)]}{[(y_1 - y_2)^2 + (z_1 - z_2)^2][(y_1y_2 + z_1z_2 - 1)^2 + (y_2z_1 - y_1z_2)^2} +$$

$$[z_2 - (\sin\theta_2 - z_2)]\delta/\alpha = 0 \qquad (26)$$

A detailed derivation of these equations is presented in Appendices A and B. The last terms in Equations (17)-(20) and (23)-(26) are the effect of the force on the vortex cut. These terms are eliminated if the force on the cut is not included in the model.

During the solution process, F1 through F6 may not be zero. As an indicator of convergence, a norm based on F1 through F6 is defined as

$$\text{Norm} = (F1^2 + F2^2 + F3^2 + F4^2 + F5^2 + F6^2)^{1/2} \tag{27}$$

Variables γ_1, γ_2, y_1, z_1, y_2 and z_2 are regarded as a set of solutions when the norm is less than or equal to 10^{-8}.

It is necessary to supplement the Kutta condition as specified in (i) above, with the condition that the flow leaves the surface at the separation line. This is because the condition that the velocity vector lies along a conical ray is satisfied at an attachment line as well as at a separation line. The difference between the two is that the flow leaves the surface at a separation line and approaches it at an attachment line. To confirm the solution, the nature of the flow near the separation line is checked. When the flow is separated, it would leave the surface to downstream side. Therefore the derivative of tangential velocity with respect to the angular position θ, $dV_t/d\theta$, should be less than zero at a correct separation point. If the derivative is greater than zero, the flow is regarded as approaching the body surface rather than leaving it. Therefore, the specified separation line is a reattachment line, not a separation line. The expression of the derivative is shown in Appendix C.

After solutions have been found, the local sectional coefficients of normal force and side force are calculated by integrating the local complex velocity potential in accordance with

the momentum principle of fluid mechanics (see Appendix D). The total force coefficients can be obtained by integrating the sectional coefficients over intervals of longitudinal stations. The results are

$$C_N = \sum_{i=1}^{n} \frac{2\alpha a_i^2}{a_B^2} \{2\gamma_{1_i} y_{1_i} (1 - \frac{1}{y_{1_i}^2 + z_{1_i}^2}) - 2\gamma_{2_i} y_{2_i} (1 - \frac{1}{y_{2_i}^2 + z_{2_i}^2}) -$$

$$2\gamma_{1_{i-1}} y_{1_{i-1}} \frac{a_{i-1}^2}{a_i^2} (1 - \frac{1}{y_{1_{i-1}}^2 + z_{1_{i-1}}^2}) +$$

$$2\gamma_{2_{i-1}} y_{2_{i-1}} \frac{a_{i-1}^2}{a_i^2} (1 - \frac{1}{y_{2_{i-1}}^2 + z_{2_{i-1}}^2}) + 1 - \frac{a_{i-1}^2}{a_i^2}\} \tag{28}$$

$$C_y = \sum_{i=1}^{n} \frac{2\alpha a_i^2}{a_B^2} \{-2\gamma_{1_i} z_{1_i} (1 - \frac{1}{y_{1_i}^2 + z_{1_i}^2}) + 2\gamma_{2_i} z_{2_i} (1 - \frac{1}{y_{2_i}^2 + z_{2_i}^2}) +$$

$$2\gamma_{1_{i-1}} z_{1_{i-1}} \frac{a_{i-1}^2}{a_i^2} (1 - \frac{1}{y_{1_{i-1}}^2 + z_{1_{i-1}}^2}) -$$

$$2\gamma_{2_{i-1}} z_{2_{i-1}} \frac{a_{i-1}^2}{a_i^2} (1 - \frac{1}{y_{2_{i-1}}^2 + z_{2_{i-1}}^2})\} \tag{29}$$

$$C_L = C_N \cos\alpha \tag{30}$$

where a_B is the radius of the base area. For a cone, the equations for force coefficients can be simplified to

$$C_N = 2\alpha\{2\gamma_1 y_1 (1 - \frac{1}{y_1^2 + z_1^2}) - 2\gamma_2 y_2 (1 - \frac{1}{y_2^2 + z_2^2}) + 1\} \tag{31}$$

$$C_y = 2\alpha\{-2\gamma_1 z_1(1 - \frac{1}{y_2^2 + z_1^2}) + 2\gamma_2 z_2(1 - \frac{1}{y_2^2 + z_2^2})\} \quad (32)$$

$$C_L = C_N \cos\alpha \quad (33)$$

A numerical scheme based on Broyden's concept (Reference 11) is used to solve the system of nonlinear algebraic equations. The advantages of this scheme are i) unlike in Newton's method, the gradient matrix is calculated by an approximate but inexpensive method; for a complicated system of equations, the computing time is significantly reduced; and ii) using an optimizer described by Broyden, even poor initial guess does not seem to affect the final convergence of the method because the optimizer tends to pull the values close to the solution. Therefore, the calculation can be restarted from where the program stops without convergence.

In finding the asymmetric solution, a function deflation technique is used. The concept of function deflation is described as follows (see Reference 12 for details). Let F(X) be the nonlinear system of equations to be solved, F representing F1, F2, F3, F4, F5, and F6 in the present case and X representing variables γ_1, γ_2, y_1, z_1, y_2, and z_2. Assuming R representing γ_{R_1}, γ_{R_2}, y_{R_1}, z_{R_1}, y_{R_2}, and z_{R_2} is one root of F(X), i.e. F(R) = 0. Dividing the original equation F(X) by $||X - R||$, the effect of root R is eliminated so that additional roots can be found. Note that $||X - R||$ represents the norm of X - R. It is defined as

$$||X - R|| = [\gamma_1 - \gamma_{R_1})^2 + (\gamma_2 - \gamma_{R_2})^2 + (y_1 - y_{R_1})^2 +$$

$$(z_1 - z_{R_1})^2 + (y_2 - y_{R_2})^2 + (z_2 - z_{R_2})^2]^{1/2} \tag{34}$$

Mathematically when X approaches the first root R_1, $F(X)/||X - R_1||$ becomes the derivative of $F(R_1)$ which does not vanish unless R_1 happens to be a multiple root. The mathematical expression is as follows:

$$G(X) = \frac{F(X)}{||X - R_1||} \tag{35}$$

$$\lim_{X \to R_1} G(X) = \lim_{X \to R_1} \frac{F(X)}{||X - R_1||} = F'(R_1) \tag{36}$$

Experience shows that using the aforementioned concept of function deflation, convergence to previously obtained roots can always be avoided.

RESULTS AND DISCUSSIONS

To investigate the flow on a cone, the separation line must first be specified. Since one of the main purposes in the present study is to show that the asymmetric vortex separation is part of the multiple solutions in the boundary value problem, the symmetric separation lines will be based on an empirical equation (Reference 13) for predicting separation angle in a laminar flow, as

$$\theta = [73 - (51.4\alpha - 450)^{1/2}][0.76 + 0.024\delta] \tag{37}$$

Equation (37) has been shown to work very well in the range of

$$10° \leq \alpha \leq 30°$$

for semi cone angles of

$$5° \leq \delta \leq 20°$$

For tangent ogives, the following equations given in Reference 14 are used to predict the separation position. That is

$$\theta = (13.12 + \delta)(3.13 - \sqrt{0.116\alpha - 1.16}) \quad \text{for} \begin{cases} 10° \leq \alpha \leq 40° \\ 0° \leq \delta \leq 15° \end{cases} \tag{38}$$

$$\theta = 3.13\ (13.12 + \delta) \quad \text{for} \begin{cases} 0° \leq \alpha \leq 10° \\ 0° \leq \delta \leq 15° \end{cases} \tag{39}$$

As explained by Schindel (Reference 13), the equation of predicted separation condition is taken from Crabbe's theory which agrees with experimental data only in some ranges of angle of attack and cone angles.

In addition, to study the separated flow on tangent ogives, an additional information is needed; that is, the axial stations downstream of which symmetric and asymmetric vortex separation will occur. Numerical experience indicated that at a small α, such as three degrees, the flow field can be assumed to be attached and the normal force coefficient can be calculated with the slender body theory (i.e. $C_N = 2\alpha$). At a slightly higher α, such as four degrees, a search is then made to find a station (called $\bar{x}_1$) at which symmetric vortex flow can be calculated: i.e., the boundary value problem has a solution. For this purpose, let

$$A_{local} = \alpha/\delta_{local} \tag{40}$$

where δ_{local} is the angle of the local surface slope. The value of A_{local} at $\bar{x}_1$, A^S_{local}, will be the one used at all angles of attack

to determine where symmetric vortex flow will begin. That is, at any station where $A_{local} \geq A^{S}_{local}$, symmetric vortex flow is assumed to exist. For a cone, A^{S}_{local} was determined to be approximately 1.2. Over the portion of the body with attached flow, the classical slender body theory is used to calculate the normal force coefficient.

For asymmetric vortex flow on a tangent ogive, note that experimental data indicated that asymmetric flow would not start until an $\alpha_{av} \simeq 2\theta_A$ (Reference 15), where θ_A is the cone half angle, or, for tangent ogives,

$$\theta_A = \tan^{-1}\left[\frac{\ell_N/d}{(\ell_N/d)^2 - 0.25}\right] \tag{41}$$

At $\alpha = \alpha_{av}$, a search is made to find the first station after which the total side force coefficient (C_y) is nearly zero (a value of 0.06 is assumed). The value of A_{local} at that station, defined as A^{a}_{local}, is then used to determine where the asymmetric vortex flow will begin at all $\alpha \geq \alpha_{av}$. For $\alpha < \alpha_{av}$, only symmetric vortex flow is assumed to exist.

Cones

Symmetric flow is investigated first, using the six models mentioned earlier. Results for symmetric flow are compared with experimental data in Figures 2 to 7. The experimental data of C_L are taken from Reference 16. In Figure 2 and Figure 3, all flow models are with a force on the vortex cut in the force-free

condition. In figure 2, the vortex core positions of a five-degree cone are presented. It is seen that flow model 4 gives good prediction of lateral core positions, but all flow models seem to underpredict the vertical positions. Vortex core positions of a ten-degree cone are shown in Figure 3. It is found that all models overpredict the lateral positions and underpredict the vertical positions. This may be explained by a large force on the vortex cut. In addition, when the angle of attack is less than 20 degrees, the theory does not predict the presence of vortices but experimental data show otherwise. In Figure 4, results without the force on the vortex cut for a five-degree cone are presented. Flow models 3 and 4 are found to have accurate prediction in both lateral and vertical positions. Results for a ten-degree cone for all models without the force on the vortex cut in the force-free condition are shown in Figure 5. The prediction of vortex core positions is more accurate than models with a force on the vortex cut in the force-free condition. In all these figures, it is seen that the effect of imposing a tangential velocity at separation points is to make core positions more inboard and lower as V_{tm} is increased.

The lift coefficients calculated by all flow models with/without a force on the vortex cut in the force-free condition are plotted in Figures 6 and 7. Both figures show that C_L is reduced by increasing V_{tm}. The force on the vortex cut seems to reduce C_L in the stagnation separation model and model 1. However, its effect is small in other flow models. Overall, it is found that

model 3 without the force on the vortex cut is the best flow model which produces results having good agreement with experimental data. Therefore, this model will be used to investigate the asymmetric vortex separation on cones and the vortex flow on tangent ogives.

After determining a symmetric solution, a function deflation technique is used to search for additional solutions. It is found that one asymmetric solution at a given α can always be found except at low α's. Pairs of symmetric and asymmetric vortex core positions on an eight-degree cone for different incidence parameters A based on flow model 3 without a force on the vortex cut in the force-free condition are shown in Figure 8. The predicted coefficients of lift and side force are compared with experimental data (Reference 16) in Figure 9. The prediction of side-force coefficient appears to be accurate, but the lift coefficient is overpredicted. This may be explained by the inaccuracy of the slender-body theory. It is well known that the slender-body theory will overpredict the lift if the fineness ratio is not large enough. Therefore, the concept of effective angle of attack as shown for delta wings (Reference 17) is used to improve the result. When the lift coefficient predicted by the slender-body theory is taken to be $2\alpha\cos\alpha$, which is equated to the lift coefficient given by a three-dimensional linear theory for a body in attached flow, an effective angle of attack, α_e, can be found. The results predicted by using effective angles of attack are shown in Figure 10. The lift coefficient agrees well with

experimental data, and the predicted side force appears to be slightly lower at high α. The effective angles of attack at different geometric α for different bodies are listed in Table 1.

When the stagnation separation model is used to predict the asymmetric separation, the left vortex (with higher vertical position) has larger circulation than the right one (with lower vertical position). As the tangential velocity, V_{tm}, on the separation line is increased, the left vortex will have smaller strength than the right one. Therefore, the effect of imposing the tangential velocity at the separation points in asymmetric case may be regarded as changing the larger vortex strength from one side to the other. The vortex strength ratio predicted by the stagnation separation model and model 3 are shown in Figure 11. The switch of vortex strength can be readily seen in the figure.

In Moore's paper (Reference 4), a branch of solution was regarded as physically meaningless and was called a lower-branch solution. Because the vortex core position is lower than the separation line, and the derivative of tangential velocity with respect to the angular position at the separation line is greater than zero, the specified separation line is actually an attachment line, not a separation line. Lower-branch solutions are also found in asymmetric cases. The pairs of lower-branch symmetric and asymmetric vortex core positions are plotted in Figure 12, and their strengths are compared with the physically meaningful (upper-branch) solutions in Figure 13. The numerical results for the upper and

lower branches for an eight-degree cone are listed in Table 2 and Table 3.

Tangent Ogives

The procedures for calculating vortex flow on tangent ogives are described as follows. The symmetric solution at a station at which A_{local} is reached is first determined. This step may require several trials to find that particular station. Symmetric solutions at stations downstream of this particular station are then calculated. These procedures are repeated for all angles of attack.

To calculate the asymmetric solution, a search is started to find the station at which A_{local} equals A^a_{local}. Then the converged symmetric solution at that station is disturbed to get an initial guess of the asymmetric solution. In the present method, the magnitudes of y_1 and γ_1 are reduced to make the initial guess asymmetric. Through the functional deflation procedure, the asymmetric solution can be found. The same idea is applied to all downstream stations.

The converged symmetric solution at a station at which A_{local} equals A^a_{local} is used as the initial guess for the next angle of attack. Then all procedures are repeated until all desired angles of attack are processed. When $\alpha < \alpha_{av}$, only symmetric solution is assumed to exist.

Two tangent ogives with fineness ratios of 5.0 and 3.5 are used for correlation. The effect of the number of integration station in

the axial direction on the predicted normal force coefficient for a tangent ogive of fineness ratio of 5.0 is presented in Figure 14. As the number of integration stations is increased, the location where the vortex separation first occurs can be more accurately predicted. It is seen from Figure 14 that for the normal force coefficient, the effect of the number of integration stations is small. In addition, the normal force coefficient remains nearly the same under the condition of symmetric or asymmetric separation until $\alpha > 30$ degrees. At these higher α's, the normal force coefficient is higher in asymmetric cases. The side force coefficient is shown in Figure 15. It is seen that the value of C_y is more sensitive to an accurate prediction of where vortex separation first occurs in the axial direction. The magnitude of C_y appears to be well predicted when the number of integration stations is adequate. At $\alpha = 30$ degrees, the C_y value starts to increase rapidly. However, its magnitude is still low and the vortex positions are therefore quite close to those in the symmetric case, as shown in Figure 16. In Figures 17 and 18 the overpredicted normal force coefficient and side force coefficient are improved by the concept of effective angle of attack.

For a tangent ogive of fineness ratio of 3.5, the lift coefficient is presented in Figure 19, and the side force coefficients in Figure 20. It is seen that the lift coefficient is overpredicted. This can again be improved by the concept of effective angle of attack, as shown in Figure 21 where the lift

coefficient is shown to agree well with experimental data. However, the predicted side-force coefficients based on effective angles of attack (Figure 22) are small and lower than the experimental data. Values of effective angles of attack at different geometric α's are listed in Table 1. Calculated vortex positions agree well with data in Reference 20, as shown in Figure 23.

Sensitivity of side force coefficients due to asymmetry of separation points is illustrated in Figures 24 and 25. In the calculation, the left separation point is kept fixed at the value used in the symmetric case, and the right separation point is shifted up ($+\Delta\theta$) and down ($-\Delta\theta$) from the symmetric case to obtain the asymmetry of separation points. The side force coefficients for a cone, being nearly zero, are seen to be insensitive to $\Delta\theta$ as shown in Figure 24. Since the separation point on the left side is kept fixed, the vortex strength is nearly the same as in the symmetric case. On the right side, the vortex strength is reduced with the separation point shifted up with the resulting vortex being more outboard. On the other hand, the side force coefficients for a tangent ogive with fineness ratio 5.0 are shown in Figure 25 to grow with $\Delta\theta$. To produce an experimental side force coefficient of 2.25, the right separation point must be shifted up by about 12 degrees.

CONCLUSIONS

Based on modified Bryson's vortex models, symmetric and asymmetric vortex separation on cones and tangent ogives were investigated. The modifications pertain to a tangential velocity imposed at the separation points and a force on the vortex cut in the force-free condition. It was concluded that

1) Adding the force on the vortex cut in the force-free condition would push the vortex core more outboard and lower, thus making an inaccurate prediction as compared with available data.
2) Increasing the imposed tangential velocity at the separation points would make the calculated vortex core more inboard and lower. The strength of the vortex with a higher vertical position (i.e. the left one) would decrease, and that of the one on the right with lower vertical position would increase in asymmetric cases.
3) Through a numerical scheme based on the concept of function deflation, multiple solutions to the problem of vortex separation on cones and tangent ogives were shown to exist. The asymmetric solutions were shown to exhibit characteristics which were observed in experiments with asymmetric vortex separation.
4) The predicted side-force coefficients for cones and tangent ogives agreed reasonably well with available data.
5) Asymmetric separation points could produce vortex solutions which generated large enough side forces as measured in experiments for tangent ogives, but not for cones.

REFERENCES

1. Bryson, A. E.: Symmetrical Vortex Separation on Circular Cylinders and Cones. Journal of Applied Mechanics, Vol. 26,1959, pp. 643-648.

2. Schindel, L. H.: Effects of Vortex Separation on the Lift Distribution on Bodies of Elliptic Cross Section. Journal of Aircraft, Vol. 6, 1969, pp. 537-543.

3. Dyer, D. E.; Fiddes, S. P.; and Smith, J. H. B.: Asymmetric Vortex Formation from Cones at Incidence--A Simple Inviscid Model. Aeronautical Quarterly, Nov. 1982, pp. 293-312.

4. Moore, K.: Line-vortex Models of Separated Flow past a Circular Cone at Incidence. RAE Technical Memorandum Aero. 1917, 1981.

5. Smith, J. H. B.: Inviscid Fluid Models, Based on Rolled-up Vortex Sheets, for Three-dimensional Separation at High Reynolds Number. Paper No. 9, AGARD-LS-94, 1978.

6. Mendenhall, M. R.; and Perkins, S. C., Jr.: Vortex Cloud Model for Body Vortex Shedding and Tracking. AIAA Progress in Astronautics and Aeronautics, Vol. 104 (Tactical Missile Aerodynamics), 1986.

7. Graham, J. E.; and Hankey, W. L.: Computation of the Asymmetric Vortex Pattern for Bodies of Revolution. AIAA Journal, Vol. 21, Nov. 1983, pp. 1500-1504.

8. Patel, M. H.: The Delta Wing in Oscillatory Gusts. AIAA Journal, Vol. 18, May 1980, pp. 481-486.

9. Smith, J. H. B.: Improved Calculations of Leading-edge Separation from Slender, Thin, Delta Wings. Proceedings of Royal Society (London), Vol. A306, 1968, pp. 67-90.

10. Ward, G. N.: Supersonic Flow Past Slender Pointed Bodies. Quarterly Journal of Mechanics and Applied Mathematics, Vol. II, Pt. 1, 1949, pp. 75-97.

11. Broyden, C. G.: A Class of Methods for Solving Nonlinear Simultaneous Equations. Math. of Computation, Vol. 19, 1965, pp. 577-593.

12. Brown, K. M.: Computer Oriented Algorithms for Solving Systems of Simultaneous Nonlinear Algebraic Equations. In Numerical Solution of Systems of Nonlinear Algebraic Equations, edited by G. D. Byrne and C. A. Hall, Academic Press, 1973.

13. Friberg, E. G.: Measurement of Vortex Separation, Part II: Three-dimensional Circular and Elliptic Bodies. MIT Aero. Lab. Technical Report 115, 1965.

14. Schindel, L. H.; and Chamberlain, J. E.: Vortex Separation on Slender Bodies of Elliptic Cross Section. MIT Aero. Lab. Technical Report 138, 1967.

15. Ericsson, L. E.; and Reding, J. P.: Asymmetric Vortex Shedding from Bodies of Revolution. AIAA Progress in Astronautics and Aeronautics, Vol. 104 (Tactical Missile Aerodynamics), 1986.

16. Coe, P. L., Jr.; Chambers, J. R.; and Letko, W.: Asymmetric Lateral-directional Characteristics of Pointed Bodies of Revolution at High Angles of Attack. NASA TN D-7095, 1973.

17. Lan, C. E.: Calculation of Asymmetric Vortex Separation on Slender Delta Wings with a Vortex-Sheet Model. AIAA Paper 86-1836, June 1986.

18. Keener, E. R.; Chapman, G. T.; Cohen, L.; and Taleghani, J.: Side Forces on Forebodies at High Angles of Attack and Mach Numbers from 0.1 to 0.7: Two Tangent Ogives, Paraboloid and Cone. NASA TM X-3438, Feb. 1977.

19. Keener, E. R.; and Taleghani, J.: Wind Tunnel Investigation of the Aerodynamic Characteristics of Five Models at High Angles of Attack at Mach numbers from 0.25 to 2. NASA TM X-73,076, 1975.

20. Ward, K. C.; and Katz, J.: Boundary Layer Separation and the Vortex Structures around an Inclined Body of Revolution. AIAA Paper 87-2276, AIAA 5th Applied Aerodynamics Conference, Monterey, CA, August 1987.

APPENDIX A

FORMULATION OF KUTTA CONDITION

The complex velocity potential at a constant $\bar{x}$ section with slope change $da/d\bar{x}$ can be written as

$$W = -iU\alpha\left(Z - \frac{a^2}{Z}\right) + Ua\frac{da}{d\bar{x}}\ell_n Z + \frac{\Gamma_1}{2\pi i}\ell_n\frac{Z - Z_1}{Z - a^2/Z_1} - \frac{\Gamma_2}{2\pi i}\frac{Z - Z_2}{Z - a^2/\bar{Z}_2} \tag{A1}$$

For a constant slope change in every section (such as a cone), $da/d\bar{x}$ can be replaced by δ. Then

$$\frac{dW}{dZ} = -iU\alpha\left(1 + \frac{a^2}{Z^2}\right) + U\alpha\frac{da}{d\bar{x}}\frac{1}{Z} + \frac{\Gamma_1}{2\pi i}\left[\frac{1}{Z - Z_1} - \frac{1}{Z - a^2/\bar{Z}_1}\right] - \frac{\Gamma_2}{2\pi i}\left[\frac{1}{Z - Z_2} - \frac{1}{Z - a^2/\bar{Z}_2}\right] \tag{A2}$$

Using nondimensionalized variables (ζ and γ) such that $z = a\zeta$ and $\Gamma = 2\pi a\alpha U\gamma$, then

$$\frac{dW}{dZ} = -iU\alpha\left(1 + \frac{1}{\zeta^2}\right) + U\frac{da}{d\bar{x}}\frac{1}{\zeta} + \frac{2\pi aU\gamma_1\alpha}{2\pi i}\left[\frac{1}{Z - Z_1} - \frac{1}{Z - a^2/Z_1}\right] - \frac{2\pi a\alpha U\gamma_2}{2\pi i}\left[\frac{1}{Z - Z_2} - \frac{1}{Z - a^2/\bar{Z}_2}\right] =$$

$$-iU\alpha\left(1 + \frac{1}{\zeta^2}\right) + U\frac{da}{d\bar{x}}\frac{1}{\zeta} - iU\gamma_1\alpha\left[\frac{1}{\zeta - \zeta_1} - \frac{\bar{\zeta}_1}{\zeta\bar{\zeta}_1 - 1}\right] + iU\gamma_2\alpha\left[\frac{1}{\zeta - \zeta_2} - \frac{\bar{\zeta}_2}{\zeta\bar{\zeta}_2 - 1}\right] \tag{A3}$$

$$\frac{1}{U\alpha}\frac{dW}{dZ} = -i\left(1 + \frac{1}{\zeta^2}\right) + \frac{da}{d\bar{x}}\frac{1}{\zeta\alpha} - i\gamma_1\left[\frac{1}{\zeta - \zeta_1} - \frac{\bar{\zeta}_1}{\zeta\bar{\zeta}_1 - 1}\right] +$$

$$i\gamma_2\left[\frac{1}{\zeta - \zeta_2} - \frac{\bar{\zeta}_2}{\zeta\bar{\zeta}_2 - 1}\right] \qquad \text{(A4)}$$

The right-side separation velocity is derived as follows:

$$V_{tm} = \mathrm{Im}\left\{-\frac{Z}{a}\frac{dW}{dZ}\right\}_{Z=ae^{i\theta_1}}$$

where V_{tm} is the mean tangential velocity and Im is the imaginary part of a complex number. Then

$$V_{tm} = \mathrm{Im}\left\{-e^{i\theta_1}\frac{dW}{dZ}\right\}_{Z=ae^{i\theta_1}}$$

$$= \mathrm{Im}\left\{-e^{i\theta_1}U\alpha\left(\frac{1}{U\alpha}\frac{dW}{dZ}\right)\right\}_{Z=ae^{i\theta_i}}$$

$$= \mathrm{Im}\left[-e^{i\theta_1}U\alpha\left\{-i\left(1 + \frac{1}{\zeta^2}\right) + \frac{da}{d\bar{x}}\frac{1}{\zeta\alpha} - i\gamma_1\left[\frac{1}{\zeta - \zeta_1} - \frac{\bar{\zeta}_1}{\zeta\bar{\zeta}_1 - 1}\right] +\right.\right.$$

$$\left.\left. i\gamma_2\left[\frac{1}{\zeta - \zeta_2} - \frac{\bar{\zeta}_2}{\zeta\bar{\zeta}_2 - 1}\right]\right\}\right]_{\zeta=e^{i\theta_1}}$$

$$= \mathrm{Im}\left[ie^{i\theta_1}\left(1 + \frac{1}{e^{2i\theta}}\right) - e^{i\theta_1}\frac{da}{d\bar{x}}\frac{1}{e^{i\theta}\alpha} +\right.$$

$$\left. ie^{i\theta_1}\gamma_1\left[\frac{1}{e^{i\theta} - \zeta_1} - \frac{\bar{\zeta}_1}{e^{i\theta}\bar{\zeta}_1 - 1}\right] - ie^{i\theta_1}\gamma_2\left[\frac{1}{e^{i\theta} - \zeta_2} - \frac{\bar{\zeta}_2}{e^{i\theta}\bar{\zeta}_2 - 1}\right]\right]_{\theta=\theta_1} \cdot U\alpha$$

$$= \mathrm{Im}\left\{i\left(e^{i\theta_1} + e^{-i\theta_1}\right) - \frac{1}{\alpha}\frac{da}{d\bar{x}} + i\gamma_1 e^{i\theta_1}\frac{\zeta_1\bar{\zeta}_1 - 1}{\left(e^{i\theta_1} - \zeta_1\right)\left(e^{i\theta_1}\bar{\zeta}_1 - 1\right)} -\right.$$

$$i\gamma_2 e^{i\theta_1} \frac{\zeta_2 \bar{\zeta}_2 - 1}{(e^{i\theta_1} - \zeta_2)(e^{i\theta_1}\bar{\zeta}_2 - 1)}\}U\alpha$$

$$= \mathrm{Im}\{i2\cos\theta_1 - \frac{1}{\alpha}\frac{da}{d\bar{x}} + i\gamma_1 \frac{\zeta_1\bar{\zeta}_1 - 1}{(e^{i\theta_1} - \zeta_1)(\bar{\zeta}_1 - e^{-i\theta_1})} -$$

$$i\gamma_2 \frac{\zeta_2\bar{\zeta}_2 - 1}{(e^{i\theta_1} - \zeta_2)(\bar{\zeta}_2 - e^{-i\theta_1})}\}U\alpha$$

$$= \{2\cos\theta_1 - \gamma_1 \frac{\zeta_1\bar{\zeta}_1 - 1}{(e^{i\theta_1} - \zeta_1)(e^{-i\theta_1} - \bar{\zeta}_1)} +$$

$$\gamma_2 \frac{\zeta_2\bar{\zeta}_2 - 1}{(e^{i\theta_1} - \zeta_2)(e^{-i\theta_1} - \bar{\zeta}_2)}\}U\alpha \qquad \text{(A5)}$$

Let $\zeta_1 = y_1 + iz_1$, $\zeta_2 = y_2 + iz_2$. Then,

$$V_{tm} = \{2\cos\theta_1 - \gamma_1 \cdot$$

$$\frac{(y_1 + iz_1)(y_1 - iz_1) - 1}{[(\cos\theta_1 + i\sin\theta_1) - (y_1 + iz_1)][(\cos\theta_1 - i\sin\theta_1) - (y_1 - iz_1)]} +$$

$$\gamma_2 \frac{(y_2 + iz_2)(y_2 - iz_2) - 1}{[(\cos\theta_1 + i\sin\theta_1) - (y_2 + iz_2)][(\cos\theta_1 - i\sin\theta_1) - (y_2 - iz_2)]}\}U\alpha$$

$$= \{2\cos\theta_1 - \gamma_1 \frac{y_1^2 + z_1^2 - 1}{[(\cos\theta_1 - y) + i(\sin\theta_1 - z_1)][(\cos\theta_1 - y_1) - i(\sin\theta_1 - z_1)]} +$$

$$\gamma_2 \frac{y_2^2 + z_2^2 - 1}{[(\cos\theta_1 - y_2) + i(\sin\theta_1 - z_2)][(\cos\theta_1 - y_2) - i(\sin\theta_1 - z_2)]}\}U\alpha$$

$$= \{2\cos\theta_1 - \gamma_1 \frac{y_1^2 + z_1^2 - 1}{(\cos\theta_1 - y_1)^2 + (\sin\theta_1 - z_1)^2} +$$

$$\gamma_2 \frac{y_2^2 + z_2^2 - 1}{(\cos\theta_1 - y_2)^2 + (\sin\theta_1 - z_2)^2}\}U\alpha \qquad \text{(A6)}$$

Define

$$XK1 \equiv \frac{y_1^2 + z_1^2 - 1}{(\cos\theta_1 - y_1)^2 + (\sin\theta_1 - z_1)^2} \qquad \text{(A7)}$$

and

$$XK2 \equiv -\frac{y_2^2 + z_2^2 - 1}{(\cos\theta_1 - y_2)^2 + (\sin\theta_1 - z_2)^2} \qquad \text{(A8)}$$

Then the separation velocity on the right side becomes

$$V_{tm} = U\alpha(2\cos\theta_1 - \gamma_1 * XK1 - y_2 * XK2)$$

or

$$U\alpha(XK1 * \gamma_1 + XK2 * \gamma_2 - 2\cos\theta_1) + V_{tm} = 0 \qquad \text{(A9)}$$

For the separation velocity on the left side,

$$V_{tm} = \mathrm{Im}\{e^{i\theta_2} \frac{dW}{dZ}\}_{Z=ae^{i\theta_2}}$$

Therefore,

$$-V_{tm} = \{2\cos\theta_2 - \gamma_1 \frac{y_1^2 + z_1^2 - 1}{(\cos\theta_2 - y)^2 + (\sin\theta_1 - z_1)^2} +$$

$$\gamma_2 \frac{y_2^2 + z_2^2 - 1}{(\cos\theta_2 - y_2)^2 + (\sin\theta_2 - z_2)^2}\}U\alpha \qquad \text{(A10)}$$

Define

$$XK3 \equiv \frac{y_1^2 + z_1^2 - 1}{(\cos\theta_2 - y_1)^2 + (\sin\theta_2 - z_1)^2} \tag{A11}$$

and

$$XK4 \equiv -\frac{y_2^2 + z_2^2 - 1}{(\cos\theta_2 - y_2)^2 + (\sin\theta_2 - z_2)^2} \tag{A12}$$

The separation velocity on the left side becomes

$$-V_{tm} = U\alpha(2\cos\theta_2 - \gamma_1 * XK3 - \gamma_2 * XK4)$$

or

$$U\alpha(-2\cos\theta_2 + \gamma_1 * XK3 + \gamma_2 * XK4) - V_{tm} = 0 \tag{A13}$$

Define

$$F1 \equiv XK1 * \gamma_1 + XK2 * \gamma_2 - 2\cos\theta_1 + V_{tm}/\alpha U \tag{A14}$$

$$F2 \equiv XK3 * \gamma_1 + XK4 * \gamma_2 - 2\cos\theta_2 - V_{tm}/\alpha U \tag{A15}$$

In Bryson's model, the separation line is required to be a stream line of the three dimensional flow, so that V_{tm}, the mean tangential cross-flow velocity component at the separation line, is zero. However, by considering the behavior of a vortex sheet model at the separation line, Smith (Reference 9) derived an expression for V_{tm}, which can be applied whether the sheet is present or not. For a body of revolution, such as a circular cone, with the separation line along a meridian, Smith's expression becomes

$$V_{tm} = \left[\frac{U}{2}\frac{d\Gamma}{dx}\right]^{1/2} \tag{A16}$$

By the assumption of conical flow, V_{tm} becomes

$$V_{tm} = \left[\frac{U}{2}\frac{\Gamma}{\bar{x}}\right]^{1/2} = U\left[\frac{\Gamma a\pi}{2U\bar{x}a\pi}\right]^{1/2} = U\left[\frac{\Gamma a\pi\alpha\delta}{2Ua\pi\alpha}\right]^{1/2} = U\alpha\sqrt{\pi\gamma\delta/\alpha} \qquad (A17)$$

For nonconical flow, it is assumed that $\partial\Gamma/\partial\bar{x} = \Delta\Gamma/\Delta\bar{x}$. Then

$$V_{tm} = \left[\frac{U\Delta\Gamma}{2\Delta\bar{x}}\right]^{1/2} = U\left[\frac{(\Gamma_i - \Gamma_{i-1})a_i\pi}{2U\Delta\bar{x}a_i\pi}\right]^{1/2} = U\left[\frac{(\Gamma_i - \Gamma_{i-1})a_i\pi\alpha}{2U\Delta\bar{x}a_i\pi\alpha}\right]^{1/2}$$

$$= U\alpha\left[(a_i\gamma_i - a_{i-1}\gamma_{i-1}) \cdot \pi/\Delta\bar{x}\alpha\right]^{1/2} \qquad (A18)$$

However, considering the vorticity flux across the boundary layer at separation, as in the vortex cloud method (Reference 6), the relationship between the vortex strength and the velocity at the boundary layer edge, U_e, may be written as

$$\frac{\partial\Gamma}{\partial t} = \int_{r_o}^{r_e} \frac{\partial U}{\partial r}\, U dr = \frac{U_e^2}{2} \qquad (A19)$$

where the nonslip condition is satisfied at r_o. In the vortex cloud model, an empirical factor, K is often used to reduce the strength of the shedding vorticity. Various investigators recommended a value in the range of $0.6 \leq K \leq 1.0$, with 0.6 being a typical value in subsonic flow. It follows that

$$\frac{\partial\Gamma}{\partial t} = U\frac{\partial\Gamma}{\partial\bar{x}} = K\frac{U_e^2}{2} \qquad (A20)$$

If V_{tm} is equated to one half of the shedding velocity, then for a cone

$$V_{tm} = \frac{U_e}{2} = \sqrt{\frac{U}{2K}\frac{\partial\Gamma}{\partial\bar{x}}} = \frac{1}{\sqrt{K}}\sqrt{\frac{U}{2}\frac{\partial\Gamma}{\partial\bar{x}}} = \frac{U\alpha}{\sqrt{K}}\sqrt{\pi\gamma\delta/\alpha} \qquad (A21)$$

For tangent ogives with $\partial\Gamma/\partial\bar{x} = \Delta\Gamma/\Delta\bar{x}$,

$$V_{tm} = \frac{U_e}{2} = \sqrt{\frac{U}{2K}\frac{\partial\Gamma}{\partial\bar{x}}} = \frac{1}{\sqrt{K}}\sqrt{\frac{U}{2}\frac{\partial\Gamma}{\partial\bar{x}}} = \frac{U\alpha}{\sqrt{K}}\sqrt{(a_i\gamma_i - a_{i-1}\gamma_{i-1}) \cdot \pi/\Delta\bar{x}\alpha} \quad \text{(A22)}$$

On the other hand, experimental data (Reference 8) showed that a vortex in a shear layer tends to be convected with a speed less than the free stream, so that

$$V_{tm} = fU_e \quad \text{(A23)}$$

where f = 0.61. If this separation condition is used, then V_{tm} for a cone becomes

$$V_{tm} = \frac{2f}{\sqrt{K}}\sqrt{\frac{U}{2}\frac{\partial\Gamma}{\partial\bar{x}}} = \frac{2fU\alpha}{\sqrt{K}}\sqrt{\pi\gamma\delta/\alpha} \quad \text{(A24)}$$

For a tangent ogive, V_{tm} is

$$V_{tm} = \frac{2f}{\sqrt{K}}\sqrt{\frac{U}{2}\frac{\partial\Gamma}{\partial\bar{x}}} = \frac{2fU\alpha}{\sqrt{K}}\sqrt{(a_i\gamma_i - a_{i-1}\gamma_{i-1})\pi/\Delta\bar{x}\alpha} \quad \text{(A25)}$$

Six models are tested for a cone based on these different separation conditions. They are

(1) Stagnation separation model ($V_{tm} = 0$)

(2) Model 1, Smith's separation condition ($V_{tm} = U\sqrt{\pi\gamma\delta/\alpha}$)

(3) Model 2, f = 0.61, and K = 1.0 ($V_{tm} = 1.220\ U\alpha\sqrt{\pi\gamma\delta/\alpha}$)

(4) Model 3, f = 0.61, and K = 0.6 ($V_{tm} = 1.575\ U\alpha\sqrt{\pi\gamma\delta/\alpha}$)

(5) Model 4, f = 1.00, and K = 1.0 ($V_{tm} = 2.000\ U\alpha\sqrt{\pi\gamma\delta/\alpha}$)

(6) Model 5, f = 1.00, and K = 0.6 ($V_{tm} = 2.585\ U\alpha\sqrt{\pi\gamma\delta/\alpha}$)

After testing, a best model with the best f and K values, f_b and K_b, is chosen to investigate asymmetric vortex separation on cones and vortex flow on tangent ogives. Based on f_b and K_b values, V_{tm} for tangent ogives becomes

$$V_{tm} = \frac{2f_bU\alpha}{\sqrt{K_b}}\sqrt{(a_i\gamma_i - a_{i-1}\gamma_{i-1})\pi/\Delta\bar{x}\alpha} \quad \text{(A26)}$$

APPENDIX B

FORMULATION OF FORCE-FREE CONDITION

There are two parts of contribution to the total force:

(i) Due to the inclination of vortex line

$$F_v = -i\rho\Gamma_v\Big[\lim_{Z\to Z_v}\Big(\frac{dW}{dZ} - \frac{\Gamma_v}{2\pi i}\frac{1}{Z - Z_v}\Big) - U\,dZ_v/d\bar{x}\Big] \tag{B1}$$

(ii) Due to potential jump on cut

$$F_e = i\rho U(d\Gamma_v/d\bar{x})(Z_v - Z_s) \tag{B2}$$

where Z_v is the vortex core position and Z_s the separation point coordinate.

The force-free condition is

$$F_v + F_c = 0,$$

or

$$\overline{F_v + F_c} = 0;$$

that is,

$$i\rho\Gamma_v\Big[\lim_{Z\to Z_v}\Big(\frac{dW}{dZ} - \frac{\Gamma_v}{2\pi i}\frac{1}{Z - Z_v} - U\frac{d\bar{Z}}{d\bar{x}}\Big] - i\rho U\frac{d\Gamma_v}{d\bar{x}}(\bar{Z}_v - \bar{Z}_s) = 0 \tag{B3}$$

Therefore,

$$\lim_{Z\to Z_v}\Big(\frac{dW}{dZ} - \frac{\Gamma_v}{2\pi i}\frac{1}{Z - Z_v}\Big) = U\frac{d\bar{Z}_v}{d\bar{x}} + \frac{U}{\Gamma_v}\frac{d\Gamma_v}{d\bar{x}}(\bar{Z}_v - \bar{Z}_s) \tag{B4}$$

Dividing both sides by $U\alpha$, it is obtained that

$$\lim_{Z\to Z_v}\Big(\frac{1}{U\alpha}\frac{dW}{dZ} - \frac{\Gamma_v}{2\pi i U\alpha a}\frac{1}{\zeta - \zeta_v}\Big) = \frac{1}{\alpha}\frac{d\bar{Z}_v}{d\bar{x}} + \frac{a}{\alpha\Gamma_v}\frac{d\Gamma_v}{d\bar{x}}(\bar{\zeta}_v - \bar{\zeta}_s)$$

Since

$$\frac{1}{U\alpha}\frac{dW}{dZ} = -i\left(1 + \frac{1}{\zeta^2}\right) + \frac{da}{d\bar{x}}\frac{1}{\zeta\alpha} - i\gamma_1\left[\frac{1}{\zeta - \zeta_1} - \frac{\bar{\zeta}_1}{\zeta\bar{\zeta}_1 - 1}\right] +$$

$$i\gamma_2\left[\frac{1}{\zeta - \zeta_2} - \frac{\bar{\zeta}_2}{\zeta\bar{\zeta}_2 - 1}\right]$$

it follows that

$$\frac{1}{U\alpha}\frac{dW}{dZ} - \frac{\gamma_1}{i}\frac{1}{\zeta - \zeta_1} = -i\left(1 + \frac{1}{\zeta^2}\right) + \frac{da}{d\bar{x}}\frac{1}{\zeta\alpha} + i\gamma_1\frac{\bar{\zeta}_1}{\zeta\bar{\zeta}_1 - 1} +$$

$$i\gamma_2\left[\frac{1}{\zeta - \zeta_2} - \frac{\bar{\zeta}_2}{\zeta\bar{\zeta}_2 - 1}\right] \tag{B5}$$

and

$$\frac{1}{U\alpha}\frac{dW}{dZ} + \frac{\gamma_2}{i}\frac{1}{\zeta - \zeta_2} = -i\left(1 + \frac{1}{\zeta^2}\right) +$$

$$\frac{da}{d\bar{x}}\frac{1}{\zeta\alpha} - i\gamma_1\left[\frac{1}{\zeta - \zeta_1} - \frac{\bar{\zeta}_1}{\zeta\bar{\zeta}_1 - 1}\right] - i\gamma_2\frac{\bar{\zeta}_2}{\zeta\bar{\zeta}_2 - 1} \tag{B6}$$

The force-free condition on the right side ($Z_v = Z_1$) becomes

$$-i\left(1 + \frac{1}{\zeta_1^2}\right) + \frac{da}{d\bar{x}}\frac{1}{\zeta_1\alpha} + i\gamma_1\frac{\bar{\zeta}_1}{\zeta_1\bar{\zeta}_1 - 1} + i\gamma_2\left[\frac{1}{\zeta_1 - \zeta_2} - \frac{\bar{\zeta}_2}{\zeta_1\bar{\zeta}_2 - 1}\right]$$

$$= \frac{1}{\alpha}\frac{d\bar{\zeta}_1}{d\bar{x}} + \frac{a}{\alpha\Gamma_1}\frac{d\Gamma_1}{d\bar{x}}\left(\bar{\zeta}_1 - \bar{\zeta}_{S_1}\right) \tag{B7}$$

and the force-free condition on the left side ($Z_v = Z_2$) becomes

$$-i\left(1 + \frac{1}{\zeta_2^2}\right) + \frac{da}{d\bar{x}} \frac{1}{\zeta_2 \alpha} - i\gamma_1 \left[\frac{1}{\zeta_2 - \zeta_1} - \frac{\bar{\zeta}_1}{\zeta_2 \bar{\zeta}_1 - 1}\right] - i\gamma_2 \frac{\bar{\zeta}_2}{\zeta_2 \bar{\zeta}_2 - 1}$$

$$= \frac{1}{\alpha} \frac{d\bar{\zeta}_2}{d\bar{x}} + \frac{a}{\alpha \Gamma_2} \frac{d\Gamma_2}{d\bar{x}} (\bar{\zeta}_2 - \bar{\zeta}_{S_2}) \qquad \text{(B8)}$$

Let

$$\zeta_1 = y_1 + iz_1, \ \zeta_2 = y_2 + iz_2, \ \zeta_{S_1} = \cos\theta_1 + i \sin\theta_1,$$

$$\zeta_{S_2} = \cos\theta_2 + i \sin\theta_2.$$

Then the force-free condition on the right side becomes

$$-i\left[1 + \frac{1}{(y_1 + iz_1)^2}\right] + \frac{1}{\alpha} \frac{da}{d\bar{x}} \frac{1}{y_1 + iz_1} + i\gamma_1 \frac{y_1 - iz_1}{(y_1 + iz_1)(y_1 - iz_1) - 1} +$$

$$i\gamma_2 \left\{\frac{(y_2 + iz_2)(y_2 - iz_2) - 1}{(y_1 + iz_1 - y_2 - iz_2)[(y_1 + iz_1)(y_2 - iz_2) - 1]}\right\} -$$

$$\frac{1}{\alpha} \frac{d\bar{\zeta}_1}{d\bar{x}} - \frac{a}{\alpha \Gamma_1} \frac{d\Gamma_1}{d\bar{x}} [(y_1 - iz_1) - (\cos\theta_1 - i \sin\theta_1)] = 0$$

$$-i\left[1 + \frac{y_1^2 - z_1^2 - i2y_1z_1}{(y_1^2 - z_1^2)^2 + 4y_1^2z_1^2}\right] + \frac{1}{\alpha} \frac{da}{d\bar{x}} \left(\frac{y_1}{y_1^2 + z_1^2} - i \frac{z_1}{y_1^2 + z_1^2}\right) +$$

$$\frac{\gamma_1(z_1 + iy_1)}{y_1^2 + z_1^2 - 1} +$$

$$i\gamma_2 \left\{\frac{(y_2^2 + z_2^2 - 1)[(y_1 - y_2) - i(z_1 - z_2)][(y_1y_2 + z_1z_2 - 1) - i(y_2z_1 - y_1z_2)]}{[(y_1 - y_2)^2 + (z_1 - z_2)^2][(y_1y_2 + z_1z_2 - 1)^2 + (y_2z_1 - y_1z_2)^2]}\right\} -$$

$$\frac{1}{\alpha} \frac{d\bar{\zeta}_1}{d\bar{x}} - \frac{a}{\alpha \Gamma_1} \frac{d\Gamma_1}{d\bar{x}} [(y_1 - \cos\theta_1) - i(z_1 - \sin\theta_1)] = 0$$

Finally, the above equation can be separated into real and imaginary parts to be

$$-2\frac{y_1z_1}{(y_1^2+z_1^2)^2}+\frac{1}{\alpha}\frac{da}{d\bar{x}}\frac{y_1}{y_1^2+z_1^2}+\gamma_1\frac{z_1}{y_1^2+z_1^2-1}+$$

$$\frac{\gamma_2(y_2^2+z_2^2-1)[(z_1-z_2)(y_1y_2+z_1z_2-1)+(y_1-y_2)(-y_1z_2+y_2z_1)]}{[(y_1-y_2)^2+(z_1-z_2)^2][(y_1y_2+z_1z_2-1)^2+(y_2z_1-y_1z_2)^2]}+$$

$$i\{-[1+\frac{y_1^2-z_1^2}{(y_1^2+z_1^2)^2}]-\frac{1}{\alpha}\frac{da}{d\bar{x}}\frac{z_1}{y_1^2+z_1^2}+\gamma_1\frac{y_1}{y_1^2+z_1^2-1}+$$

$$\frac{\gamma_2(y_2^2+z_2^2-1)[(y_1-y_2)(y_1y_2+z_1z_2-1)-(z_1-z_2)(-y_1z_2+y_2z_1)]}{[(y_1-y_2)^2+(z_1-z_2)^2][(y_1y_2+z_1z_2-1)^2+(y_2z_1-y_1z_2)^2]}\}-$$

$$\frac{1}{\alpha}\frac{d\bar{\zeta}_1}{d\bar{x}}-\frac{a}{\alpha\Gamma_1}\frac{d\Gamma_1}{d\bar{x}}[(y_1-\cos\theta_1)-i(z_1-\sin\theta_1)]=0 \qquad (B9)$$

Using a simple difference to represent the derivatives, that is

$$\frac{da}{d\bar{x}}=\frac{\Delta a}{\Delta\bar{x}}=\frac{a_i-a_{i-1}}{\Delta\bar{x}},$$

$$\frac{d\bar{\zeta}}{d\bar{x}}=\frac{\bar{\zeta}_i-\bar{\zeta}_{i-1}\cdot a_{i-1}/a_i}{\Delta\bar{x}}$$

$$=\frac{(y_i-y_{i-1}\cdot a_{i-1}/a_i)-i(z_i-z_{i-1}\cdot a_{i-1}/a_i)}{\Delta\bar{x}},$$

$$\frac{d\Gamma}{d\bar{x}}=\frac{\Gamma_i-\Gamma_{i-1}}{\Delta\bar{x}}$$

then the force-free condition on the right side, with y_1, z_1, etc.

representing y_{1_i}, z_{1_i}, etc., becomes

$$-2\frac{y_1z_1}{(y_1^2+z_1^2)^2}+\frac{1}{\alpha}\frac{a_i-a_{i-1}}{\bar{\Delta x}}\frac{y_1}{y_1^2+z_1^2}+\gamma_1\frac{z_1}{y_1^2+z_1^2-1}+$$

$$\frac{\gamma_2(y_2^2+z_2^2-1)[(z_1-z_2)(y_1y_2+z_1z_2-1)+(y_1y_2)(-y_1z_2+y_2z_1)]}{[(y_1-y_2)^2+(z_1-z_2)^2][(y_1y_2+z_1z_2-1)^2+(y_2z_1-y_1z_2)^2]}+$$

$$i\{-[1+\frac{y_1^2-z_1^2}{(y_1^2+z_1^2)^2}]-\frac{1}{\alpha}\frac{a_i-a_{i-1}}{\bar{\Delta x}}\frac{z_1}{y_1^2+z_1^2}+\gamma_1\frac{y_1}{y_1^2+z_1^2-1}+$$

$$\frac{\gamma_2(y_2^2+z_2^2-1)[(y_1-y_2)(y_1y_2+z_1z_2-1)-(z_1-z_2)(-y_1z_2+y_2z_1)]}{[(y_1-y_2)^2+(z_1-z_2)^2][(y_1y_2+z_1z_2-1)^2+(y_2z_1-y_1z_2)^2]}-$$

$$\frac{a_i}{\alpha}\frac{(y_{1_i}-y_{1_{i-1}}\cdot a_{i-1}/a_i)-i(z_{1_i}-z_{1_{i-1}}\cdot a_{i-1}/a_i)}{\bar{\Delta x}}-$$

$$\frac{a_i}{\alpha\gamma_{1_i}}\frac{\gamma_{1_i}-\gamma_{1_{i-1}}\cdot a_{i-1}/a_i}{\bar{\Delta x}}[(y_1-\cos\theta_1)-i(z_1-\sin\theta_1)]=0$$

(B10)

Similarly the force-free condition on the left side becomes

$$-2\frac{y_2z_2}{(y_2^2+z_2^2)^2}+\frac{1}{\alpha}\frac{a_i-a_{i-1}}{\bar{\Delta x}}\frac{y_2}{y_2^2+z_2^2}-\gamma_2\frac{z_2}{y_2^2+z_2^2-1}+$$

$$\frac{\gamma_1(y_1^2+z_1^2-1)[(z_1-z_2)(y_1y_2+z_1z_2-1)+(y_1-y_2)(-y_1z_2+y_2z_1)]}{[(y_1-y_2)^2+(z_1-z_2)^2][(y_1y_2+z_1z_2-1)^2+(y_2z_1-y_1z_2)^2]}+$$

$$i\{-[1+\frac{y_2^2-z_2^2}{(y_2^2+z_2^2)^2}]-\frac{a_i-a_{i-1}}{\alpha\bar{\Delta x}}\frac{z_2}{y_2^2+z_2^2}-\gamma_2\frac{y_2}{y_2^2+z_2^2-1}+$$

$$\frac{\gamma_1(y_1^2 + z_1^2 - 1)[(y_1 - y_2)(y_1y_2 + z_1z_2 - 1) - (z_1 - z_2)(-y_1z_2 + y_2z_1)]}{[(y_1 - y_2)^2 + (z_1 - z_2)^2][(y_1y_2 + z_1z_2 - 1)^2 + (y_2z_1 - y_1z_2)^2]} -$$

$$\frac{a_i}{\alpha}\frac{(y_{2_i} - y_{2_{i-1}} \cdot a_{i-1}/a_i) - i(z_{2_i} - z_{2_{i-1}} \cdot a_{i-1}/a_i)}{\Delta\bar{x}} -$$

$$\frac{a_i}{\alpha}\frac{\gamma_{1_i} - \gamma_{1_{i-1}} \cdot a_{i-1}/a_i}{\gamma_{1_i}\Delta\bar{x}}[(y_2 - \cos\theta_2) - i(z_2 - \sin\theta_2)] = 0 \qquad \text{(B11)}$$

Define:

$$F3 \equiv -2\frac{y_1z_1}{(y_1^2 + z_1^2)^2} + \frac{1}{\alpha}\frac{a_i - a_{i-1}}{\Delta\bar{x}}\frac{y_1}{y_1^2 + z_1^2} + \gamma_1\frac{z_1}{y_1^2 + z_1^2 - 1} +$$

$$\frac{\gamma_2(y_2^2 + z_2^2 - 1)[(z_1 - z_2)(y_1y_2 + z_1z_2 - 1) + (y_1 - y_2)(-y_1z_2 + y_2z_1)]}{[(y_1 - y_2)^2 + (z_1 - z_2)^2][(y_1y_2 + z_1z_2 - 1)^2 + (y_2z_1 - y_1z_2)^2]} -$$

$$\frac{a_i}{\alpha}\frac{y_{1_i} - y_{1_{i-1}} \cdot a_{i-1}/a_i}{\Delta\bar{x}} - \frac{a_i}{\alpha}\frac{\gamma_{1_i} - \gamma_{1_{i-1}} \cdot a_{i-1}/a_i}{\Delta\bar{x}\gamma_{1_i}}(y_1 - \cos\theta_1) = 0 \qquad \text{(B12)}$$

$$F4 \equiv -\left[1 + \frac{y_1^2 - z_1^2}{(y_1^2 + z_1^2)^2}\right] - \frac{1}{\alpha}\frac{a_i - a_{i-1}}{\Delta\bar{x}}\frac{z_1}{y_1^2 + z_1^2} + \gamma_1\frac{y_1}{y_1^2 + z_1^2 - 1} +$$

$$\frac{\gamma_2(y_2^2 + z_2^2 - 1)[(y_1 - y_2)(y_1y_2 + z_1z_2 - 1) - (z_1 - z_2)(-y_1z_2 + y_2z_1)]}{[(y_1 - y_2)^2 + (z_1 - z_2)^2][(y_1y_2 + z_1z_2 - 1)^2 + (y_2z_1 - y_1z_2)^2]} +$$

$$\frac{a_i}{\alpha}\frac{z_{1_i} - z_{1_{i-1}} \cdot a_{i-1}/a_i}{\Delta\bar{x}} + \frac{a_i}{\alpha}\frac{\gamma_{1_i} - \gamma_{1_{i-1}} \cdot a_{i-1}/a_i}{\Delta\bar{x}\gamma_{1_i}}(z_1 - \sin\theta_1) = 0 \qquad \text{(B13)}$$

$$F5 \equiv -2\frac{y_2z_2}{(y_2^2 + z_2^2)^2} + \frac{1}{\alpha}\frac{a_i - a_{i-1}}{\Delta\bar{x}}\frac{y_2}{y_2^2 + z_2^2} - \gamma_2\frac{z_2}{y_2^2 + z_2^2 - 1} +$$

$$\frac{\gamma_1(y_1^2 + z_1^2 - 1)[(z_1 - z_2)(y_1y_2 + z_1z_2 - 1) + (y_1 - y_2)(-y_1z_2 + y_2z_1)]}{[(y_1 - y_2)^2 + (z_1 - z_2)^2][(y_1y_2 + z_1z_2 - 1)^2 + (y_2z_1 - y_1z_2)^2]} -$$

$$\frac{a_i}{\alpha}\frac{y_{2_i} - y_{2_{i-1}} \cdot a_{i-1}/a_i}{\Delta\bar{x}} - \frac{a_i}{\alpha}\frac{\gamma_{1_i} - \gamma_{1_{i-1}} \cdot a_{i-1}/a_i}{\Delta\bar{x}\gamma_{1_i}}(y_2 - \cos\theta_2) = 0 \qquad \text{(B14)}$$

$$F6 \equiv -\left[1 + \frac{y_2^2 - z_2^2}{(y_2^2 + z_2^2)^2}\right] - \frac{1}{\alpha}\frac{a_i - a_{i-1}}{\Delta\bar{x}}\frac{z_2}{y_2^2 + z_2^2} - \gamma_2\frac{y_2}{y_2^2 + z_2^2 - 1} +$$

$$\frac{\gamma_1(y_1^2 + z_1^2 - 1)[(y_1 - y_2)(y_1y_2 + z_1z_2 - 1) - (z_1 - z_2)(-y_1z_2 + y_2z_1)]}{[(y_1 - y_2)^2 + (z_1 - z_2)^2][(y_1y_2 + z_1z_2 - 1)^2 + (y_2z_1 - y_1z_2)^2]} +$$

$$\frac{a_i}{\alpha}\frac{z_{2_i} - z_{2_{i-1}} \cdot a_{i-1}/a_i}{\Delta\bar{x}} + \frac{a_i}{\alpha}\frac{\gamma_{1_i} - \gamma_{1_{i-1}} \cdot a_{i-1}/a_i}{\Delta\bar{x}\gamma_{1_i}}(z_2 - \sin\theta_2) = 0 \qquad \text{(B15)}$$

For a conical flow, the derivative terms can be approximated by

$$\frac{da}{d\bar{x}} = \frac{a}{\bar{x}} \approx \delta, \quad \frac{d\bar{\zeta}}{d\bar{x}} = \frac{\bar{\zeta}}{\bar{x}} = \frac{\delta\bar{\zeta}}{a}, \quad \frac{d\Gamma}{d\bar{x}} = \frac{\Gamma}{\bar{x}} = \frac{\delta\Gamma}{a}$$

Therefore,

$$F3 \equiv -2\frac{y_1z_1}{(y_1^2 + z_1^2)^2} + \frac{1}{A}\frac{y_1}{y_1^2 + z_1^2} + \frac{\gamma_1z_1}{y_1^2 + z_1^2 - 1} +$$

$$\gamma_2\frac{(y_2^2 + z_2^2 - 1)[(z_1 - z_2)(y_1y_2 + z_1z_2 - 1) + (y_1 - y_2)(-y_1z_2 + y_2z_1)]}{[(y_1 - y_2)^2 + (z_1 - z_2)^2][(y_1y_2 + z_1z_2 - 1)^2 + (y_2z_1 - y_1z_2)^2]} -$$

$$[y_1 + (y_1 - \cos\theta_1)]/A = 0 \qquad \text{(B16)}$$

$$F4 \equiv -\left[1 + \frac{y_1^2 - z_1^2}{(y_1^2 + z_1^2)^2}\right] - \frac{1}{A}\frac{z_1}{y_1^2 + z_1^2} + \frac{\gamma_1 y_1}{y_1^2 + z_1^2 - 1} +$$

$$\gamma_2 \frac{(y_2^2 + z_2^2 - 1)[(y_1 - y_2)(y_1y_2 + z_1z_2 - 1) - (z_1 - z_2)(-y_1z_2 + y_2z_1)]}{[(y_1 - y_2)^2 + (z_1 - z_2)^2][y_1y_2 + z_1z_2 - 1)^2 + (y_2z_1 - y_1z_2)^2]} +$$

$$[z_1 - (\sin\theta_1 - z_1)]/A = 0 \qquad \text{(B17)}$$

$$F5 \equiv -2\frac{y_2z_2}{(y_2^2 + z_2^2)^2} + \frac{1}{A}\frac{y_2}{y_2^2 + z_2^2} - \gamma_2 \frac{z_2}{y_2^2 + z_2^2 - 1} +$$

$$\gamma_1 \frac{(y_1^2 + z_1^2 - 1)[z_1 - z_2)(y_1y_2 + z_1z_2 - 1) + (y_1 - y_2)(-y_1z_2 + y_2z_1)]}{[(y_1 - y_2)^2 + (z_1 - z_2)^2][(y_1y_2 + z_1z_2 - 1)^2 + (y_2z_1 - y_1z_2)^2]} -$$

$$[y_2 + (y_2 - \cos\theta_2)]/A = 0 \qquad \text{(B18)}$$

$$F6 \equiv -\left[1 + \frac{y_2^2 - z_2^2}{(y_2^2 + z_2^2)^2}\right] - \frac{1}{A}\frac{z_2}{y_2^2 + z_2^2} - \frac{\gamma_2 y_2}{y_2^2 + z_2^2 - 1} +$$

$$\frac{\gamma_1(y_1^2 + z_1^2 - 1)[(y_1 - y_2)(y_1y_2 + z_1z_2 - 1) - (z_1 - z_2)(-y_1z_2 + y_2z_1)]}{[(y_1 - y_2)^2 + (z_1 - z_2)^2][(y_1y_2 + z_1z_2 - 1)^2 + (y_2z_1 - y_1z_2)^2]} +$$

$$[z_2 - (\sin\theta_2 - z_2)]/A = 0 \qquad \text{(B19)}$$

where $A = \alpha/\delta$.

Define

$$\text{Norm} \equiv [F1^2 + F2^2 + F3^2 + F4^2 + F5^2 + F6^2]^{1/2}$$

Variables y_1, y_2, z_1, z_2, γ_1, and γ_2 satisfying the requirement that the Norm be less than or equal to 10^{-8} are regarded as a set of solutions.

The last terms of Equations (B12) to (B19) are the effect of the vortex cut. When testing models without this effect, these terms are eliminated.

APPENDIX C

FORMULATION OF THE DERIVATIVE d $V_{tm}/d\theta$

Since the mean tangential velocity on the body is

$$V_{tm} = \left\{2\cos\theta - \gamma_1 \frac{\zeta_1\bar{\zeta}_1 - 1}{(e^{i\theta} - \zeta_1)(e^{-i\theta} - \bar{\zeta}_1)} + \gamma_2 \frac{\zeta_2\bar{\zeta}_2 - 1}{(e^{i\theta} - \zeta_2)(e^{-i\theta} - \bar{\zeta}_2)}\right\} U\alpha$$

then

$$\frac{1}{U\alpha}\frac{dV_{tm}}{d\theta} = -2\sin\theta + \gamma_1 \frac{(\zeta_1\bar{\zeta}_1 - 1)[i(e^{-i\theta} - \bar{\zeta}_1)e^{i\theta} - ie^{-i\theta}(e^{i\theta} - \zeta_1)}{(e^{i\theta} - \zeta_1)^2(e^{-i\theta} - \bar{\zeta}_1)^2} -$$

$$\gamma_2 \frac{(\zeta_2\bar{\zeta}_2 - 1)[ie^{i\theta}(e^{-i\theta} - \bar{\zeta}_2) - ie^{-i\theta}(e^{i\theta} - \zeta_2)]}{(e^{i\theta} - \zeta_2)^2(e^{-i\theta} - \bar{\zeta}_2)^2}$$

$$= -2\sin\theta + i\gamma_1 \frac{(\zeta_1\bar{\zeta}_1 - 1)(\zeta_1 e^{-i\theta} - \bar{\zeta}_1 e^{i\theta})}{(e^{i\theta} - \zeta_1)^2(e^{-i\theta} - \bar{\zeta}_1)^2} -$$

$$i\gamma_2 \frac{(\zeta_2\bar{\zeta}_2 - 1)(\zeta_2 e^{-i\theta} - \bar{\zeta}_2 e^{i\theta})}{(e^{i\theta} - \zeta_2)^2(e^{-i\theta} - \bar{\zeta}_2)^2} \qquad \text{(C1)}$$

Let

$$\zeta_1 = y_1 + \zeta_1$$

$$\zeta_2 = y_2 + iz_2.$$

It follows that

$$\frac{1}{U\alpha}\frac{dV_{tm}}{d\theta} = -2\sin\theta + i\gamma_1.$$

$$\frac{[(y_1+iz_1)(y_1-iz_1)-1][(y_1+iz_1)(\cos\theta - i\sin\theta)-(y_1-iz_1)(\cos\theta+i\sin\theta)]}{[(\cos\theta-y_1)+i(\sin\theta-z_1)]^2[(\cos\theta-y_1)-i(\sin\theta-z_1)]^2} -$$

$$i\gamma_2 \frac{[(y_2+iz_2)(y_2-iz_2)-1][(y_2+iz_2)(\cos\theta-i\sin\theta)-(y_2-iz_2)(\cos\theta+i\sin\theta)}{[(\cos\theta-y_2)+i(\sin\theta-z_2)]^2[(\cos\theta-y_2)-i(\sin\theta-z_2)]^2}$$

$$= -2\sin\theta - 2\gamma_1 \frac{(y_1^2+z_1^2-1)(z_1\cos\theta - y_1\sin\theta)}{[(\cos\theta-y_1)^2+(\sin\theta-z_1)^2]^2} +$$

$$2\gamma_2 \frac{(y_2^2+z_2^2-1)(z_2\cos\theta - y_2\sin\theta)}{[(\cos\theta-y_2)^2+(\sin\theta-z_2)^2]^2} \qquad \text{(C2)}$$

A line represents an actual separation line if $dV_{tm}/d\theta|_{\theta_1} < 0$ on the right side and $dV_{tm}/d\theta|_{\theta_2} > 0$ on the left side.

APPENDIX D

FORMULATION OF THE COEFFICIENTS OF AERODYNAMIC FORCES

The lateral force is, based on the momentum theory,

$$\vec{F} = \int \rho\vec{V}(-\vec{V} \cdot d\vec{A})$$

From Reference 10, the local force can be calculated as

$$\frac{F_i}{1/2\ \rho U^2} = -2i \oint_{C_{B_{out}}} \frac{W'}{U}\, dZ + 2i \oint_{C_{B_{in}}} \frac{W'}{U}\, dZ - 2iS_{out}(\alpha - i\beta) + 2iS_{in}(\alpha - i\beta) \tag{D1}$$

where $C_{B_{out}}$ is the contour of the out-flow plane, with area S_{out}, and $C_{B_{in}}$ is the contour of the in-flow plane, with area S_{in}.

Note that

$$\oint \frac{W}{U}\, dZ = -2\pi a_i^2\alpha - \frac{\Gamma_{1_i}}{U}\left(Z_{1_i} - \frac{a_i^2}{\bar{Z}_{1_i}}\right) + \frac{\Gamma_{2_i}}{U}\left(Z_{2_i} - \frac{a_i^2}{\bar{Z}_{2_i}}\right)$$

$$= -2\pi a_i^2\alpha - \frac{2\pi a_i^2\Gamma_{1_i}\alpha}{2\pi a_i U\alpha}\left(\zeta_{1_i} - \frac{1}{\bar{\zeta}_{1_i}}\right) + \frac{2\pi a_i^2\Gamma_{2_i}\alpha}{2\pi a_i U\alpha}\left(\zeta_{2_i} - \frac{1}{\bar{\zeta}_{2_i}}\right)$$

$$= -2\pi a_i^2\alpha\left[1 + \gamma_{1_i}\left(\zeta_{1_i} - \frac{1}{\bar{\zeta}_{1_i}}\right) - \gamma_{2_i}\left(\zeta_{2_i} - \frac{1}{\bar{\zeta}_{2_i}}\right)\right] \tag{D2}$$

To obtain the coefficients of aerodynamic forces, lateral force is nondimensionalized by the base area. That is,

$$C_{y_i} + iC_{N_i} = \frac{1}{\pi a_B^2}\left(\frac{F_i}{1/2\ \rho U^2}\right) \tag{D3}$$

For cases in this report, no sideslip effect is assumed. Therefore

$$C_{y_i} + iC_{N_i} = \frac{-2i}{\pi a_B^2} \{-2\pi a_i^2 \alpha[1 + \gamma_{1_i}(\zeta_{1_i} - \frac{1}{\bar{\zeta}_{1_i}}) - \gamma_{2_i}(\zeta_{2_i} - \frac{1}{\bar{\zeta}_{2_i}})] +$$

$$2\pi a_{i-1}^2 \alpha[1 + \gamma_{1_{i-1}}(\zeta_{1_{i-1}} - \frac{1}{\bar{\zeta}_{1_{i-1}}}) - \gamma_{2_{i-1}}(\zeta_{2_{i-1}} - \frac{1}{\bar{\zeta}_{2_{i-1}}})]\} -$$

$$\frac{2i}{\pi a_B^2} \pi a_i^2 \alpha + \frac{2i}{\pi a_B^2} \pi a_{i-1}^2 \alpha$$

$$= \frac{i\alpha}{a_B^2} \{4a_i^2[\gamma_{1_i}(\zeta_{1_i} - \frac{1}{\bar{\zeta}_{1_i}}) - \gamma_{2_i}(\zeta_{2_i} - \frac{1}{\bar{\zeta}_{2_i}})] -$$

$$4a_{i-1}^2[\gamma_{1_{i-1}}(\zeta_{1_{i-1}} - \frac{1}{\bar{\zeta}_{1_{i-1}}}) - \gamma_{2_{i-1}}(\zeta_{2_{i-1}} - \frac{1}{\bar{\zeta}_{2_{i-1}}})] + 2a_i^2 - 2a_{i-1}^2\} \tag{D4}$$

Let

$$\zeta_{1_i} = y_{1_i} + z_{1_i} \text{ and } \zeta_{2_i} = y_{2_i} + z_{2_i}.$$

Then

$$C_{y_i} + iC_{N_i} = \frac{i\alpha}{a_B^2} \{4a_i^2[\gamma_{1_i}\{(y_{1_i} + iz_{1_i}) - \frac{y_{1_i} + iz_{1_i}}{y_{1_i}^2 + z_{1_i}^2}\} -$$

$$\gamma_{2_i}\{(y_{2_i} + iz_{2_i}) - \frac{y_{2_i} + iz_{2_i}}{y_{2_i}^2 + z_{2_i}^2}\}] - 4a_{i-1}^2[\gamma_{1_{i-1}}\{(y_{1_{i-1}} + iz_{1_{i-1}}) -$$

$$\frac{y_{1_{i-1}} + iz_{1_{i-1}}}{y_{1_{i-1}}^2 + z_{1_{i-1}}^2}\} - \gamma_{2_{i-1}}\{(y_{2_{i-1}} + iz_{2_{i-1}}) - \frac{y_{2_{i-1}} + iz_{2_{i-1}}}{y_{2_{i-1}}^2 + z_{2_{i-1}}^2}\}] +$$

$$2a_i^2 - 2a_{i-1}^2\}$$

$$= \frac{2\alpha}{a_B^2} \{-2a_i^2[\gamma_{1_i} z_{1_i}(1 - \frac{1}{y_{1_i}^2 + z_{1_i}^2}) + \gamma_{2_i} z_{2_i}(1 - \frac{1}{y_{2_i}^2 + z_{2_i}^2})] +$$

$$2a_{i-1}^2[\gamma_{1_{i-1}} z_{1_{i-1}} (1 - \frac{1}{y_{1_{i-1}}^2 + z_{1_{i-1}}^2}) -$$

$$\gamma_{2_{i-1}} z_{2_{i-1}} (1 - \frac{1}{y_{2_{i-1}}^2 + z_{2_{i-1}}^2})]\} +$$

$$i \frac{2\alpha}{a_B^2} \{2a_i^2[\gamma_{1_i} y_{1_i} (1 - \frac{1}{y_{1_i}^2 + z_{1_i}^2}) - \gamma_{2_i} y_{2_i} (1 - \frac{1}{y_{2_i}^2 + z_{2_i}^2})] -$$

$$2a_{i-1}^2[\gamma_{1_{i-1}} y_{1_{i-1}} (1 - \frac{1}{y_{1_{i-1}}^2 + z_{1_{i-1}}^2}) -$$

$$\gamma_{2_{i-1}} y_{2_{i-1}} (1 - \frac{1}{y_{2_{i-1}}^2 + z_{2_{i-1}}^2})] + a_i^2 - a_{i-1}^2\} \qquad \text{(D5)}$$

It follows that

$$C_{y_i} = \frac{2\alpha a_i^2}{a_B^2} \{-2\gamma_{1_i} z_{1_i} (1 - \frac{1}{y_{1_i}^2 + z_{1_i}^2}) + 2\gamma_{2_i} z_{2_i} (1 - \frac{1}{y_{2_i}^2 + z_{2_i}^2}) +$$

$$2\gamma_{1_{i-1}} z_{1_{i-1}} \frac{a_{i-1}^2}{a_i^2} (1 - \frac{1}{y_{1_{i-1}}^2 + z_{1_{i-1}}^2}) -$$

$$2\gamma_{2_{i-1}} z_{2_{i-1}} \frac{a_{i-1}^2}{a_i^2} (1 - \frac{1}{y_{2_{i-1}}^2 + z_{2_{i-1}}^2})\} \qquad \text{(D6)}$$

$$C_{N_i} = \frac{2\alpha a_i^2}{a_B^2} \{2\gamma_{1_i} y_{1_i} (1 - \frac{1}{y_{1_i}^2 + z_{1_i}^2}) - 2\gamma_{2_i} y_{2_i} (1 - \frac{1}{y_{2_i}^2 + z_{2_i}^2}) -$$

$$2\gamma_{1_{i-1}} y_{1_{i-1}} \frac{a_{i-1}^2}{a_i^2} (1 - \frac{1}{y_{1_{i-1}}^2 + z_{1_{i-1}}^2}) +$$

$$2\gamma_{2_{i-1}} y_{2_{i-1}} \frac{a_{i-1}^2}{a_i^2}\left(1 - \frac{1}{y_{2_{i-1}}^2 + z_{2_{i-1}}^2}\right) + 1 - \frac{a_{i-1}^2}{a_i^2}\} \tag{D7}$$

and

$$C_y = \sum_i C_{y_i} \tag{D8}$$

$$C_N = \sum_i C_{N_i} \tag{D9}$$

For conical flow (such as on a cone), all flow properties changing with respect to $\bar{x}$ are constant. Therefore,

$$C_y = 2\alpha\{-2\gamma_1 z_1\left(1 - \frac{1}{y_1^2 + z_1^2}\right) + 2\gamma_2 z_2\left(1 - \frac{1}{y_2^2 + z_2^2}\right)\} \tag{D10}$$

$$C_N = 2\alpha\{2\gamma_1 y_1\left(1 - \frac{1}{y_1^2 + z_1^2}\right) - 2\gamma_2 y_2\left(1 - \frac{1}{y_2^2 + z_2^2}\right) + 1\} \tag{D11}$$

$$C_L = C_N \cos\alpha$$

Table 1: Effective Angles of Attack for Three Bodies

α = Geometric Angle of Attack

α_e = Effective Angle of Attack

f.r. = Fineness ratio

α	8 Deg. cone α_e	Tangent Ogive of f.r. = 3.5 α_e	Tangent Ogive of f.r. = 5.0 α_e
5.0	---	4.56	4.74
10.0	8.93	9.09	9.43
12.0	10.69	10.88	11.29
14.0	12.44	12.66	13.12
16.0	14.17	14.42	14.95
18.0	15.89	16.16	16.75
20.0	17.58	17.88	18.53
22.0	19.25	19.57	20.27
24.0	20.89	21.24	21.99
26.0	22.51	22.88	23.66
28.0	24.09	24.48	25.31
30.0	25.64	26.05	26.90
35.0	---	29.78	30.65
40.0	---	33.16	---

--- not calculated

Table 2: Numerical Results for an Eight-Degree Cone

"It." stands for "iterations."

All roots satisfy the requirement that Norm $< 10^{-8}$.

	α deg.	θ_1 deg.	A	y_1	z_1	y_2	z_2	γ_1	γ_2	It.
Init. Guess	14	53.86	1.750	0.300	1.100	-0.300	1.200	0.300	0.300	
Sym. Root				0.299	1.130	-0.299	1.130	0.182	0.182	23
Asym. Root				0.462	0.971	-0.188	1.665	0.157	0.107	38
Init. Guess	16	51.12	2.000	0.300	1.100	-0.300	1.250	0.180	0.180	
Sym. Root				0.317	1.157	-0.317	1.157	0.226	0.226	25
Asym. Root				0.379	1.075	-0.247	1.769	0.259	0.213	36
Init. Guess	18	48.74	2.250	0.320	1.100	-0.320	1.300	0.250	0.250	
Sym. Root				0.355	1.181	-0.335	1.181	0.269	0.269	32
Asym. Root				0.320	1.156	-0.323	1.842	0.340	0.340	48

Table 2 (continued)

	α deg.	θ_1 deg.	A	y_1	z_1	y_2	z_2	γ_1	γ_2	It.
Init. Guess	20	46.61	2.500	0.350	1.200	-0.350	1.400	0.250	0.250	
Sym. Root				0.353	1.202	-0.353	1.202	0.311	0.311	30
Asym. Root				0.282	1.222	-0.401	1.904	0.412	0.311	38
Init. Guess	22	44.66	2.750	0.370	1.200	-0.370	1.400	0.300	0.300	
Sym. Root				0.372	1.223	-0.372	1.223	0.352	0.352	31
Asym. Root				0.256	1.277	-0.477	1.962	0.481	0.361	42
Init. Guess	24	42.85	3.000	0.380	1.200	-0.380	1.400	0.350	0.350	
Sym. Root				0.390	1.243	-0.390	1.243	0.393	0.393	24
Asym. Root				0.239	1.327	-0.550	2.016	0.548	0.411	44
Init. Guess	26	41.15	3.250	0.400	1.200	-0.400	1.400	0.400	0.400	
Sym. Root				0.408	1.262	-0.408	1.262	0.433	0.433	21

Table 2 (continued)

	α deg.	θ_1 deg.	A	y_1	z_1	y_2	z_2	γ_1	γ_2	It.
Asym. Root				0.228	1.372	-0.619	2.069	0.613	0.462	45
Init. Guess	28	39.55	3.500	0.420	1.250	-0.420	1.450	0.450	0.450	
Sym. Root				0.425	1.280	-0.425	1.280	0.473	0.473	31
Asym. Root				0.221	1.414	-0.685	2.119	0.678	0.513	49
Init. Guess	30	38.04	3.750	0.440	1.300	-0.440	1.450	0.500	0.500	
Sym. Root				0.442	1.297	-0.442	1.297	0.512	0.512	25
Asym. Root				0.217	1.453	-0.748	2.167	0.741	0.563	67

Table 3: Lower-Branch Solutions for an Eight-Degree Cone

	α deg.	θ_1 deg.	A	y_1	z_1	y_2	z_2	γ_1	γ_2	It.
				Symmetric Cases						
Init. Guess	10	61.88	1.250	0.750	0.740	-0.750	0.740	0.100	0.100	
Root				0.580	0.851	-0.580	0.851	0.065	0.065	62
Init. Guess	12	57.20	1.500	0.820	0.610	-0.820	0.619	0.200	0.200	
Root				0.746	0.738	-0.746	0.738	0.133	0.133	53
Init. Guess	14	53.86	1.750	0.850	0.610	-0.850	0.610	0.200	0.200	
Root				0.842	0.651	-0.842	0.651	0.186	0.186	45
Init. Guess	16	51.12	2.000	0.850	0.610	-0.850	0.610	0.250	0.250	
Root				0.904	0.583	-0.904	0.583	0.232	0.232	33
Init. Guess	18	48.74	2.250	0.850	0.610	-0.850	0.610	0.330	0.330	
Root				0.949	0.529	-0.949	0.529	0.271	0.271	46
Init. Guess	20	46.61	2.500	0.850	0.610	-0.850	0.610	0.330	0.330	
Root				0.982	0.485	-0.982	-.485	0.305	0.305	40

Table 3 (continued)

	α deg.	θ_1 deg.	A	y_1	z_1	y_2	z_2	γ_1	γ_2	It.
Init. Guess	22	44.66	2.750	0.850	0.610	-0.850	0.610	0.330	0.330	
Root				1.009	0.448	-1.009	0.448	0.333	0.333	72
Init. Guess	24	42.85	3.000	0.850	0.610	-0.850	0.610	0.350	0.350	
Root				1.030	0.416	-1.030	0.416	0.357	0.357	28
Init. Guess	26	41.15	3.250	1.050	0.400	-1.050	0.400	1.200	1.200	
Root				1.046	0.388	-1.046	0.388	0.377	0.377	48
Init. Guess	28	39.55	3.500	1.050	0.400	-1.050	0.400	1.300	1.300	
Root				1.060	0.364	-1.060	0.364	0.393	0.393	16
Init. Guess	30	38.04	3.750	1.050	0.400	-1.050	0.400	1.500	1.500	
Root				1.071	0.342	-1.071	0.342	0.406	0.406	29

Table 3 (continued)

	Asymmetric Cases									
	α deg.	θ_1 deg.	A	y_1	z_1	y_2	z_2	γ_1	γ_2	It.
Init. Guess				0.840	00.580	-0.640	1.890	0.210	0.630	
Root	14	53.86	1.750	0.695	0.771	-0.182	1.719	0.112	0.165	60
Root	16	51.12	2.000	0.785	0.707	-0.213	1.958	0.179	0.204	78
Root	18	48.74	2.250	0.844	0.655	-0.247	2.200	0.230	0.242	60
Root	20	46.61	2.500	0.887	0.612	-0.282	2.443	0.271	0.281	40
Root	22	44.66	2.750	0.919	0.575	-0.319	2.687	0.304	0.319	43
Root	24	42.85	3.000	0.944	0.543	-0.355	2.932	0.331	0.356	80
Root	26	41.15	3.250	0.964	0.515	-0.390	3.177	0.353	0.392	89
Root	28	39.55	3.500	0.979	0.490	-0.425	3.423	0.371	0.427	106
Root	30	38.04	3.750	0.992	0.467	-0.459	3.670	0.385	0.461	108

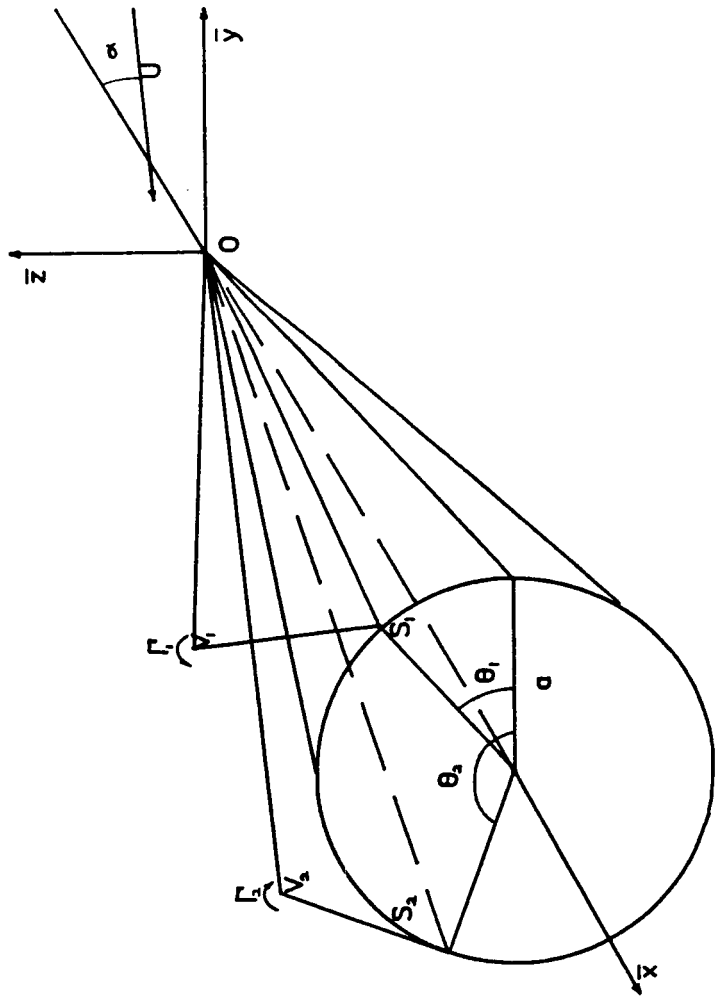

Fig.1 Configuration and Coordinate System

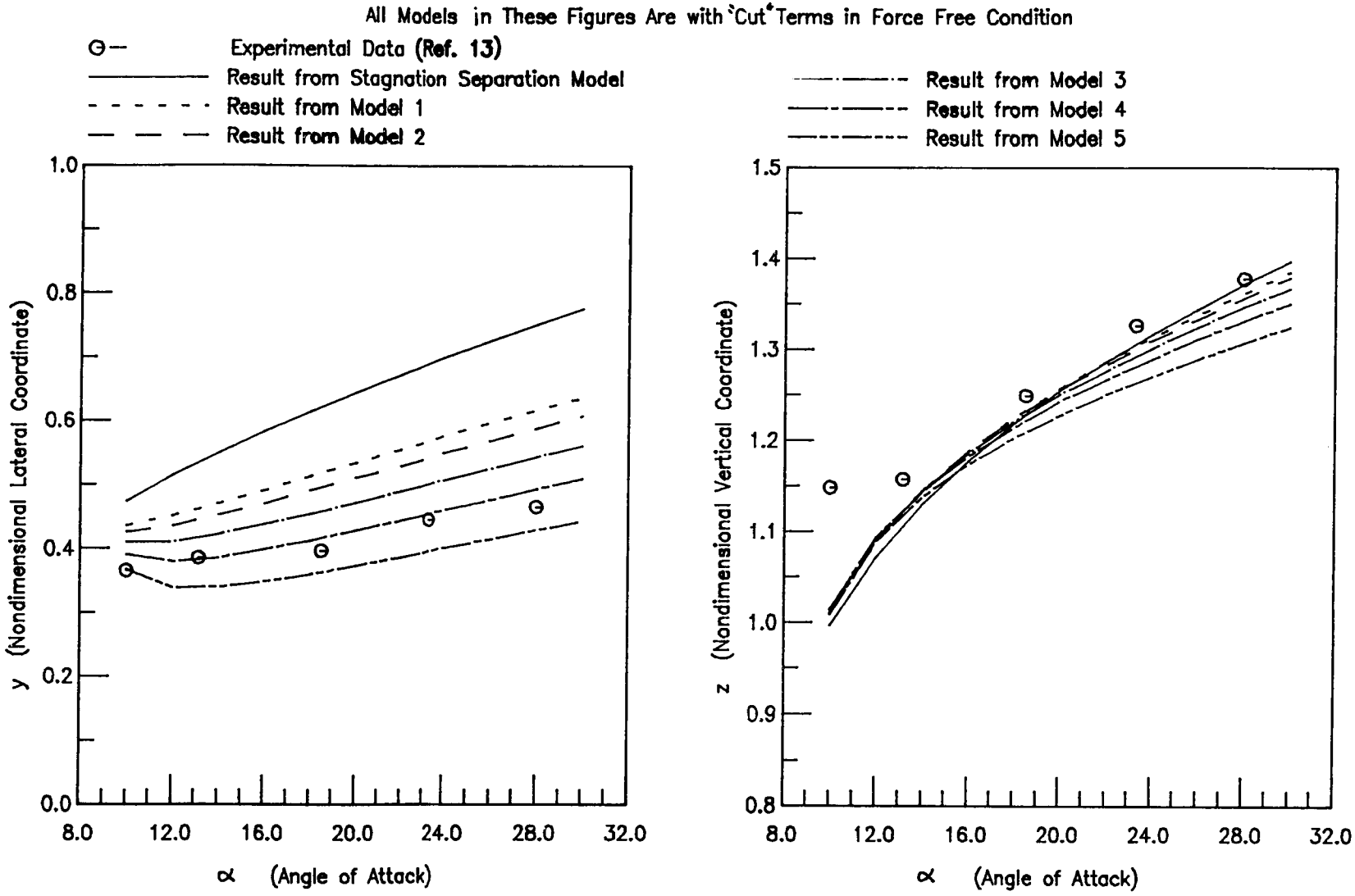

Fig.2 Right Vortex Core Positions for Different Models of a 5 Deg. Cone as a Function of Angle of Attack (Symmetric Case)

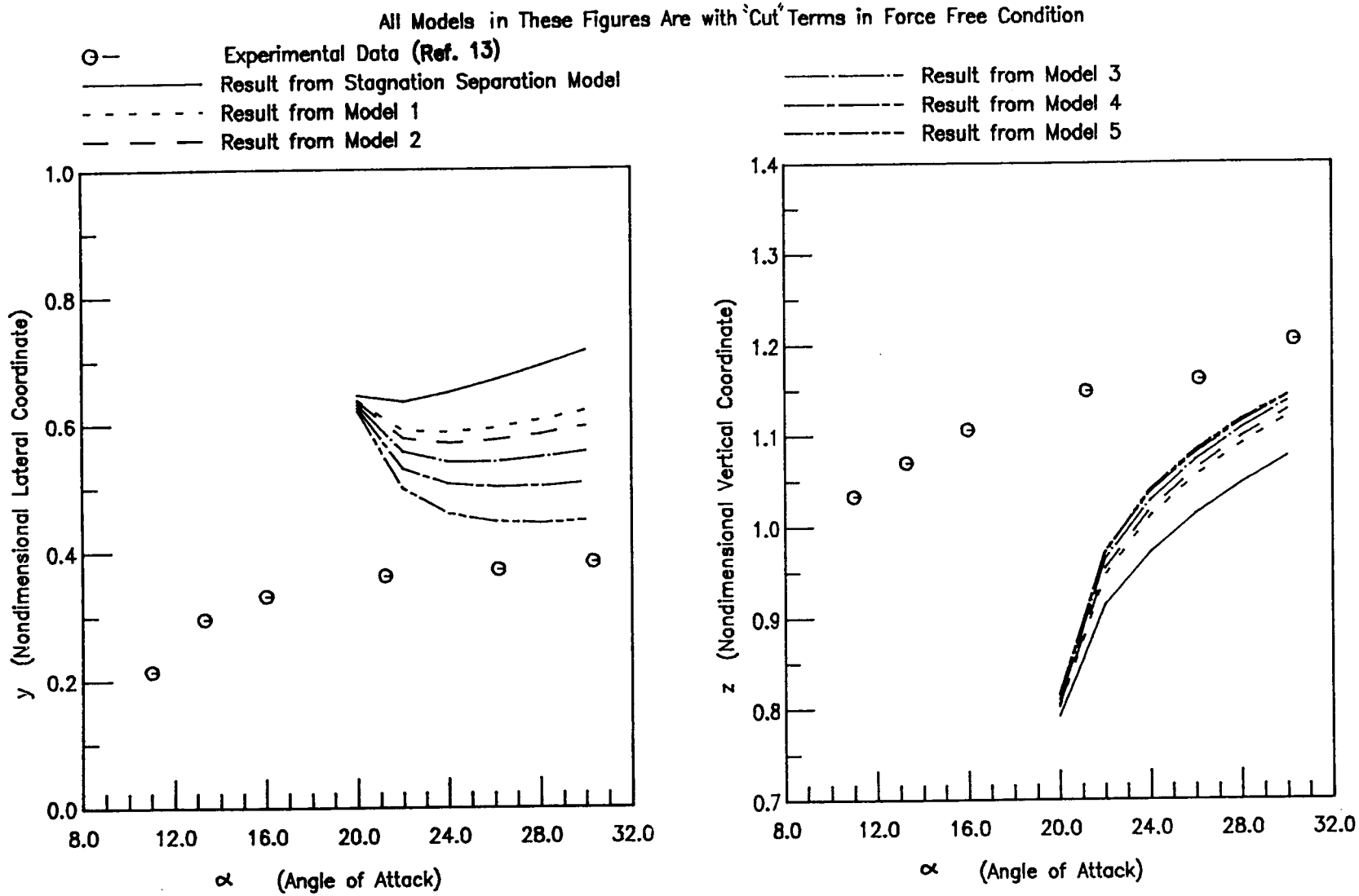

Fig.3 Right Vortex Core Positions for Different Models of a 10 Deg. Cone as a Function of angle of Attack (Symmetric Case)

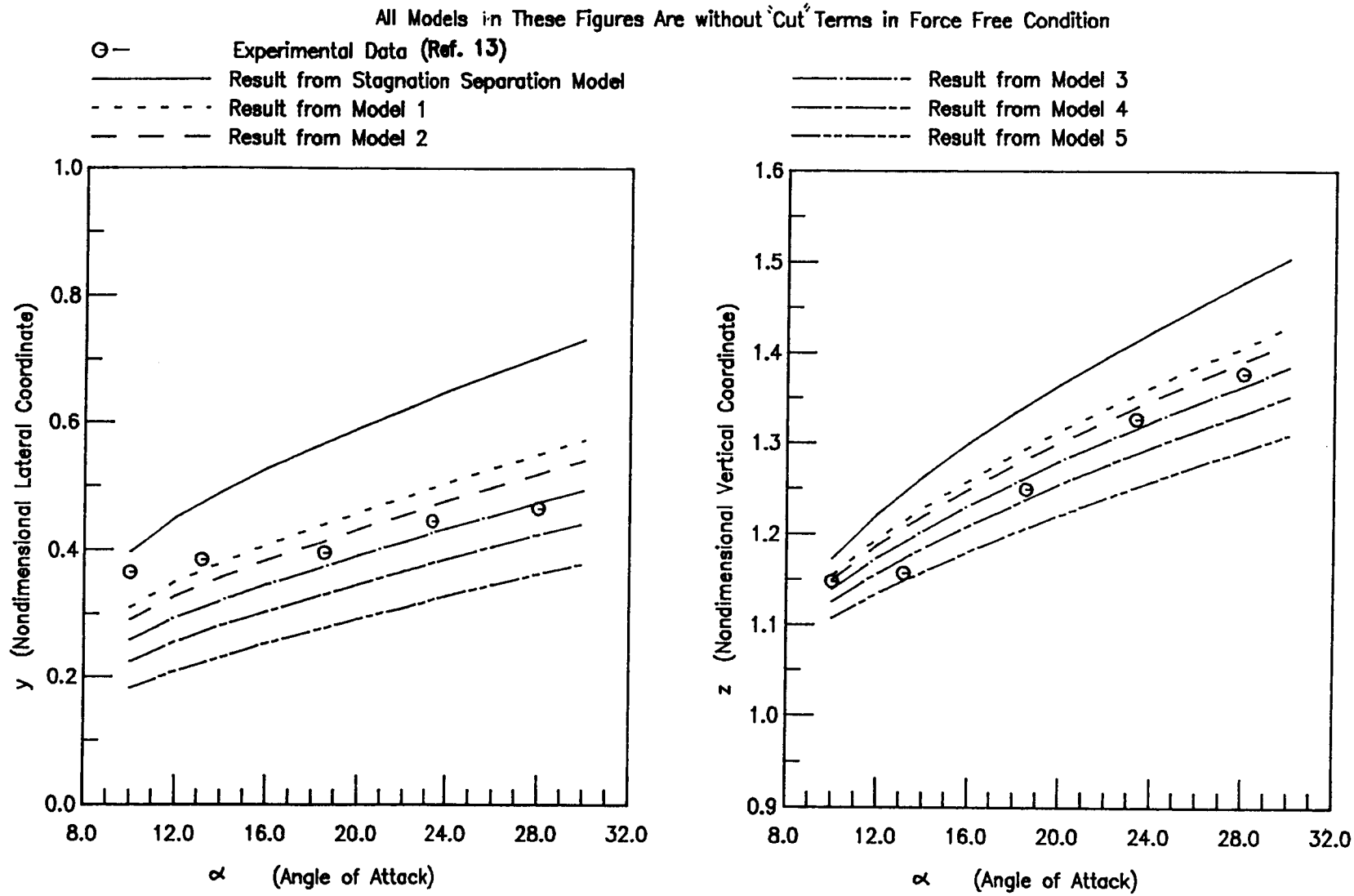

Fig.4 Right Vortex Core Positions for Different Models of a 5 Deg. Cone as a Function of Angle of Attack (Symmetric Case)

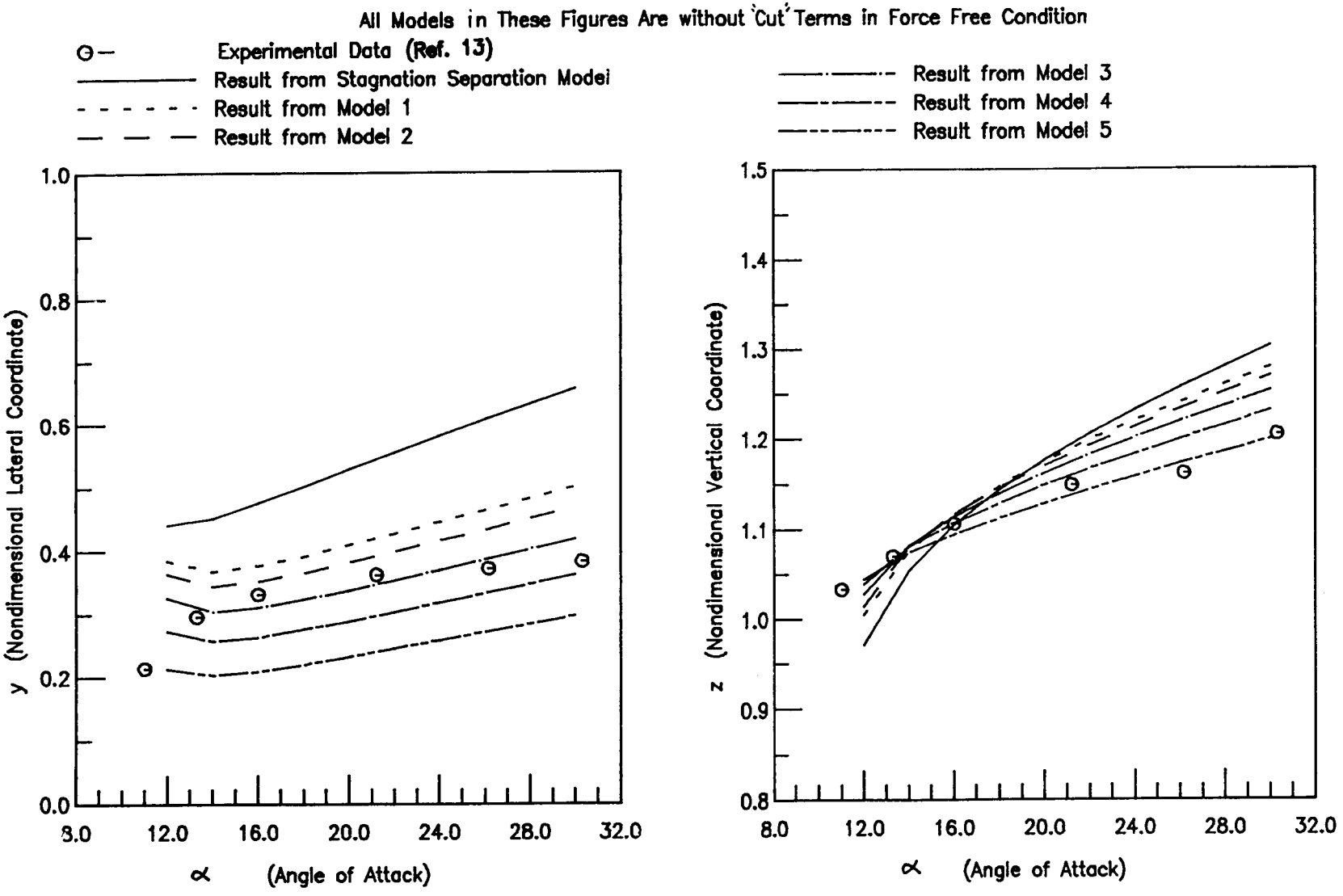

Fig.5 Right Vortex Core Positions for Different Models of a 10 Deg. Cone as a Function of Angle of Attack (Symmetric Case)

All Models in This Figure Are With 'Cut' Terms in Force Free Condition

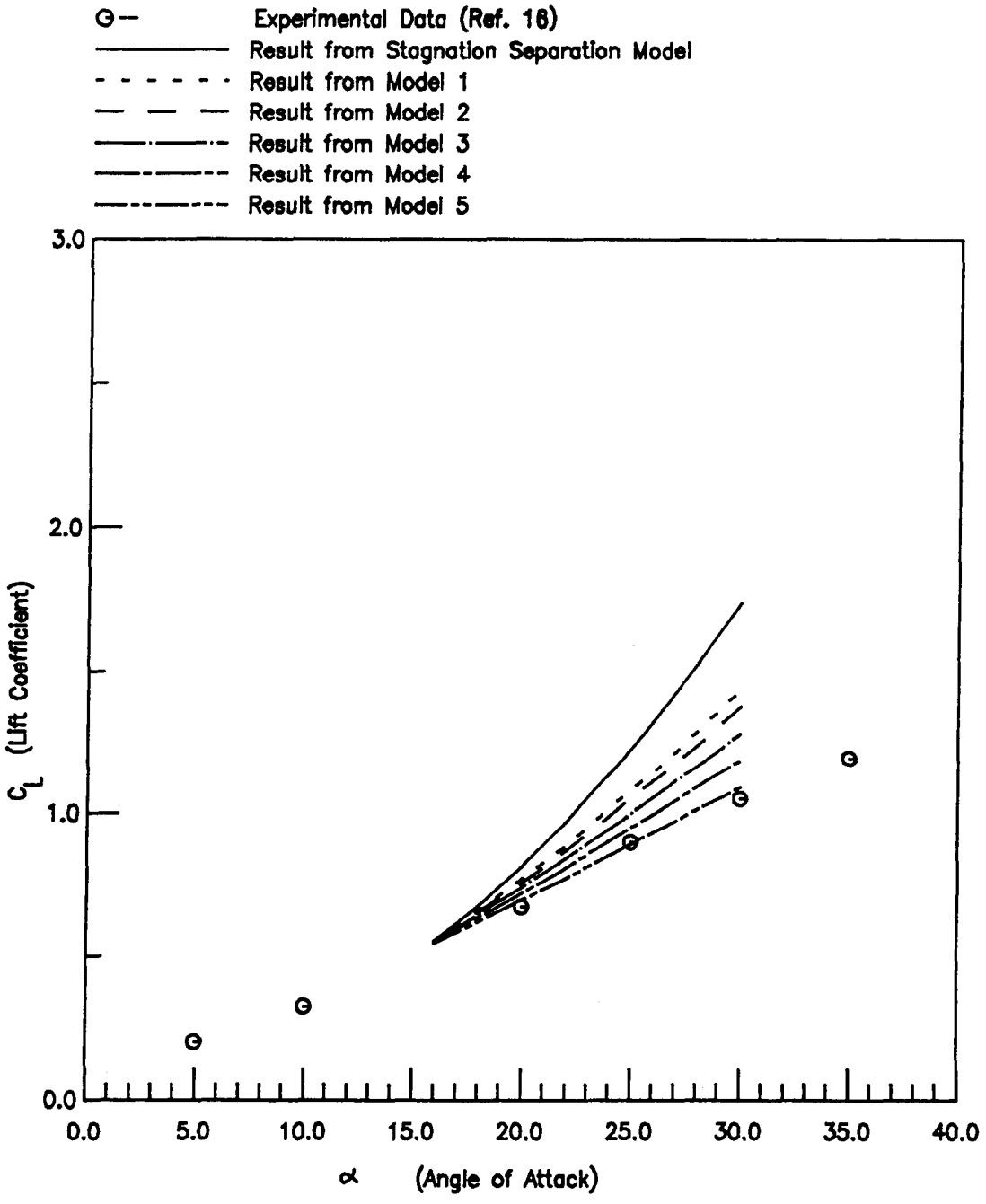

Fig.6 Lift Coefficient of a 8 Deg. Cone as a Function of Angle of Attack(Symmetric Case)

All Models in This Figure Are Without 'Cut' Terms in Force Free Condition

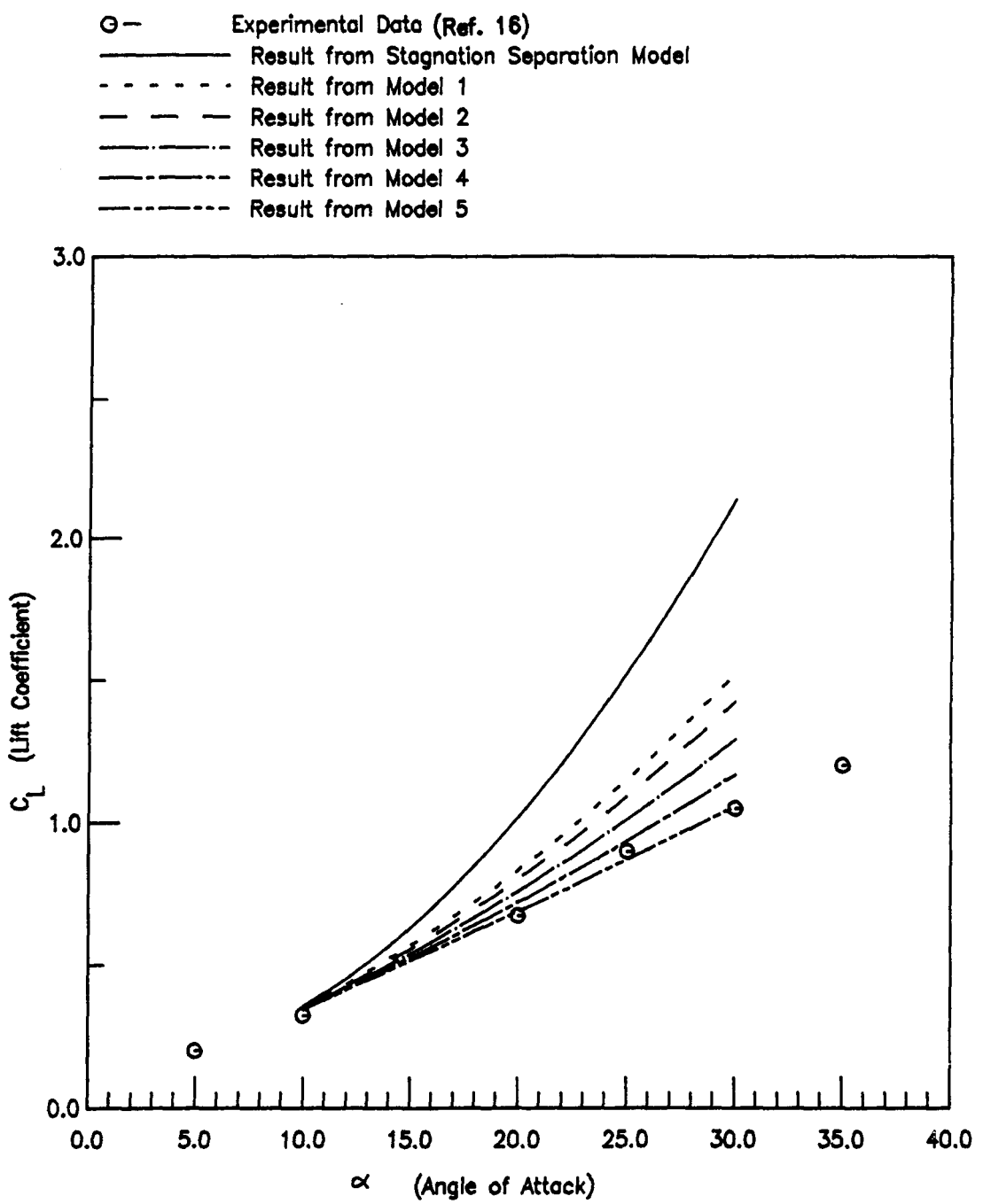

Fig.7 Lift Coefficient of a 8 Deg. Cone as a Function of Angle of Attack(Symmetric Case)

Result from Model 3 Without 'Cut' Terms in Force Free Condition

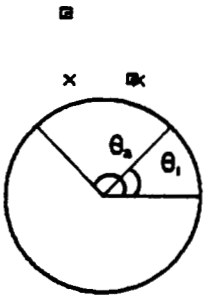

A = 2.500
θ_1 = 46.61

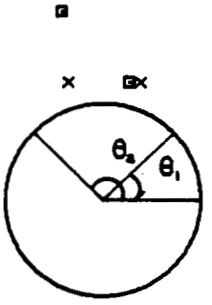

A = 2.750
θ_1 = 44.66

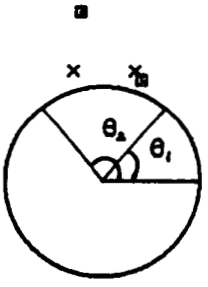

A = 2.000
θ_1 = 51.12

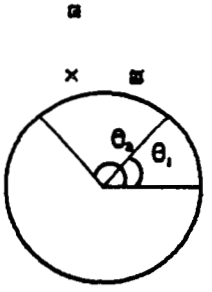

A = 2.250
θ_1 = 48.74

Fig.8 Symmetric and Asymmetric Vortex Core Positions of a 8 Deg. Cone as a Function of Incidence Parameter A ($\theta_1 + \theta_2 = 180$)

Result from Model 3 Without 'Cut' Terms in Force Free Condition

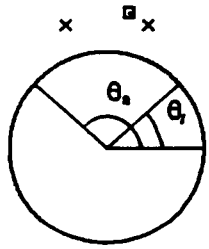

A = 3.500
θ_1 = 39.55

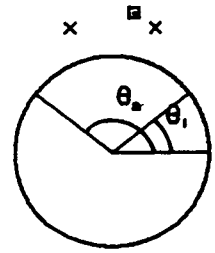

A = 3.750
θ_1 = 38.04

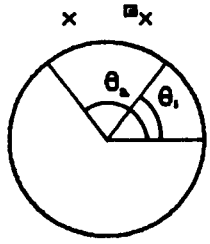

A = 3.000
θ_1 = 42.85

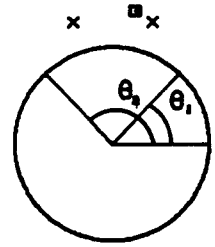

A = 3.250
θ_1 = 41.15

Fig.8 Concluded

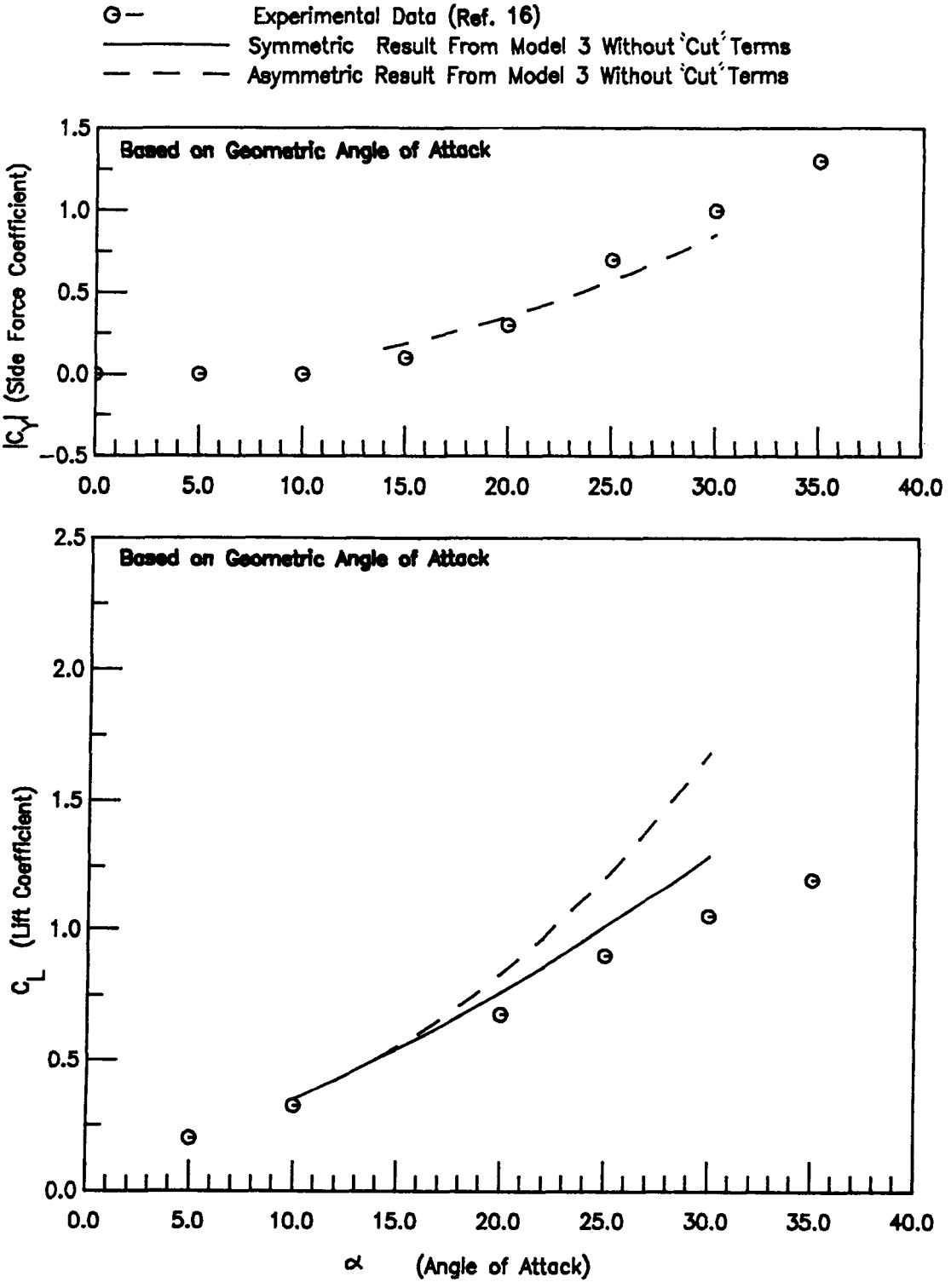

FIG.9 Lift Coefficient and Side Force Coefficient of a 8 Deg. Cone as a Function of Angle of Attack

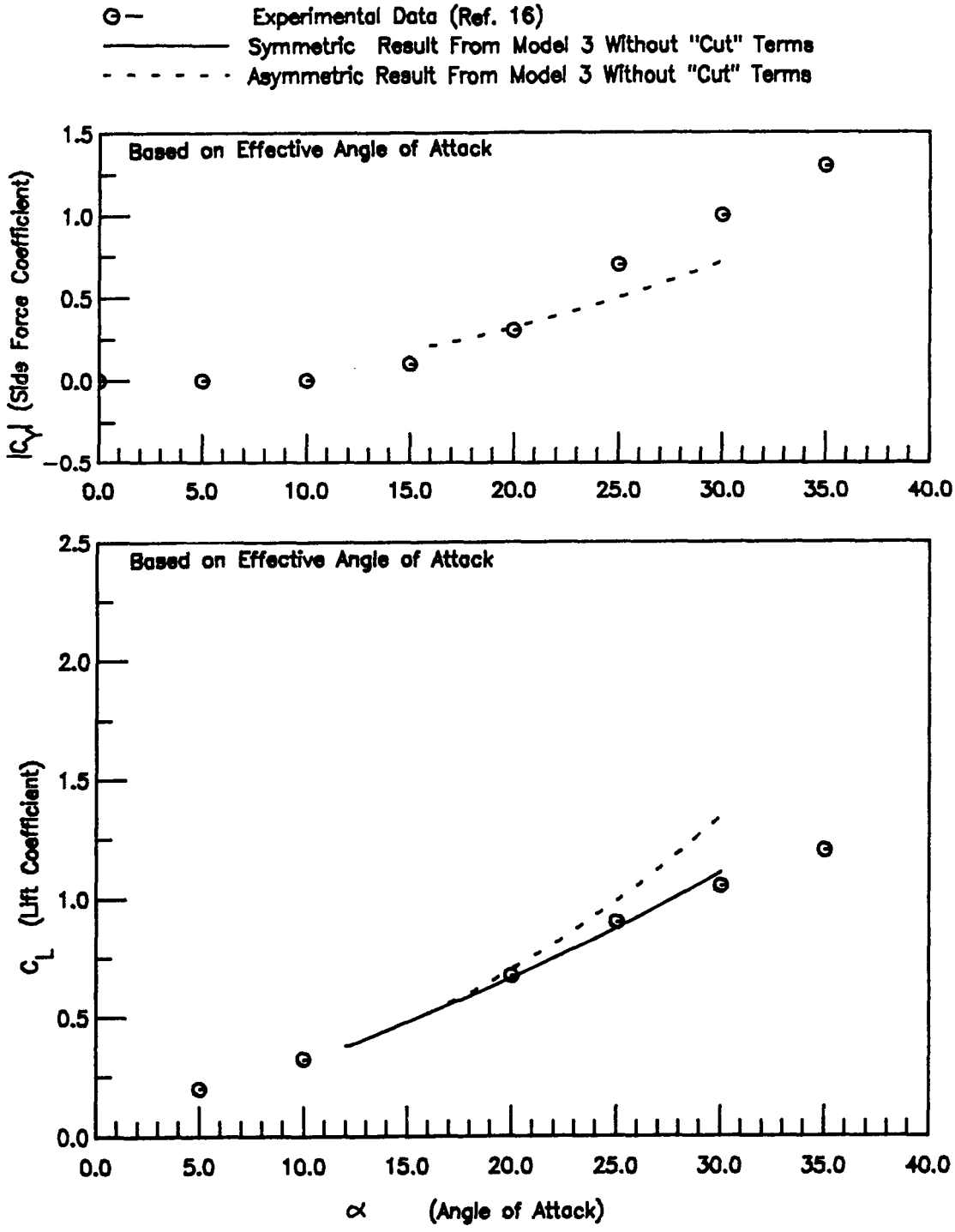

Fig.10 Lift Coefficient and Side Force Coefficient Calculated at Effective Angle of Attack of a 8 Deg. Cone as a Function of Angle of Attack

All Models in These Figures Are Without 'Cut' Terms in Force Free Condition

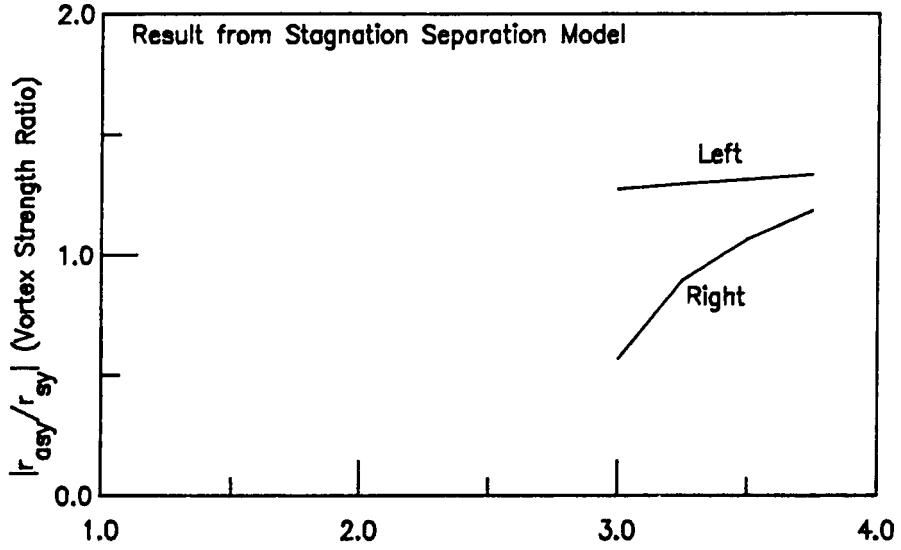

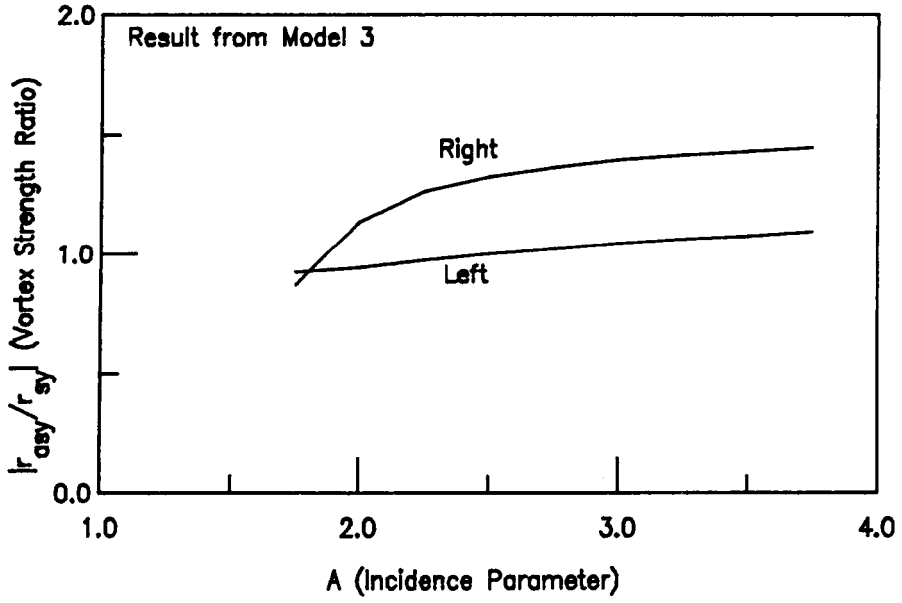

Fig.11 Vortex Strength Ratio for Different Models of a 8 Deg. Cone as a Function of Incidence Parameter A

Result from Model 3 Without 'Cut' Terms in Force Free Condition

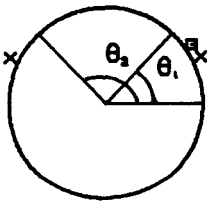

A = 2.500
θ1 = 46.61

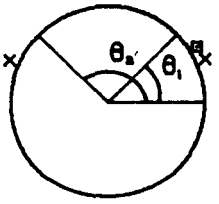

A = 2.750
θ1 = 44.66

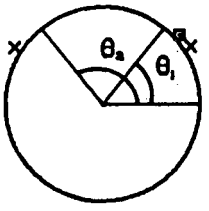

A = 2.000
θ1 = 51.12

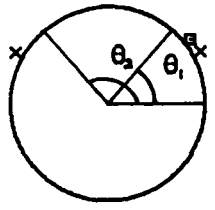

A = 2.250
θ1 = 48.74

Fig.12 Low Branch Symmetric and Asymmetric Vortex Core Positions of a 8 Deg. Cone as a Function of Incidence Parameter A ($\theta_1 + \theta_2 = 180$)

Result from Model 3 Without 'Cut' Terms in Force Free Condition

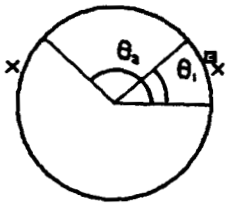

A = 3.500
θ1 = 39.55

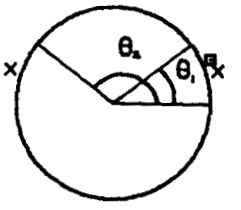

A = 3.750
θ1 = 38.04

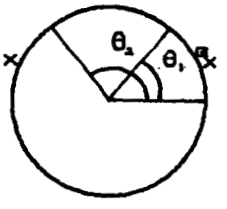

A = 3.000
θ1 = 42.85

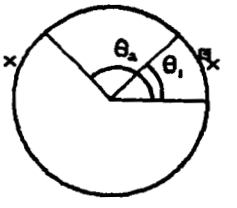

A = 3.250
θ1 = 41.15

Fig.12 Concluded

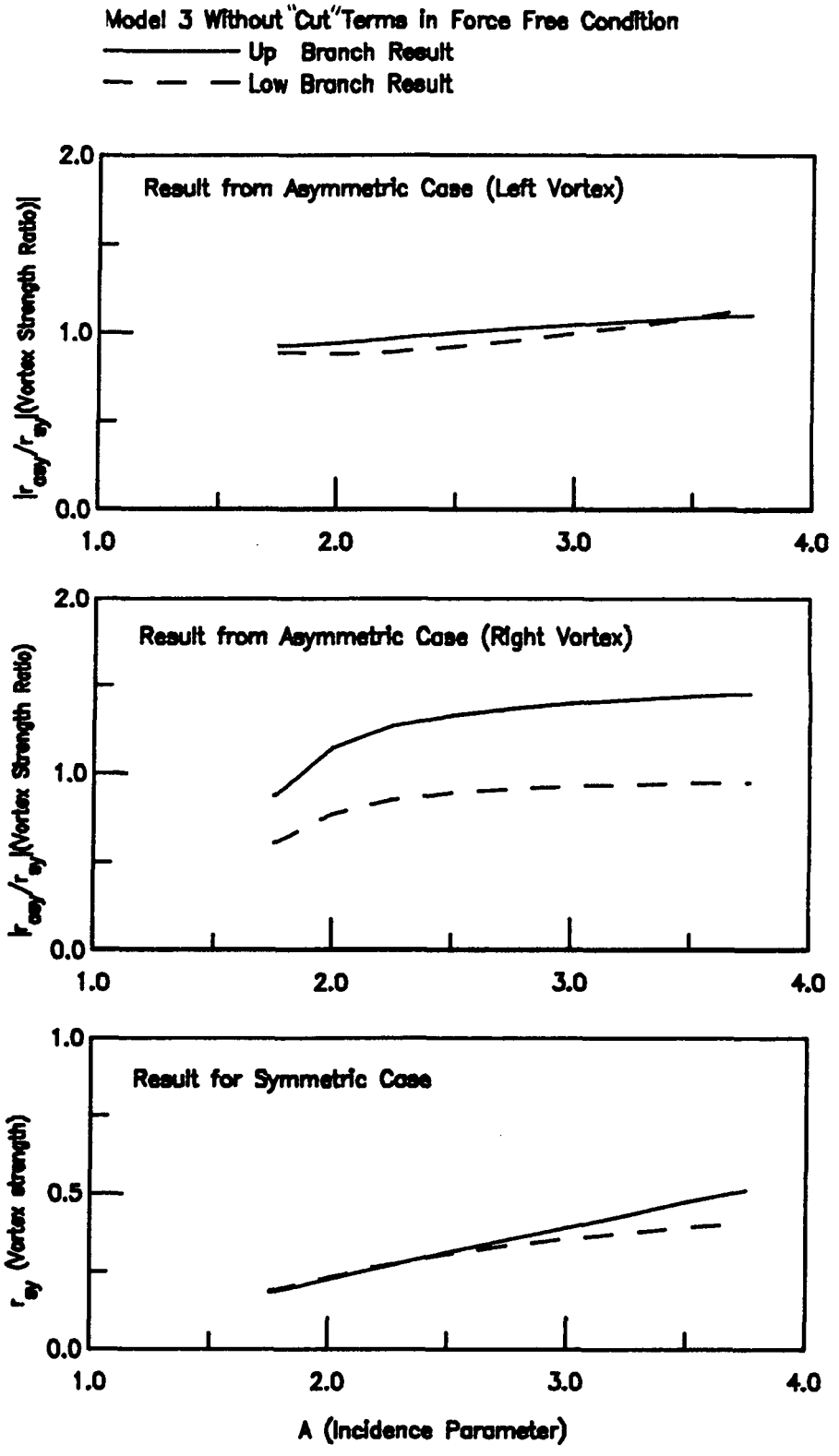

Fig.13 Vortex Strength Ratio for Both Branchs of a 8 Deg. Cone as a Function of Incidence Parameter A

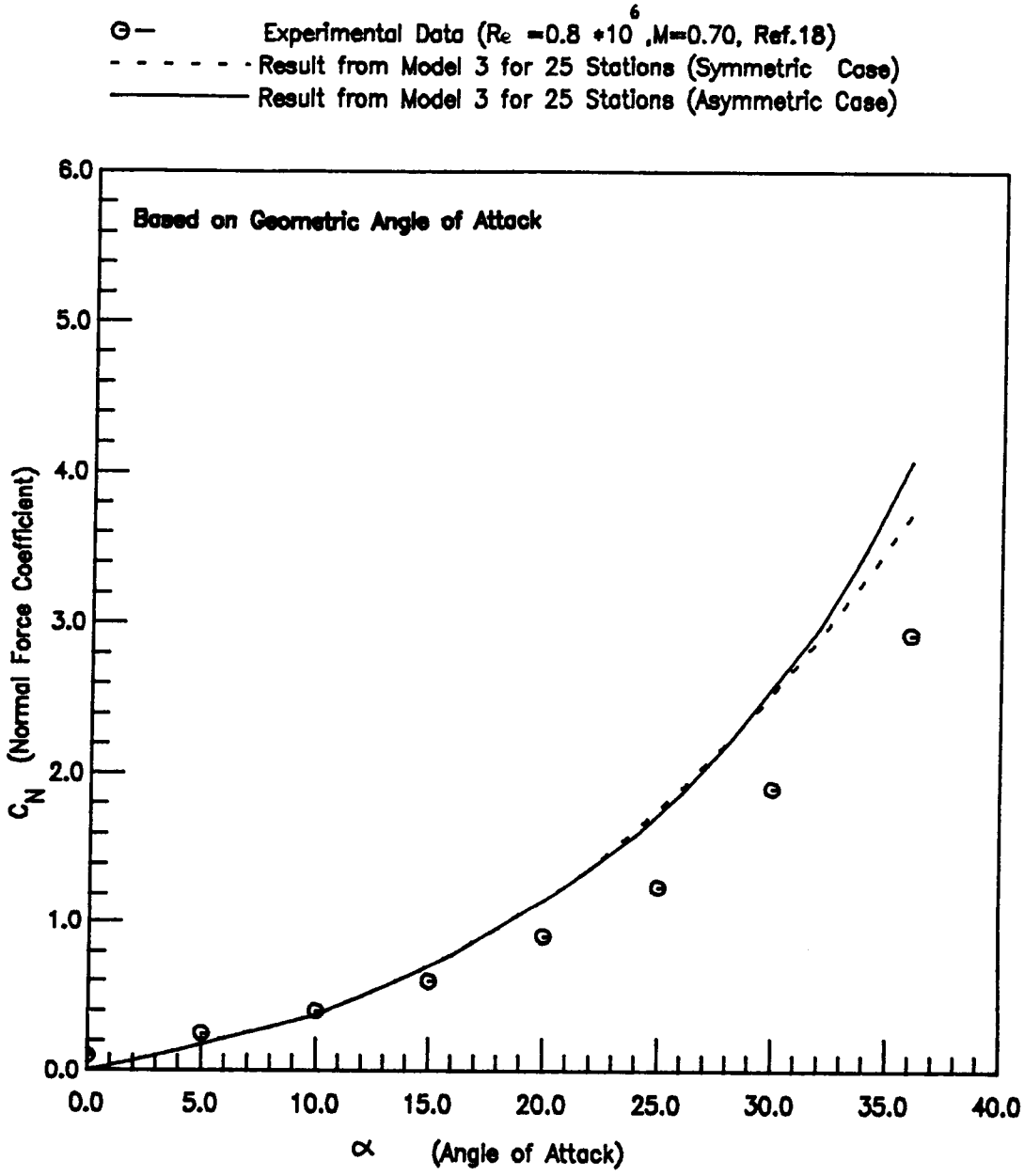

Fig.14 Normal Force Coefficient of a Tangent Ogive (Fineness Ratio = 5.) as a Function of Angle of Attack

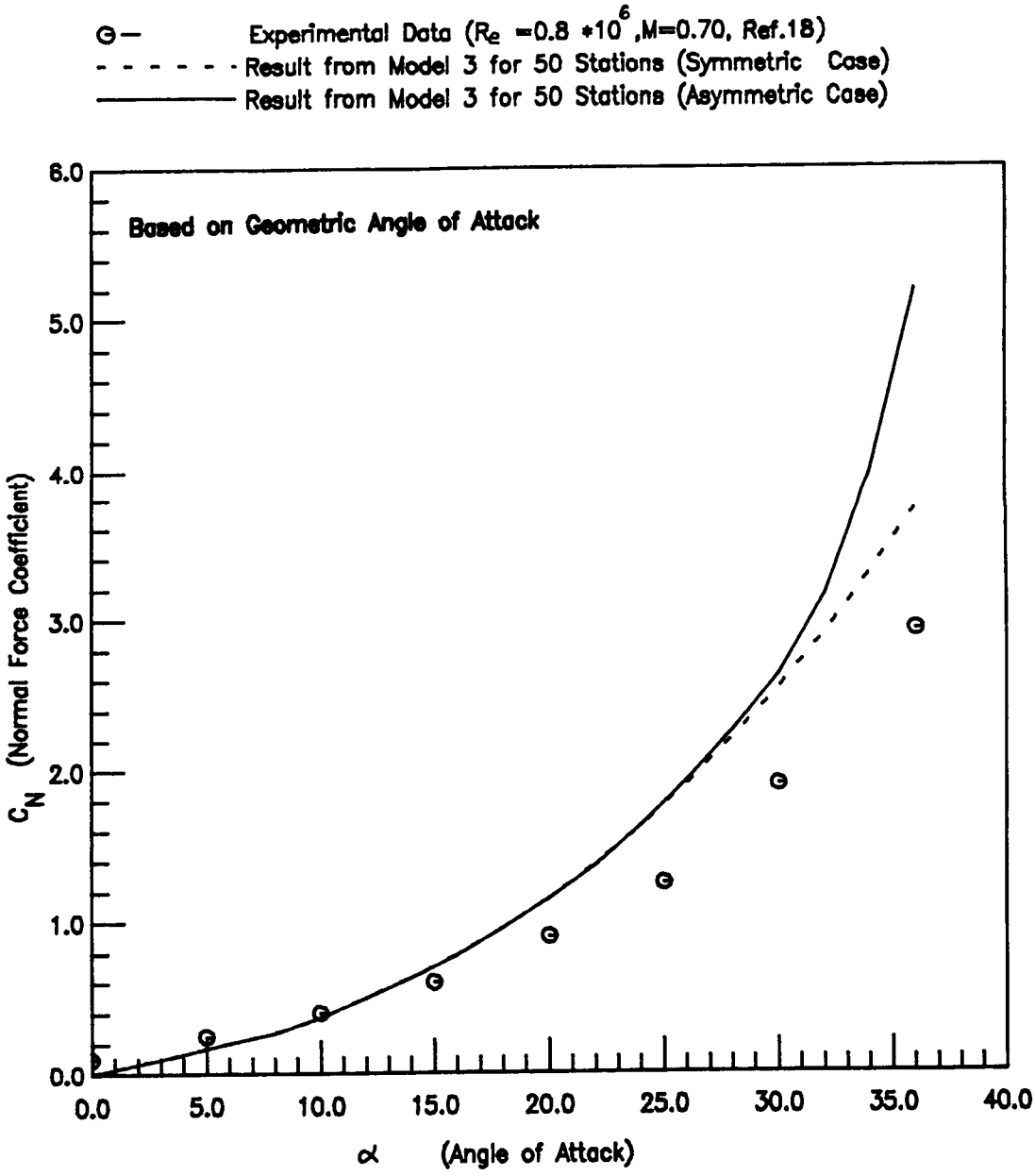

Fig.14 Concluded

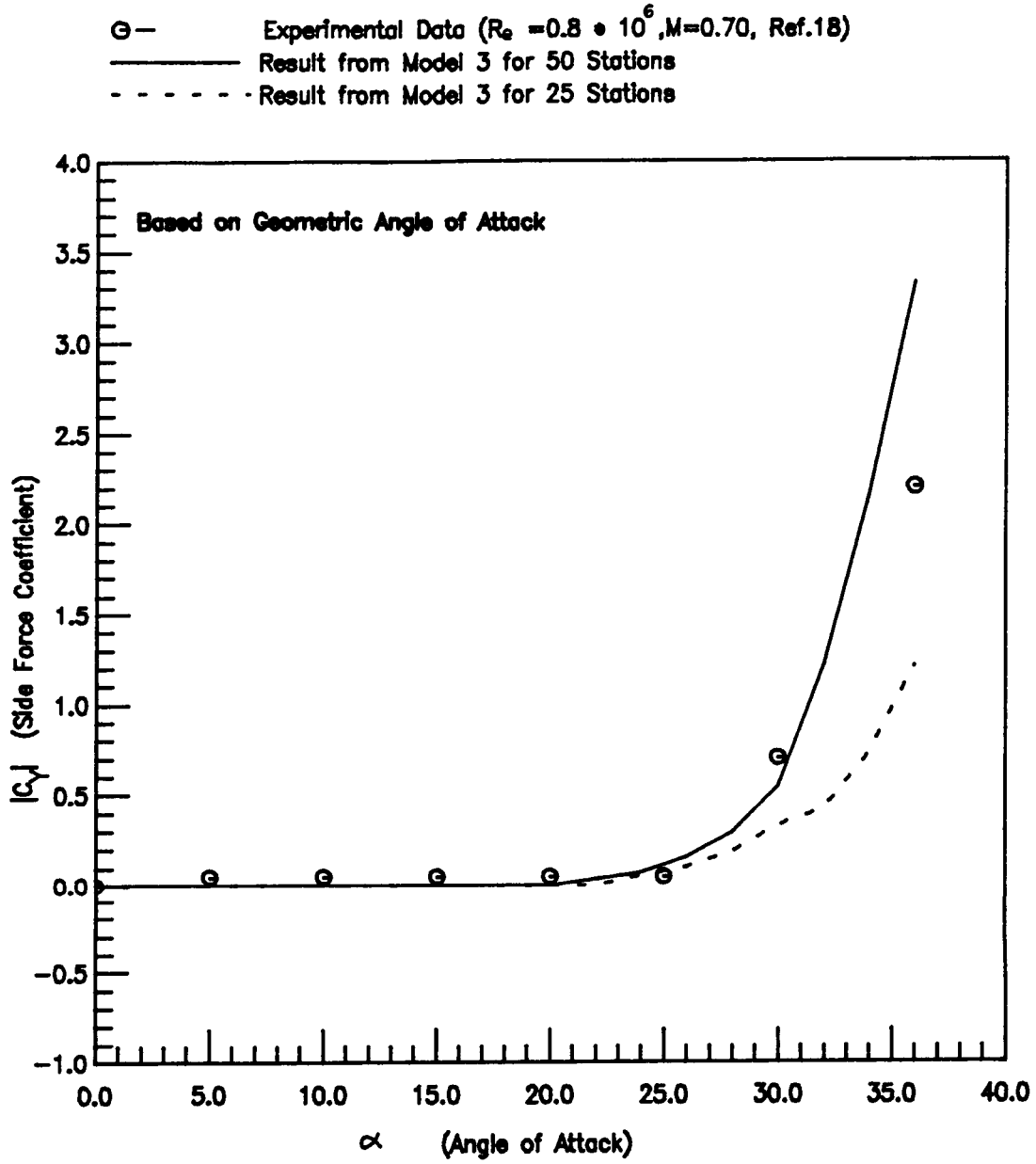

Fig.15 Side Force Coefficient of a Tangent Ogive (Fineness Ratio = 5.) as a Function of Angle of Attack (Asymmetric Case)

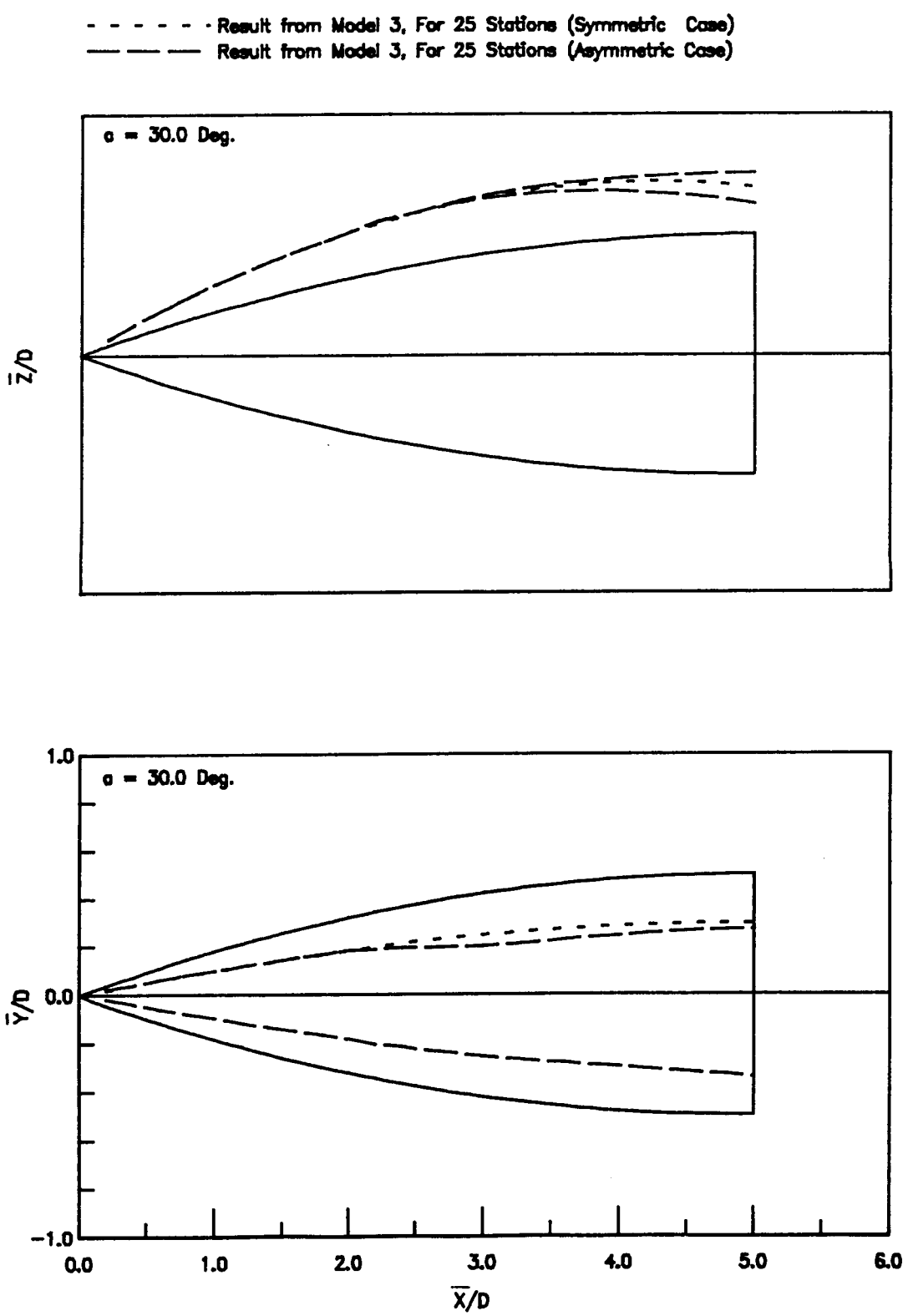

Fig.16 Tracing of Vortex Core Position in a Tangent Ogive (Fineness Ratio = 5).

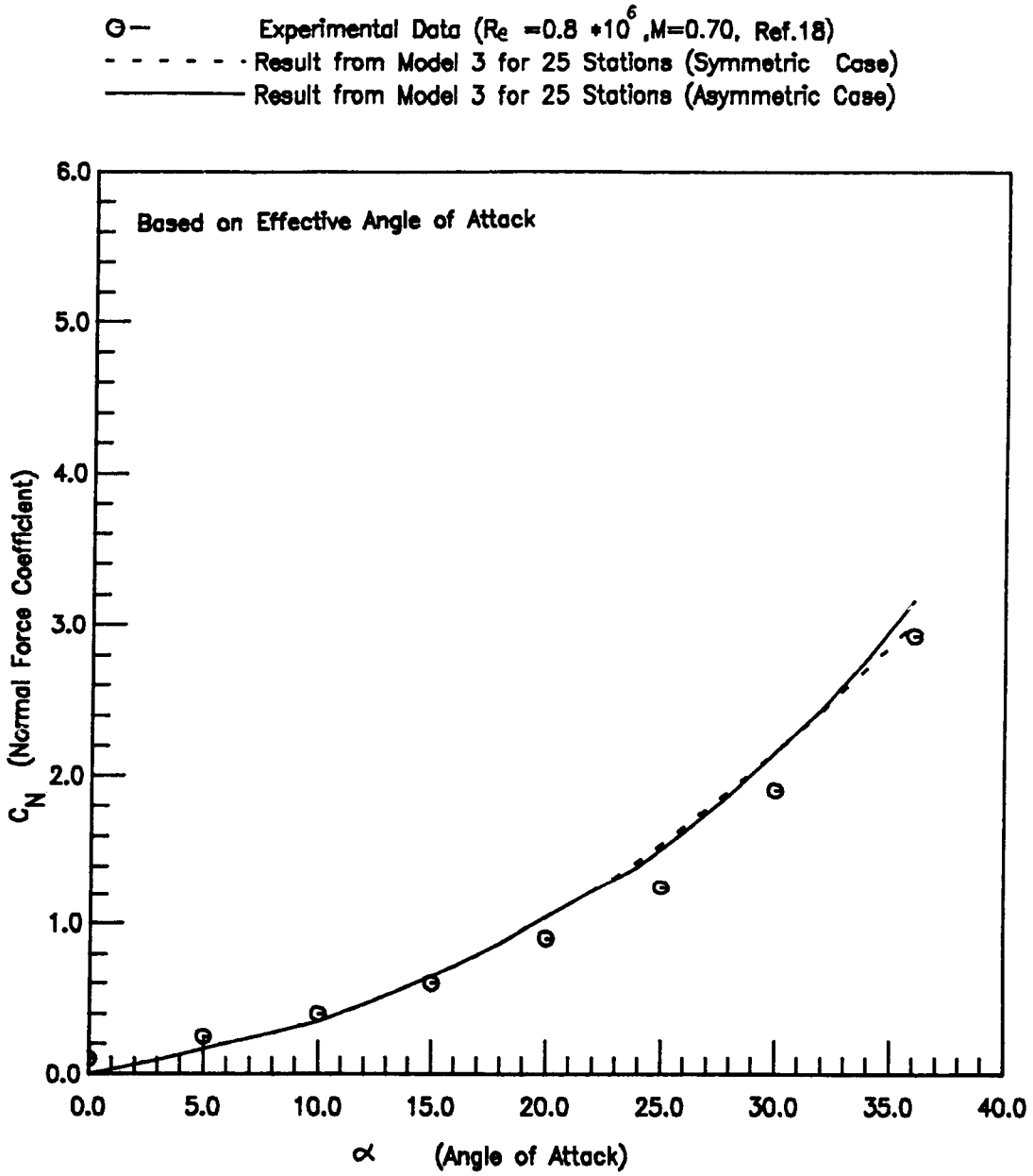

Fig.17 Normal Force Coefficient Calculated at Effective Angle of Attack of a Tangent Ogive (Fineness Ratio = 5.) as a Function of Angle of Attack

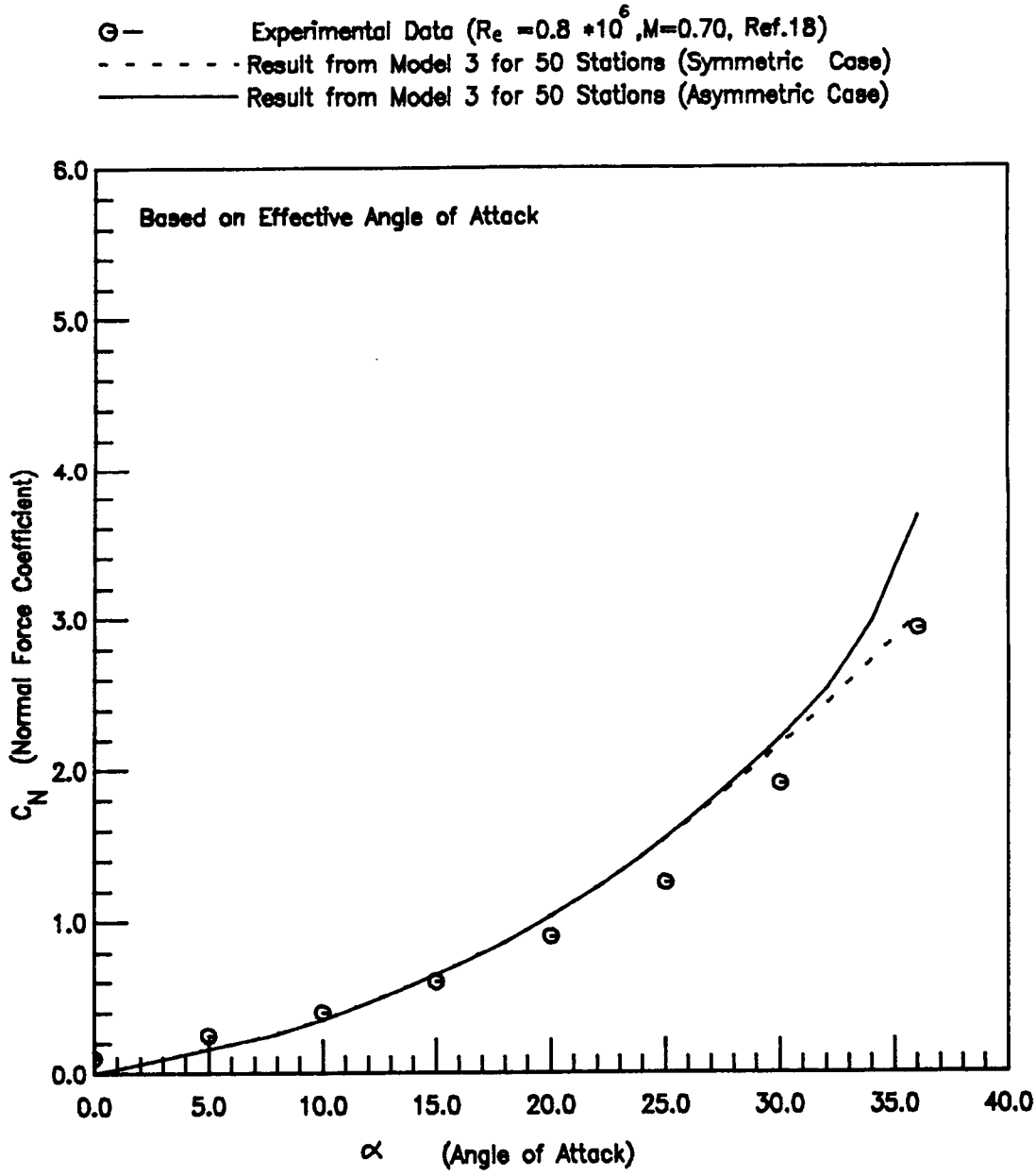

Fig.17 Concluded

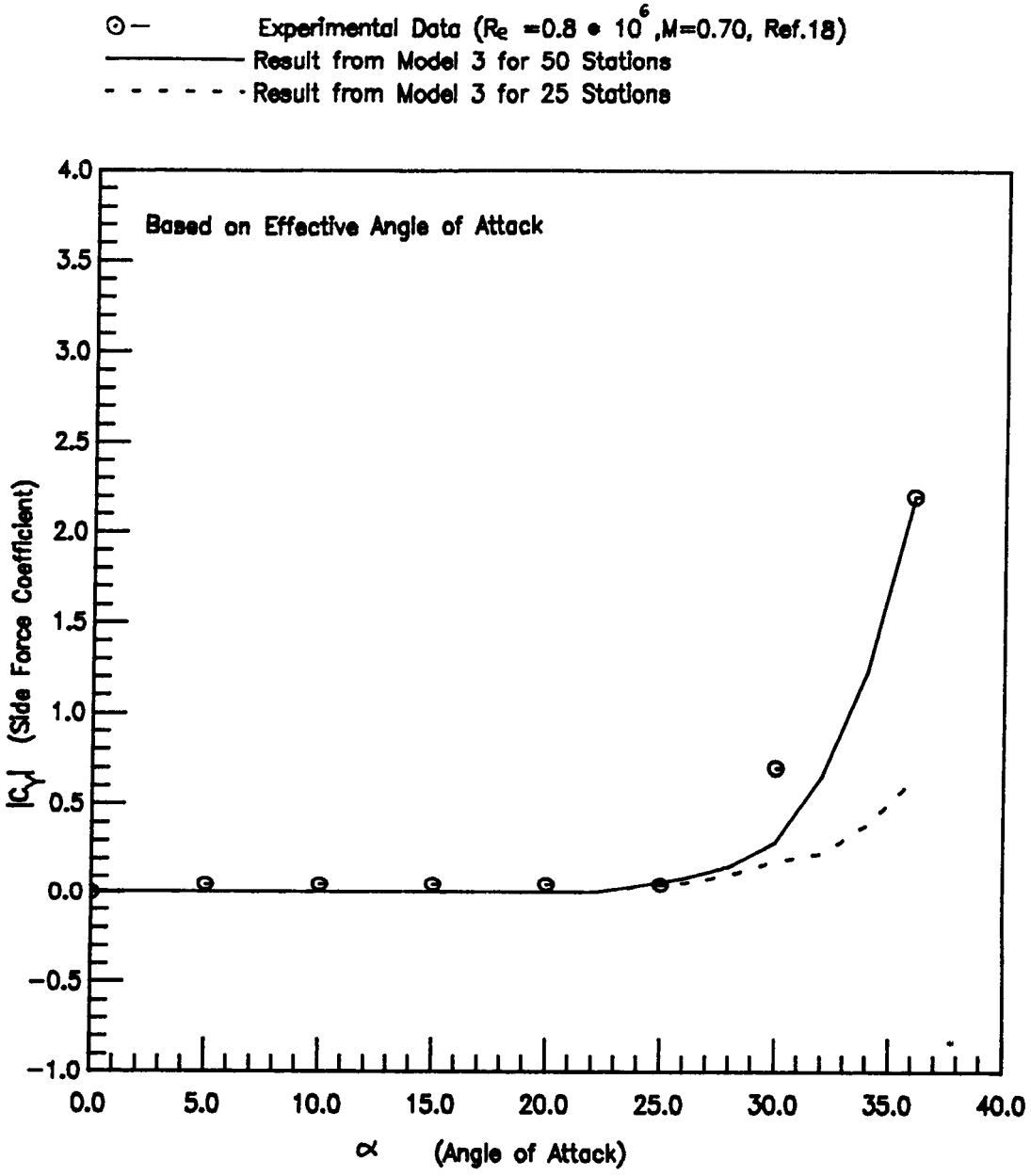

Fig.18 Side Force Coefficient Calculated at Effective Angle of Attack of a Tangent Ogive (Fineness Ratio = 5.) as a Function of Angle of Attack (Asymmetric Case)

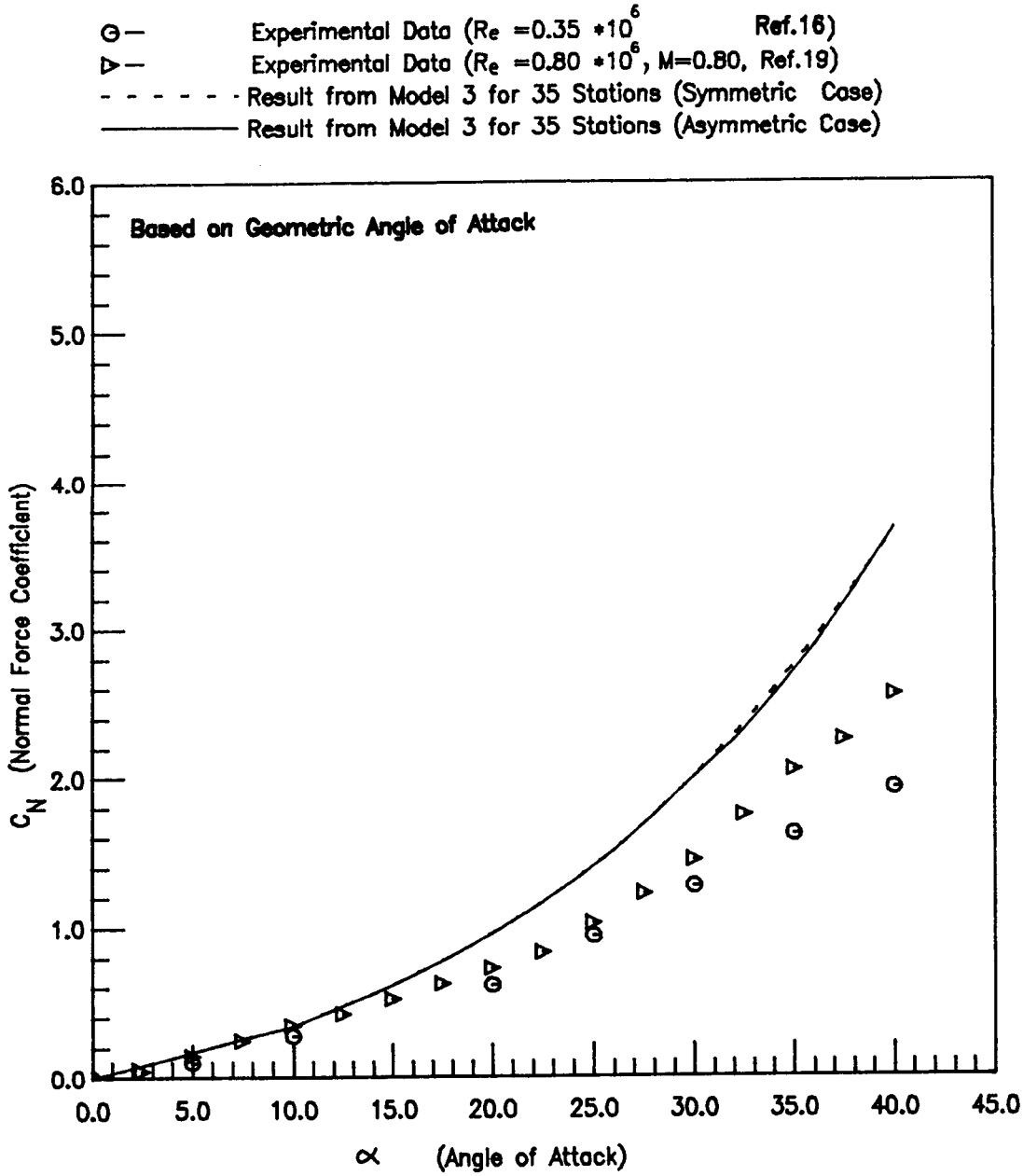

Fig.19 Normal Force Coefficient of a Tangent Ogive (Fineness Ratio 3.5) as a Function of Angle of Attack

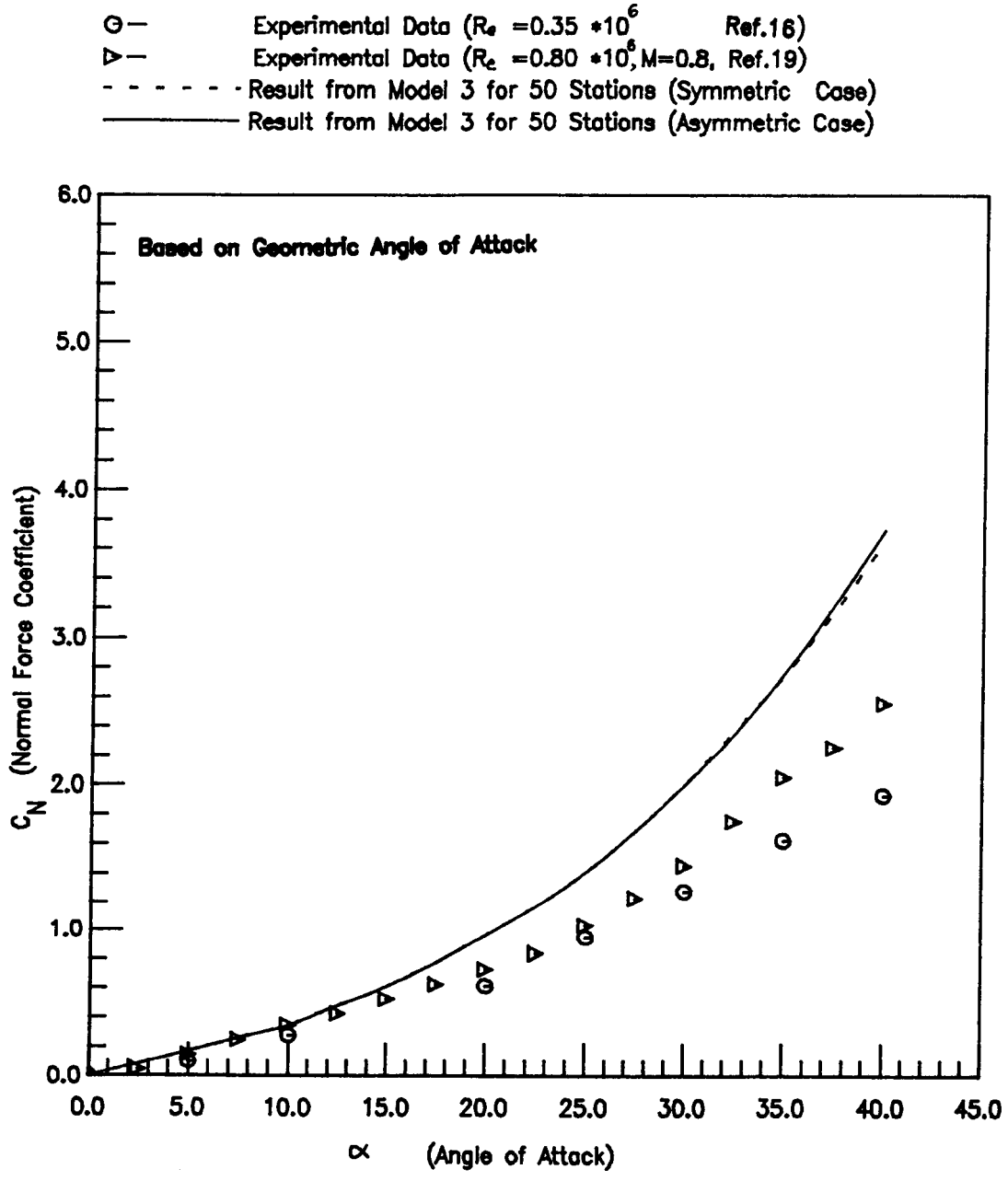

Fig.19 Concluded

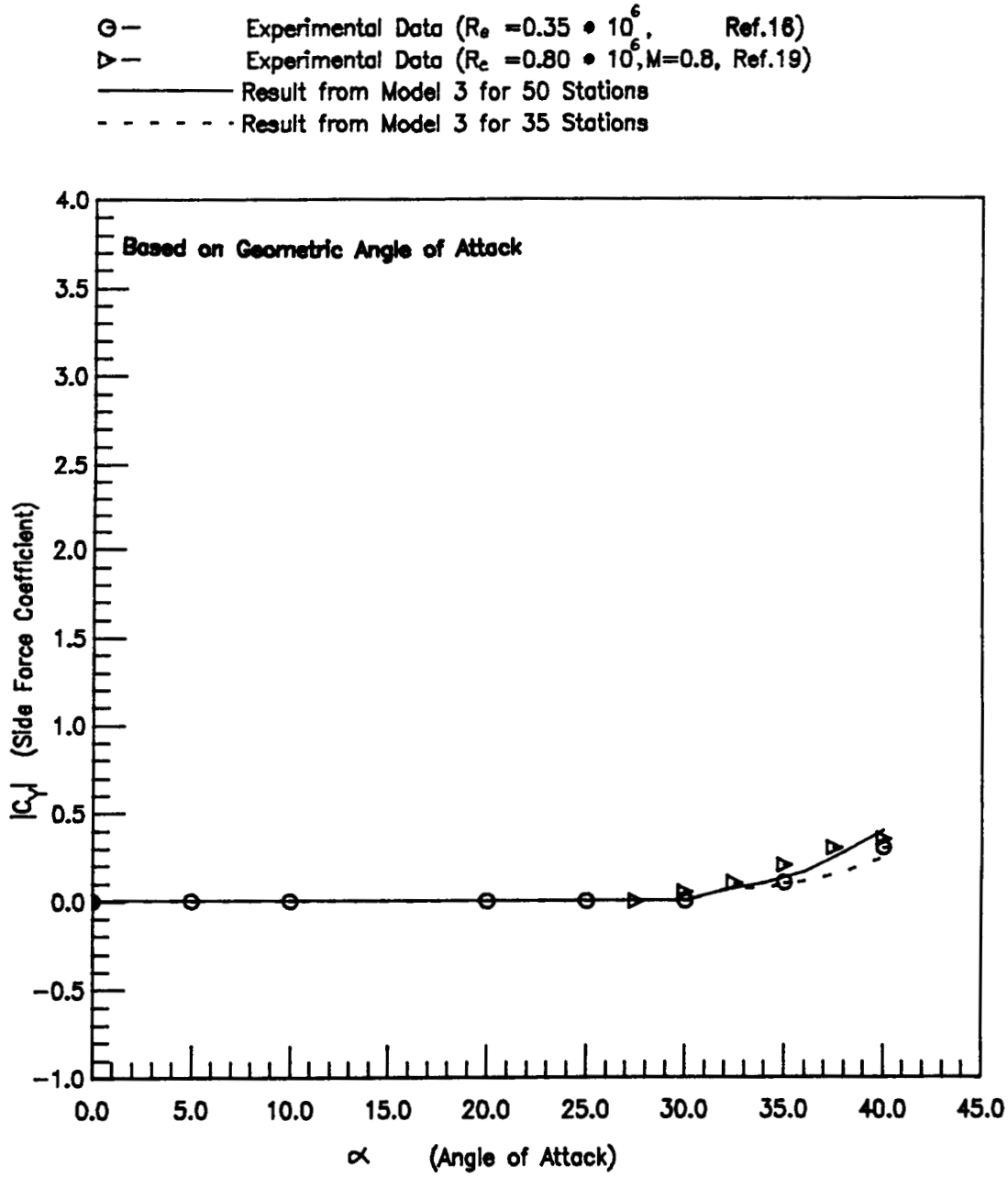

Fig.20 Side Force Coefficient of a Tangent Ogive (Fineness Ratio = 3.5) as a Function of Angle of Attack (Asymmetric Case)

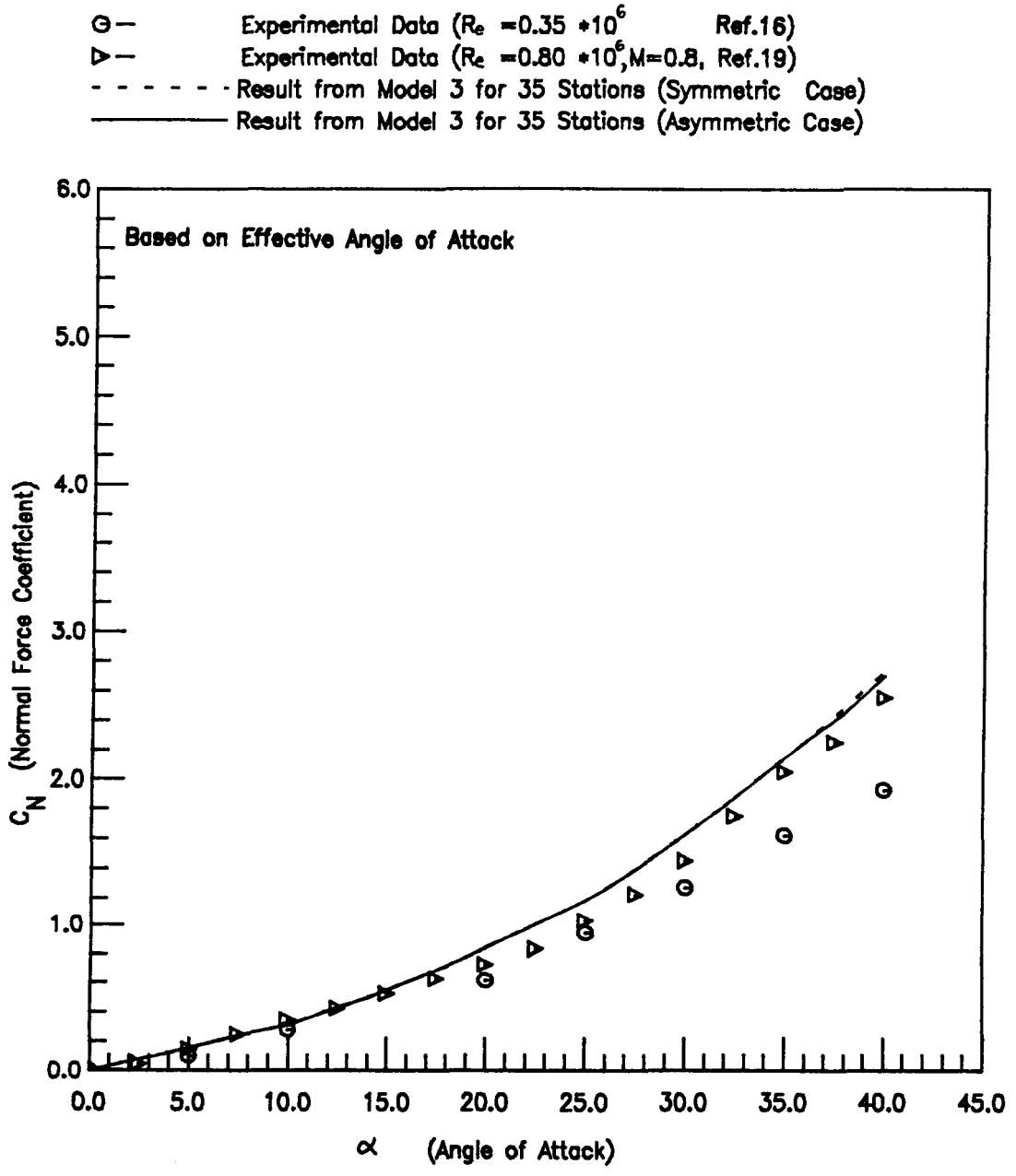

Fig.21 Normal Force Coefficient Calculated at Effective Angle of Attack of a Tangent Ogive (Fineness Ratio = 3.5) as a Function of Angle of Attack

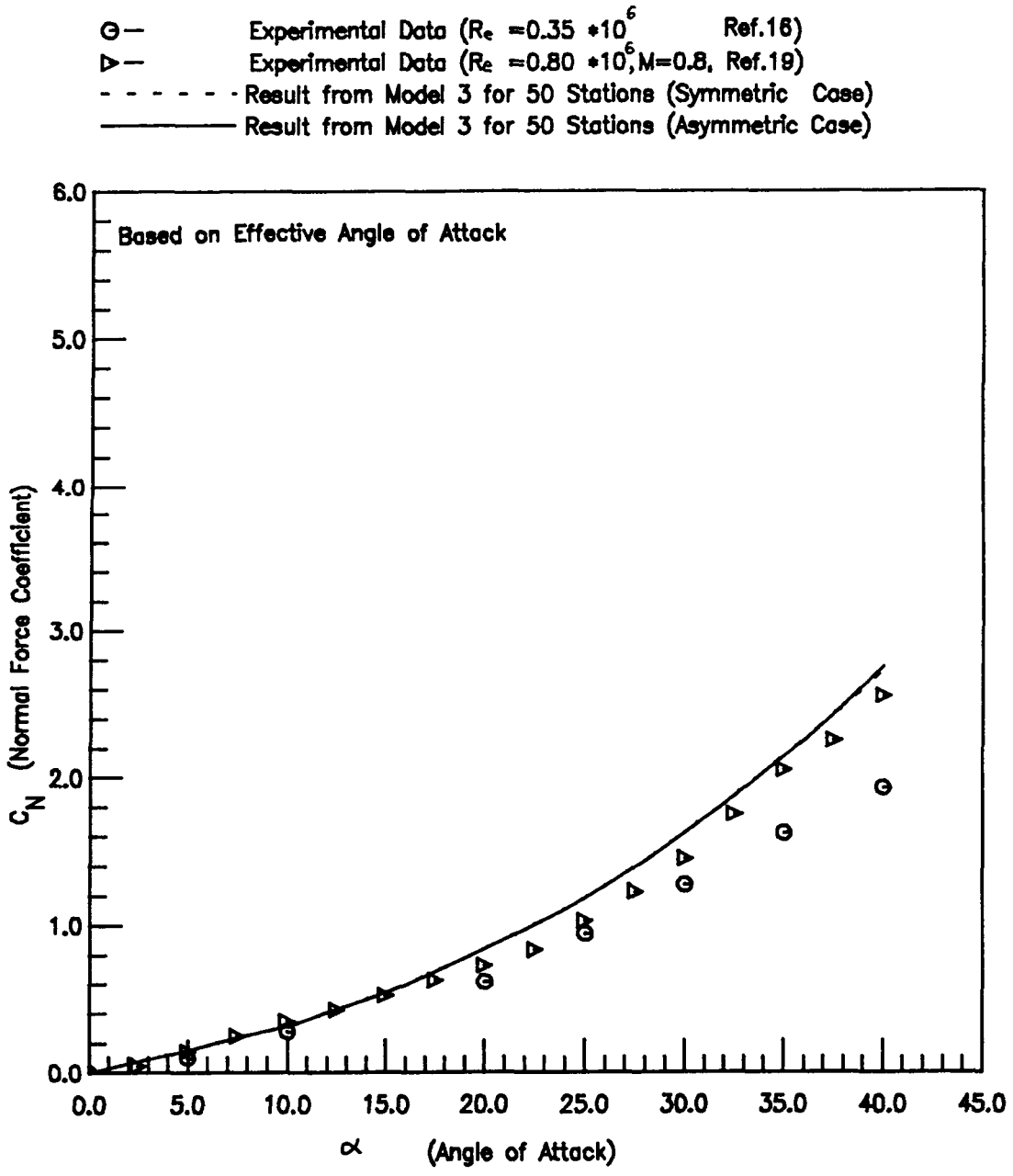

Fig.21 Concluded

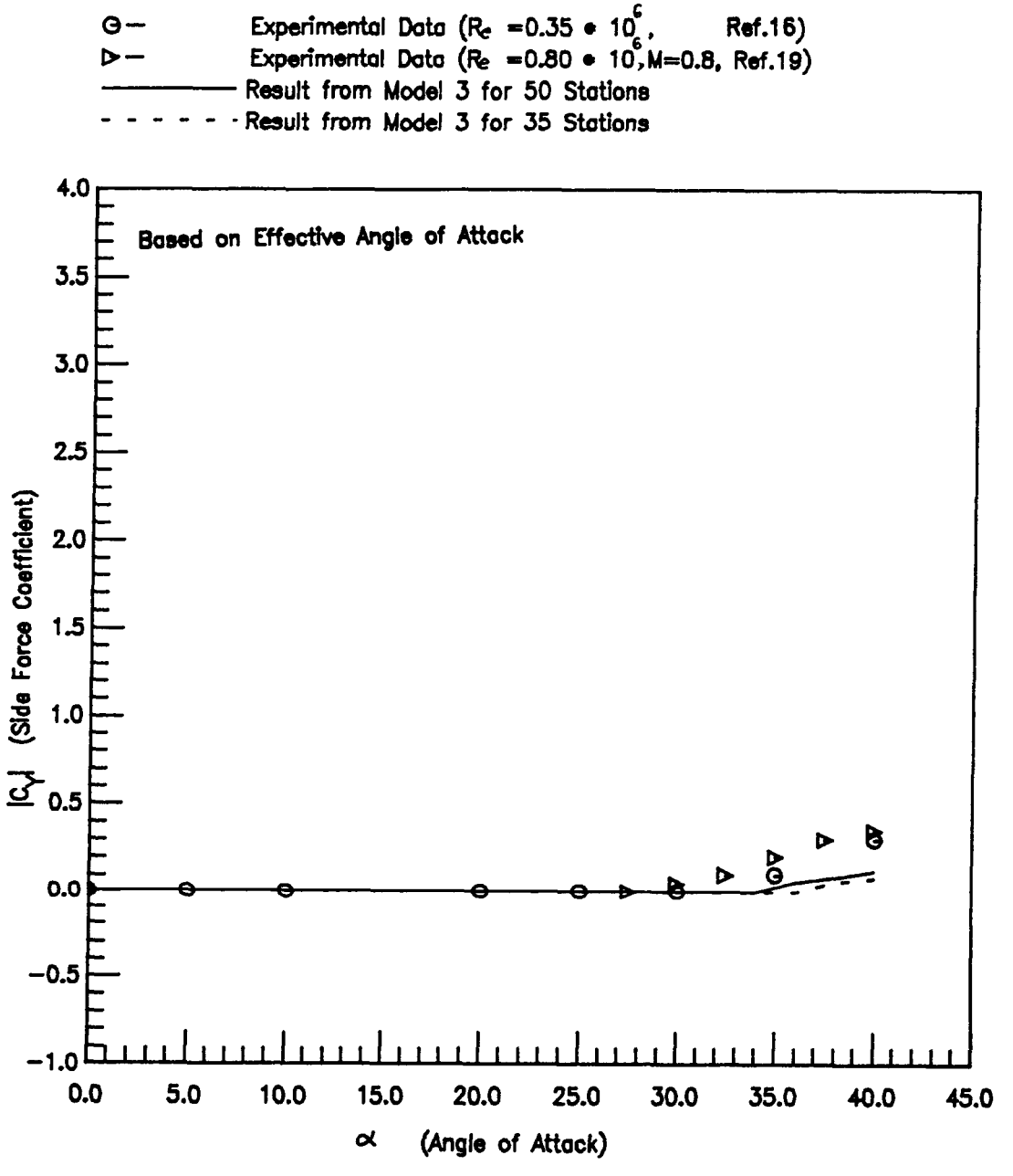

Fig.22 Side Force Coefficient Calculated at Effective Angle of Attack of a Tangent Ogive (Fineness Ratio = 3.5) as a as a Function of Angle of Attack (Asymmetric Case)

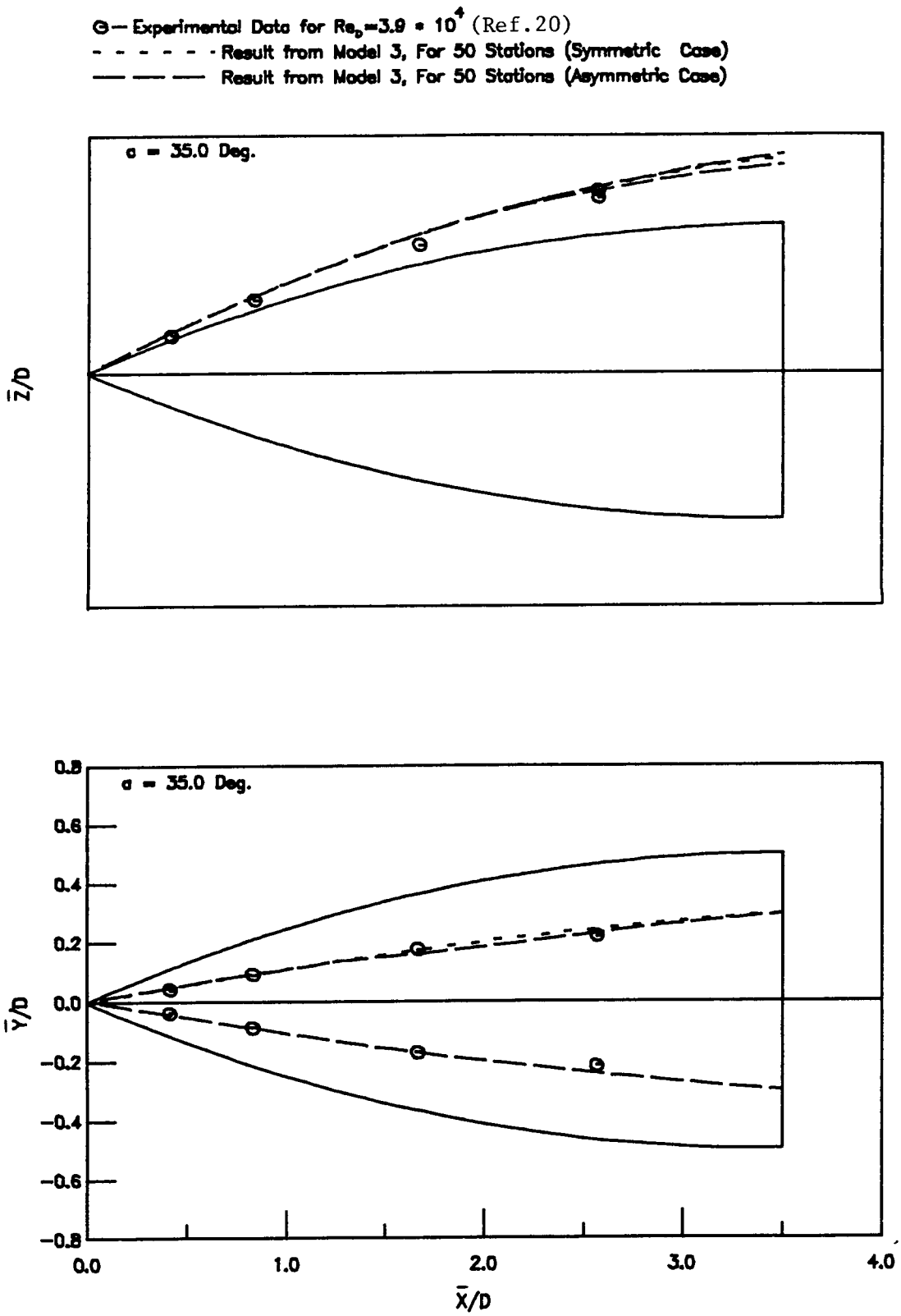

Fig.23 Vortex Core Positions for a Tangent Ogive of Fineness Ratio of 3.5

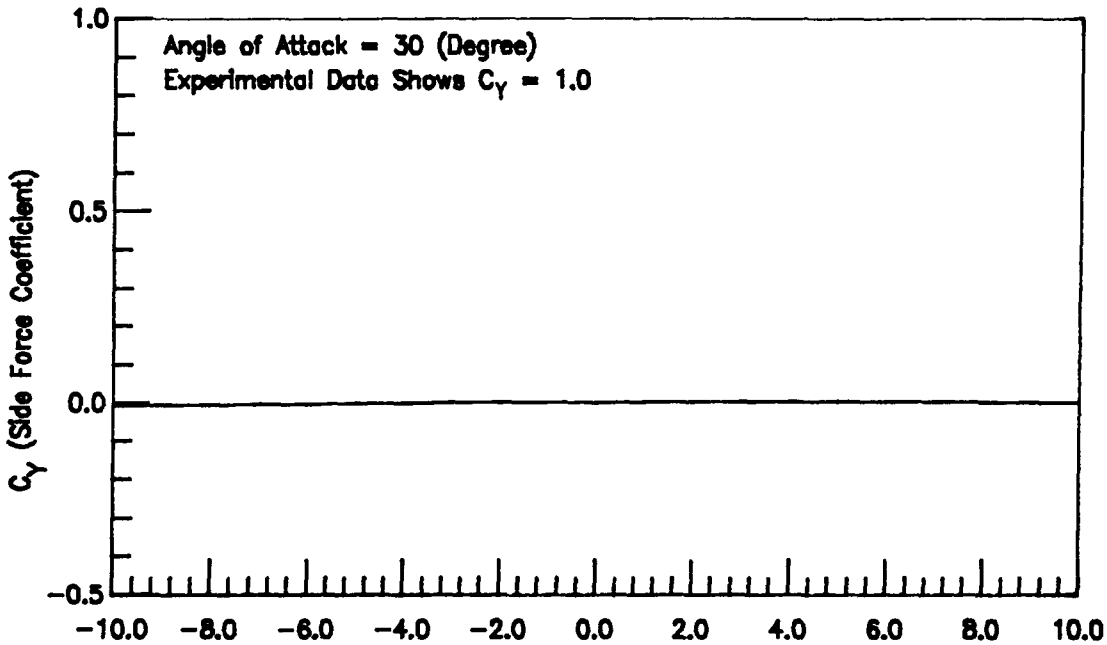

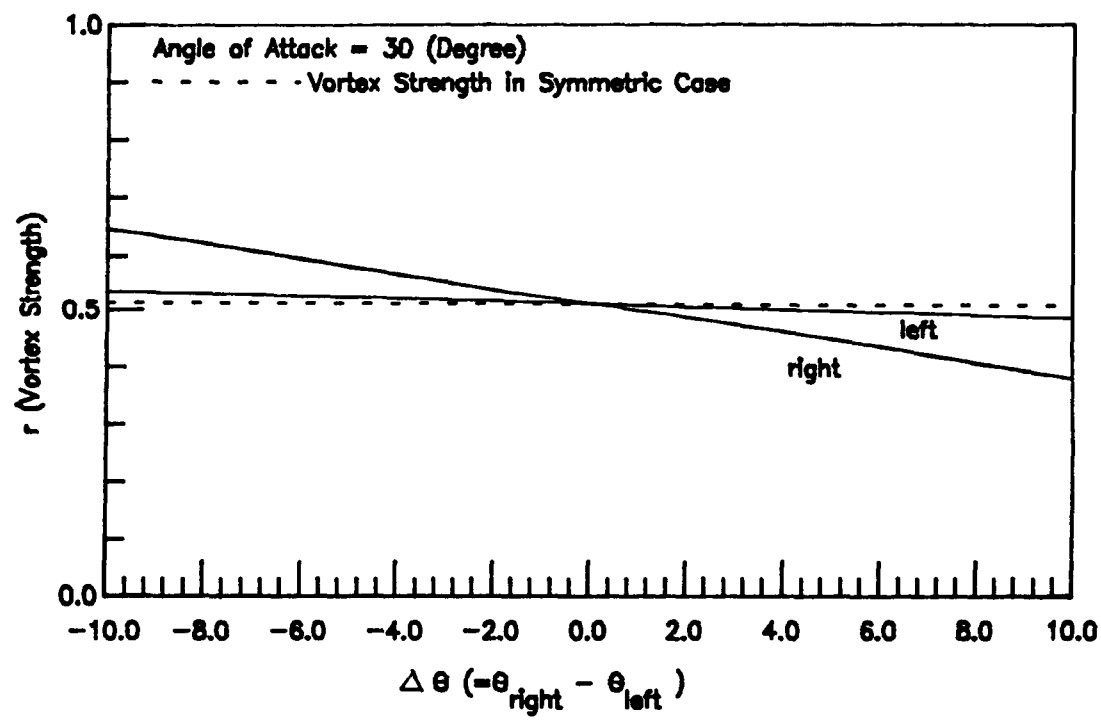

Fig. 24 The Sensitivity of Vortex Strength and Side Force Coefficient Due to The Asymmetry of Separation Points on an 8 Degree Cone

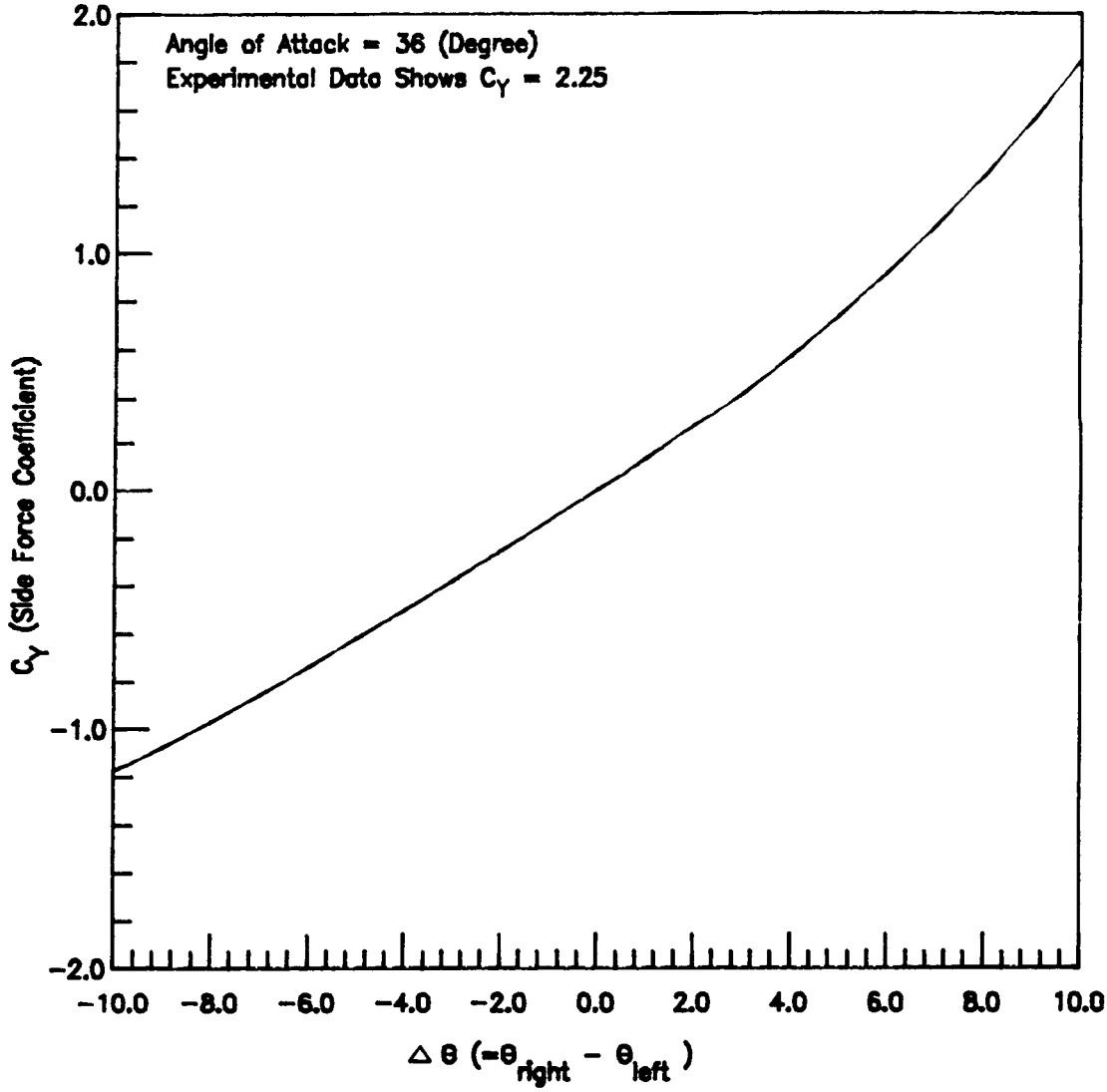

Fig. 25 The Sensitivity of Side Force Coefficient Due to The Asymmetry of Separation Points on a Tangent Ogive (Fineness Ratio = 5.0)

1. Report No.	2. Government Accession No.	3. Recipient's Catalog No.
NASA CR-4122		

4. Title and Subtitle	5. Report Date
Calculation of Symmetric and Asymmetric Vortex Separation on Cones and Tangent Ogives Based on Discrete Vortex Models	February 1988
	6. Performing Organization Code
7. Author(s)	8. Performing Organization Report No.
S. Chin and C. Edward Lan	CRINC-FRL-426-4
	10. Work Unit No.
9. Performing Organization Name and Address	505-61-71-03
Flight Research Laboratory University of Kansas Center for Research, Inc. Lawrence, Kansas 66045-2969	11. Contract or Grant No.
	Grant NSG-1629
	13. Type of Report and Period Covered
12. Sponsoring Agency Name and Address	Contractor Report
National Aeronautics and Space Administration Langley Research Center Hampton, VA 23665-5225	14. Sponsoring Agency Code

15. Supplementary Notes

Technical Monitor: Thomas Gainer, Langley Research Center, Hampton, Virginia.

16. Abstract

An inviscid discrete vortex model, with newly derived expressions for the tangential velocity imposed at the separation points, is used to investigate the symmetric and asymmetric vortex separation on cones and tangent ogives. The circumferential locations of separation are taken from experimental data. Based on a slender body theory, the resulting simultaneous nonlinear algebraic equations in a cross-flow plane are solved with Broyden's modified Newton-Raphson method. Total force coefficients are obtained through momentum principle with new expressions for nonconical flow. It is shown through the method of function deflation that multiple solutions exist at large enough angles of attack, even with symmetric separation points. These additional solutions are asymmetric in vortex separation and produce side force coefficients which agree well with data for cones and tangent ogives.

17. Key Words (Suggested by Author(s))	18. Distribution Statement
Asymmetric Vortex Flow Symmetric Vortex Flow Cones Tangent Ogives	Unclassified - Unlimited Subject Category 02

19. Security Classif. (of this report)	20. Security Classif. (of this page)	21. No. of Pages	22. Price
Unclassified	Unclassified	90	A05

For sale by the National Technical Information Service, Springfield, Virginia 22161

NASA-Langley, 1988